KfK 3376
Juli 1983

BACCHUS-3D/SP
A Computer Programme for the Three-Dimensional Description of Sodium Single-Phase Flow in Bundle Geometry

M. Bottoni, B. Dorr, Ch. Homann, D. Struwe
Institut für Reaktorentwicklung
Projekt Schneller Brüter

Kernforschungszentrum Karlsruhe

KERNFORSCHUNGSZENTRUM KARLSRUHE

Institut für Reaktorentwicklung

Projekt Schneller Brüter

KfK 3376

BACCHUS-3D/SP

A Computer Programme for the Three-Dimensional Description of Sodium Single-Phase Flow in Bundle Geometry

M. Bottoni

B. Dorr

Ch. Homann

D. Struwe

Kernforschungszentrum Karlsruhe G.m.b.H., Karlsruhe

Kernforschungszentrum Karlsruhe GmbH
ISSN 0303-4003

Abstract

The computer programme BACCHUS implemented at KfK includes a steady-state version, a two-dimensional and a three-dimensional transient single-phase flow version describing the thermal-hydraulic behaviour of the coolant (sodium or water) in bundle geometry under nominal or accident conditions. All versions are coupled with a pin model describing the temperature distribution in fuel (or electrical heaters) and cladding. The report describes the programme from the viewpoints of the geometrical model, the mathematical foundations and the numerical treatment of the basic equations. Although emphasis is put on the three-dimensional version, the two-dimensional and the steady state versions are also documented in self-consistent sections.

BACCHUS-3D/SP, ein Rechenprogramm für die dreidimensionale Beschreibung der einphasigen Natriumströmung in Bündelgeometrie

Zusammenfassung

Das Computerprogramm BACCHUS, das im KfK implementiert ist, enthält eine stationäre, eine zwei- und eine dreidimensionale transiente einphasige Version zur Beschreibung der Thermohydraulik eines Kühlmittels (Natrium oder Wasser) in einer Bündelgeometrie unter Nominal- oder Unfallbedingungen. Alle Versionen sind mit einem Stabmodell zur Beschreibung der Temperaturverteilung im Brennstoff (oder dem elektrischen Heizer) und der Hülle gekoppelt. Im Bericht wird das Programm hinsichtlich des geometrischen Modells, der mathematischen Grundgleichungen und ihrer numerischen Behandlung beschrieben. Obwohl die dreidimensionale Version im Vordergrund steht, werden auch die zweidimensionale und die stationäre Version in sich abgeschlossen dokumentiert.

Contents

List of tables

List of figures

Introduction

The three-dimensional version of the computer programme BACCHUS has been developed at KFK since the beginning of 1980. The starting point for this development were two two-dimensional programmes delivered from the CEN Research Centre of Grenoble (France) in the frame of a French-German cooperation. The two programmes were: a) BACCHUS-P /1/, /2/ describing steady state single-phase and two-phase flow of sodium in reactor bundles; b) BACCHUS -T /3/ a transient programme version describing sodium single phase flow under accident conditions like pump run-down, up to boiling inception. In these programmes only thermal-hydraulic effects were described without a fuel pin model.

Work done at KFK concentrated first to assess the performances of the two-dimensional transient BACCHUS-T programme by calculating three 7-pin bundle out-of-pile experiments performed in the sodium loop (NSK) at the Institut für Reaktorentwicklung at KfK /4/. Results of the calculations showed that at least in case of rapid transients a pin model was necessary for describing the temperature distribution in the fuel elements, hence the transient heat fluxes into the coolant. Therefore, the first programme implementation consisted in coupling the thermal-hydraulic calculation to a fuel pin model, as explained in section C 4. Results of the programme verification against bundle experiments will be shown in Part III of this documentation.

Some further programme improvements, concerning the two-dimensional version, aimed at accelerating the convergence of the iterative solution for the coolant pressure field and are reported in section C 3.

The largest part of this report is dedicated to the new development of the three-dimensional programme version done at KfK. The new programme makes use of a different technique for solving the Poisson-like equation describing the coolant pressure field, namely the Alternating Direction Implicit (ADI) method derived from the original work by Peaceman and Rachford /5/. It offers the great advantage of reducing the solution of a three-dimensional problem to the solution of simpler one-dimensional problems. However, an iteration procedure is still required. The problem of accelerating the convergence of the ADI scheme has not yet been dealt with and may be object of future development. Due to the large number of cells in the three-dimensional case, a numerical solution by a direct method, for instance by a matrix inversion

technique, is not efficient with regard to computing time. In the two-dimensional case, however, a direct matrix inversion method has been incorporated as an alternative to the several iteration schemes based on the SOR method. It has been found to be superior to the iterative methods because it eliminates spurious oscillations in the time and space distributions of the dependent variables.

For the sake of completeness, the two-dimensional programme version, which still exists as an independent programme, is also documented in this report in a self-consistent section (C 3).

The two- and three-dimensional BACCHUS programmes are in continuous development. This report documents the versions of July 1982.

PART I - The physical model and the mathematical foundations

A) Geometrical model

We consider separately the geometrical model adopted for the thermal-hydraulic calculation and that used for the fuel or electrically heated pins. We assume that the pins are arranged on a hexagonal lattice, as shown in Fig. 1.

1. Thermal-hydraulic calculation

1.1 Control volumes

The conservation equations describing the sodium single-phase flow are written first in a local form, then integrated over appropriate control volumes. According to the ICE technique, explained in section C 2.1, a staggered mesh is used for defining the several dependent variables (components of coolant velocity, pressure, enthalpy) and correspondingly different cells are used for making the macroscopic balances.

With reference to Fig. 2, taken from reference /2/, we consider the following control volumes. The control cells are bounded in radial direction by planes parallel to the bundle z axis through the pin axes. Let Δr be the distance between the internal and external bounding planes, i.e. the width of the hexagonal ring. Planes perpendicular to the z axis define the following control cells of length Δz in the axial direction:

- Control volume V_I is bounded in axial direction by two planes perpendicular to the bundle z axis and a distance Δz apart, in radial direction by planes through the pin axes. This control cell is used for volume-averaging the coolant energy equation, and the continuity equation.

- Control volume V_{II} is obtained by displacing V_I by $\Delta r/2$ in radial direction. It is therefore bounded in the radial direction by planes parallel to the bundle axis passing midway between the pin axes. This control cell is used for volume - averaging the radial component of the coolant momentum equation.

- Control volume V_{III} is obtained by displacing V_I by $\Delta z/2$ in axial direction. It is used for volume - averaging the axial component of the coolant momentum equation.

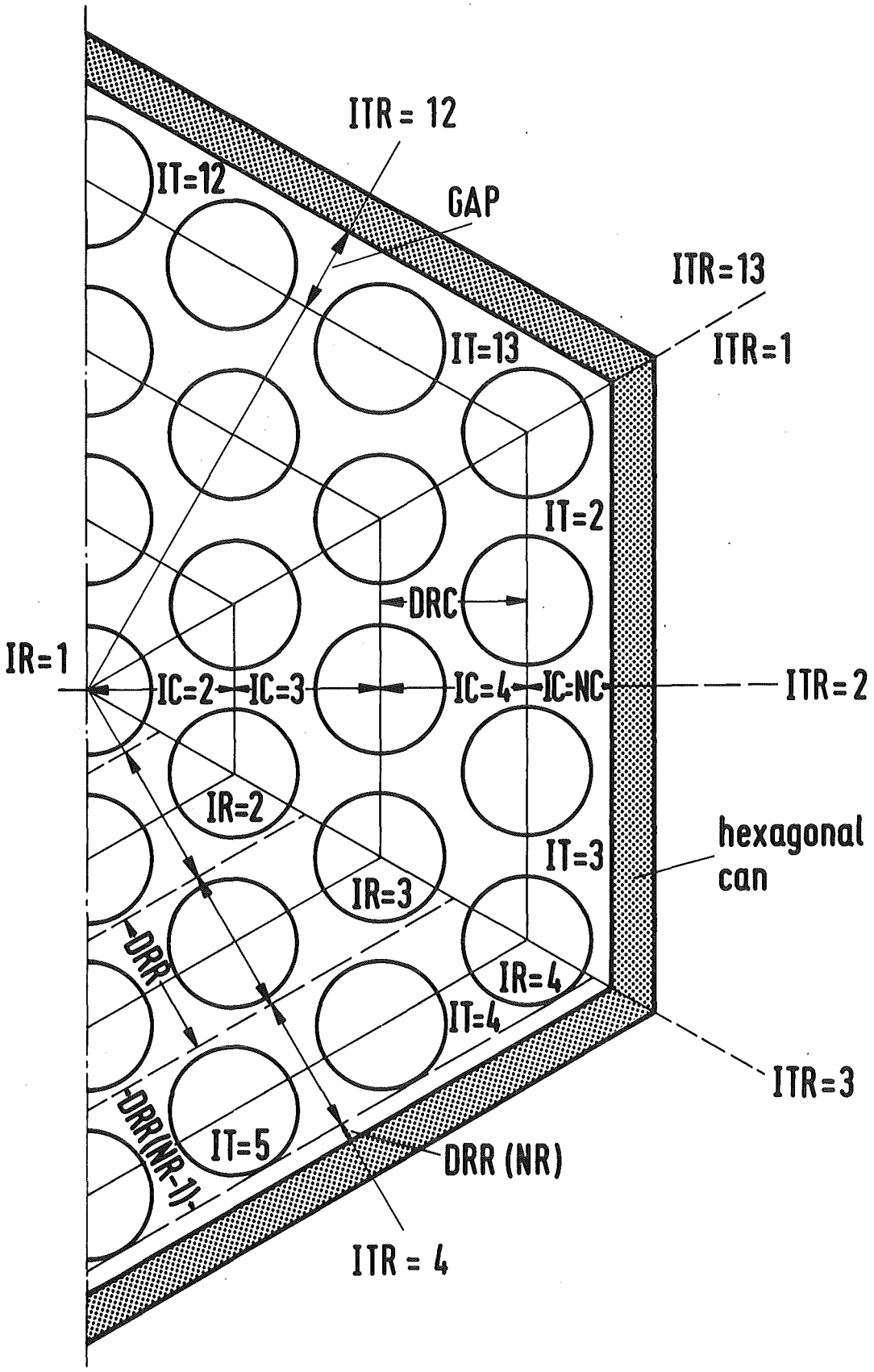

Fig. 1: Indexing of control cells in radial and azimuthal directions

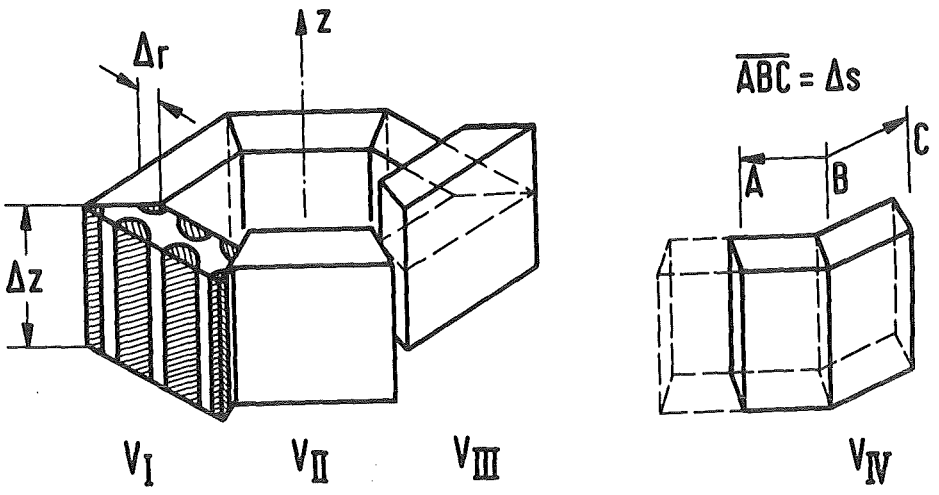

Fig. 2a

Fig. 2: Control volumes used for macroscopic balances

Fig. 2a) Perspective view

V_I for the energy equation

V_{II} for the radial component of the momentum equation

V_{III} for the axial component of the momentum equation

V_{IV} for the azimuthal component of the momentum equation

Fig. 2b) Cross section

$2b_1$) V_I, V_{III} centred or axially displaced control volume

$2b_2$) V_{II} radially displaced control volume

$2b_3$) V_{IV} control volume displaced in the azimuthal negative direction

$2b_4$) V_{IV} control volume displaced in the azimuthal positive direction

Fig. 2b) Cross section

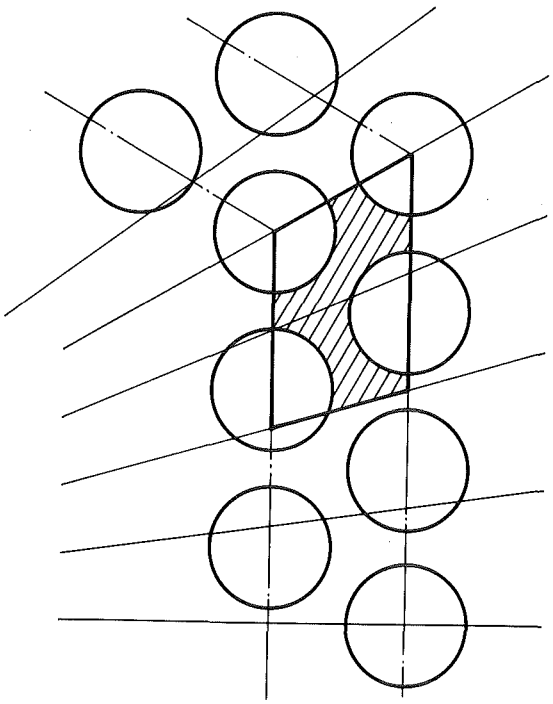

Fig. $2b_1$) V_I, V_{III} centred or axially displaced control volume

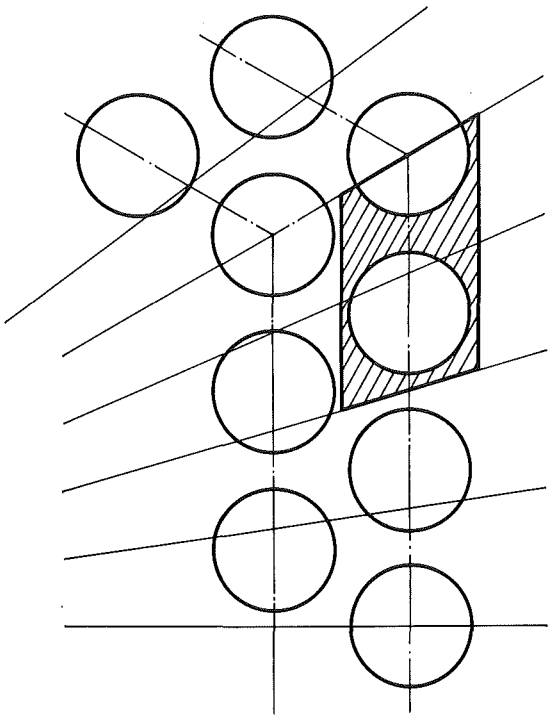

Fig. $2b_2$) V_{II} radially displaced control volume

Fig. 2b) Cross section

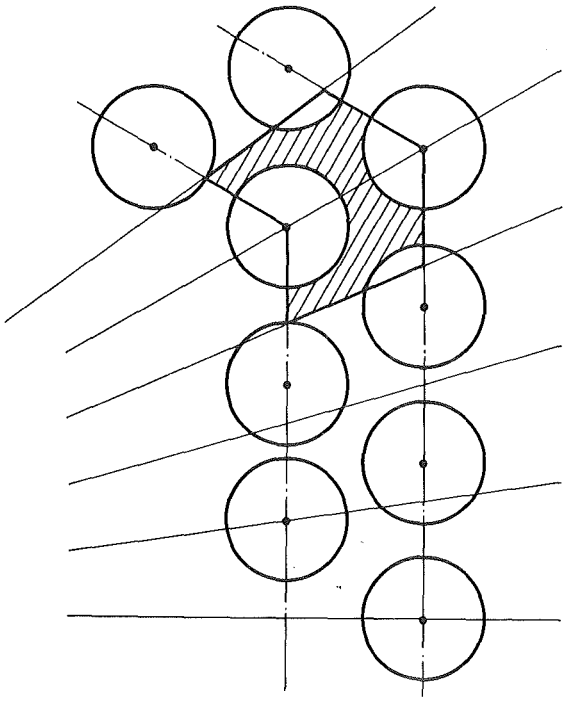

Fig. $2b_3$) V_{IV} control volume displaced in the azimuthal negative direction

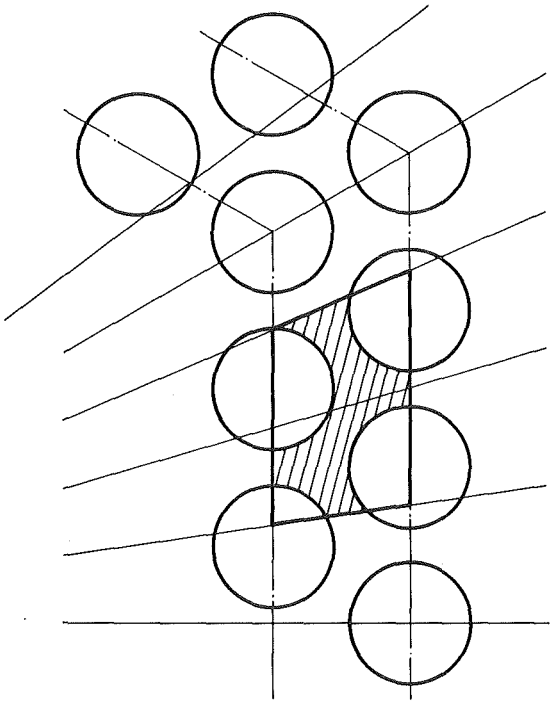

Fig. $2b_4$) V_{IV} control volume displaced in the azimuthal positive direction

Control volumes V_I to V_{III} are bounded in the azimuthal direction by two planes passing through the bundle axis and forming an angle of 30 degrees. One of these planes is perpendicular to the hexagonal can, the other passes through the axis of a corner pin. The full bundle is thus divided azimuthally into twelve sectors.

- Control volume V_{IV} is obtained by taking the two adjacent halves of cells like V_I. V_{IV} is used for volume-averaging the azimuthal component of the coolant momentum equation.

1.2 Indexing conventions

Following conventions are adopted for indexing the control cells:

- Axial direction. Index JC = 2, 3, ... MC denotes the control volumes V_I of length Δz = DZC (JC). Control volumes V_{III}, displaced by $\pm\Delta z/2$ are indexed by JZ = 2, 3, ... MZ.

  Meshes JC = 2 ÷ MC and JZ = 2 ÷ MZ correspond to physical partitions of the bundle in axial direction. Meshes JC = 1 and JC = MC + 1 are dummy meshes used for introducing boundary conditions.

- Radial direction. Index IC = 2, 3, ... NC denotes the control volumes V_I. IC = 2 refers to the inner hexagonal control volume; IC = NC is the control volume bounded externally by the hexagonal can and internally by a plane through the axes of the outermost pins. Meshes IC = 1 and IC = NC + 1 are dummy meshes used for introducing boundary conditions.

Index IR = 1,2, ... NR refers to the control volumes V_{II}. IR = 1 is a mesh centred on the axis of the central pin with width $\Delta r/2$. IR = NR is the control volume bounded externally by the hexagonal can and internally by a plane tangent to the outermost pins.

- Azimuthal direction. Index IT = 2, 3, ... NTH = 13 refers to the twelve azimuthal sectors bounded by planes passing through the bundle axis and forming 30 degrees angles. Index ITR = 1, 2 ... 13 denotes these planes (planes ITR = 1 and ITR = 13 coincide). Meshes IT = 1 and IT = NTH + 1 are dummy meshes used for deriving boundary conditions when integrating with the ADI method along the azimuthal direction.

Control cells and indexing conventions are shown in Fig. 1 for the case of a 37-pin bundle.

(IC, JC, IT) is indexed as node (i, j, k). The cells faces are indexed as $i \pm 1/2$, $j \pm 1/2$, $k \pm 1/2$ respectively.

1.3 Definition of dependent variables

According to the ICE technique, described in section C.2.1, space discretization of the conservation equations describing the fluid flow is done with reference to staggered meshes. Scalar quantities, like coolant pressure, enthalpy and other physical properties of the fluid, are defined at the centre point (i, j, k) of a control volume. Velocity components of the coolant (u, w, v for the r, z, s directions respectively) are defined at the mid points of the boundary faces. These conventions are shown in Fig. 3.

1.4 Volume Porosity and Surface Permeabilities

All cells are characterized by a total volume V, a volume occupied by the fluid V_f, an area A_w of the solid (wall)-fluid interfaces, by the areas of the lateral faces, S_t, S_b, (top, bottom, perpendicular to the z axis of the bundle), S_i, S_e (internal, external, perpendicular to the radial coordinate r), S_m, S_p (bounding the cell in the azimuthal direction, where the subscripts m (minus), p (plus) denote the sequence considered in the positive clockwise direction). These geometrical elements are used to define volumetric porosities and surface permeabilities for every cell.

Let S_{f_t}, S_{f_b}, S_{f_i}, S_{f_e}, S_{f_m}, S_{f_p} be the flow areas of the bounding faces. We define the surface permeabilities as ratios of the flow areas to the total areas, i.e.:

$\varepsilon_t = S_{f_t}/S_t$ Surface permeability at the top cross section (1)

$\varepsilon_b = S_{f_b}/S_b$ Surface permeability at the bottom cross section (2)

$\psi_i = S_{f_i}/S_i$ Surface permeability at the inner cross section (3)

$\psi_e = S_{f_e}/S_e$ Surface permeability at the outer cross section (4)

$\xi_m = S_{f_m}/S_m$ Surface permeability at the azimuthal left cross section (5)

$\xi_p = S_{f_p}/S_p$ Surface permeability at the azimuthal right cross section (6)

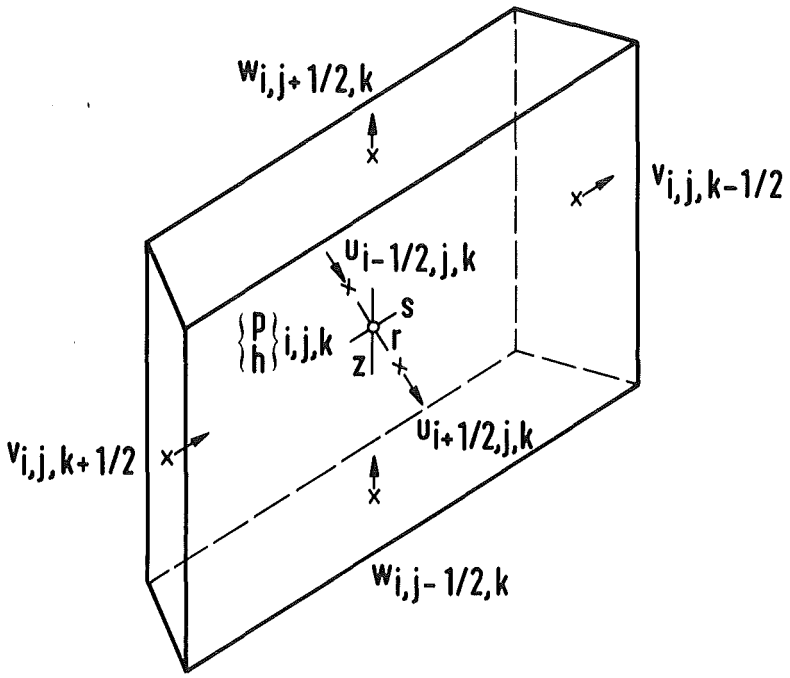

Fig. 3: Definition of velocity components and scalar quantities on staggered meshes

The volume porosity of a cell is defined as the ratio of the volume occupied by the fluid to the total cell volume, i.e.:

$$\varepsilon = V_f/V \tag{7}$$

In an undisturbed geometry the volume porosity is equal to the surface permeabilities in the axial direction:

$$\varepsilon = \varepsilon_t = \varepsilon_b \tag{8a}$$

or

$$V_f/V = S_{f_t}/S_t = S_{f_b}/S_b \tag{8b}$$

The definition of the surface permeabilities for the radial direction is shown in detail in Fig. 4 with reference to the centred cells V_I and to the displaced cells V_{II}. The following nomenclature has been adopted:

a) Centred cells V_I

$$\Psi_i = \text{PSI (IC)} \tag{9}$$

b) Displaced cells V_{II}

$$\Psi_{i+1/2} = \text{PSIR (IR)} \tag{10}$$

where index i denotes the node at the centre of control volume V_I and $i \pm 1/2$ refer to its radial boundary faces.

In the volume averaged conservation equations one must consider the surface to volume ratios. With reference to Fig. 5 these ratios are obtained for the radial direction as follows:

a) Centred cells V_I (Control volume (ABFE) $\cdot \Delta z$)

Inner surface $S_i = EA \cdot \Delta z = (EC - AC) \cdot \Delta z = \left(\Delta s - \frac{\sqrt{3}}{6}\Delta r\right)\Delta z$ (11)

outer surface $S_e = FB \cdot \Delta z = (FD + DB) \cdot \Delta z = \left(\Delta s + \frac{\sqrt{3}}{6}\Delta r\right)\Delta z$ (12)

with $\Delta s = MN$ (13)

The radial surface to volume ratios are then

$$\frac{S_i}{V} = \frac{\left(\Delta\vartheta - \frac{\sqrt{3}}{6}\Delta r\right)\Delta z}{\Delta r \cdot \Delta\vartheta \cdot \Delta z} = \frac{\left(1 - \frac{\sqrt{3}}{6}\right)\frac{\Delta r}{\Delta\vartheta}}{\Delta r} = \frac{FACCM(IC)}{\Delta r} = \frac{S_i / S_{mi}}{\Delta r} \qquad (14)$$

$$\frac{S_e}{V} = \frac{\left(\Delta\vartheta + \frac{\sqrt{3}}{6}\Delta r\right)\Delta z}{\Delta r \cdot \Delta\vartheta \cdot \Delta z} = \frac{\left(1 + \frac{\sqrt{3}}{6}\right)\frac{\Delta r}{\Delta\vartheta}}{\Delta r} = \frac{FACCP(IC)}{\Delta r} = \frac{S_e / S_{mi}}{\Delta r} \qquad (15)$$

with $$FACCM(IC) = \left(1 - \frac{\sqrt{3}}{6}\right)\frac{\Delta r}{\Delta\vartheta} = S_i / S_{mi} \qquad (16)$$

$$FACCP(IC) = \left(1 + \frac{\sqrt{3}}{6}\right)\frac{\Delta r}{\Delta\vartheta} = S_e / S_{mi} \qquad (17)$$

b) Displaced cells V_{II} (Control volume (MNVT)$\cdot\Delta z$)

Inner surface $$S_{mi} = MN \cdot \Delta z = (FB - DB)\,\Delta z = \left(FB - \frac{\sqrt{3}}{6}\Delta r\right)\Delta z \qquad (18)$$

outer surface $$S_{me} = TV \cdot \Delta z = (FB + HV)\,\Delta z = \left(FB + \frac{\sqrt{3}}{6}\Delta r\right)\Delta z \; ; \qquad (19)$$

with $$FB = \frac{\Delta s}{12} + \frac{\Delta r}{2\sqrt{3}} \qquad (20)$$

one has

$$\frac{S_{mi}}{V} = \frac{1}{\Delta r}\left(1 - \frac{6\Delta r}{\sqrt{3}\cdot PFC(IC) + 6\Delta r}\right) = \frac{FACRM(IR)}{\Delta r} = \frac{S_{mi} / S_e}{\Delta r} \qquad (21)$$

$$\frac{S_{me}}{V} = \frac{1}{\Delta r}\left(1 + \frac{6\Delta r}{\sqrt{3}\cdot PFC(IC) + 6\Delta r}\right) = \frac{FACRP(IR)}{\Delta r} = \frac{S_{me} / S_e}{\Delta r} \qquad (22)$$

where

$$FACRM(IR) = 1 - \frac{6\Delta r}{\sqrt{3}\cdot PFC(IC) + 6\Delta r} = S_{mi} / S_e \qquad (23)$$

$$FACRP(IR) = 1 + \frac{6\Delta r}{\sqrt{3}\cdot PFC(IC) + 6\Delta r} = S_{me} / S_e = \qquad (24)$$

$$= 2 - FACRM(IR) \, .$$

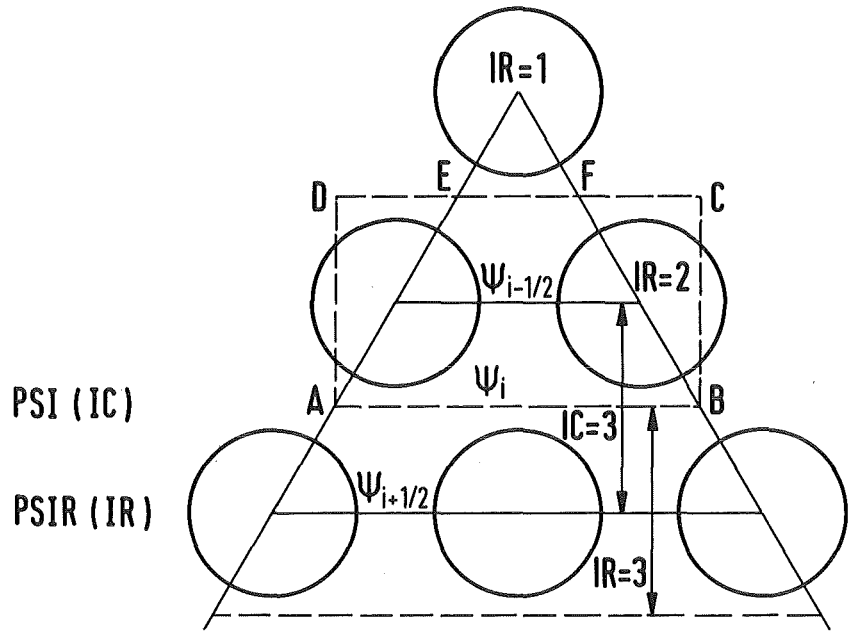

Fig. 4: Definition of radial surface permeabilities

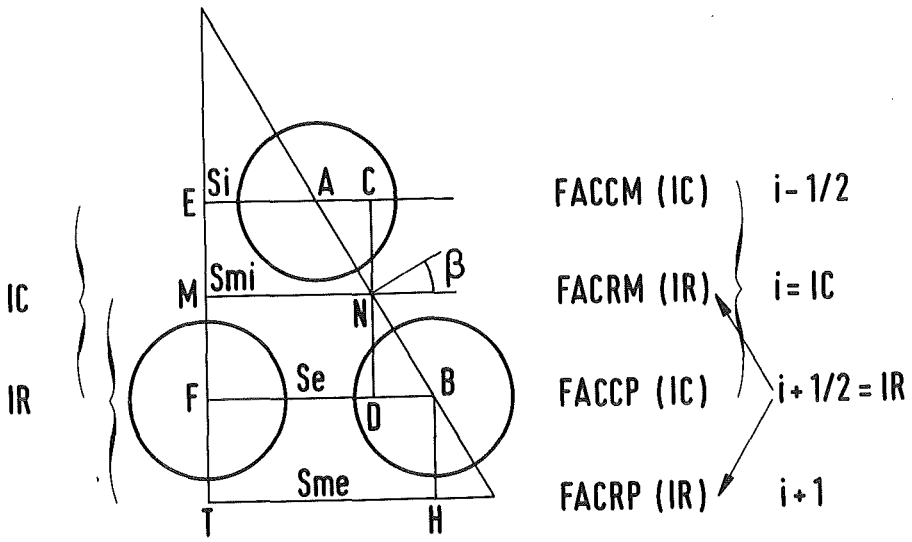

Fig. 5: Definition of geometry coefficients

2. Fuel pin model and structure

Every control volume V_I of the bundle is associated to an equivalent fuel pin with geometrical data corresponding to those of the real pins. Fig. 6a shows the fractions of the fuel pins associated to the control volume ABCD which are considered for defining the equivalent pin of Fig. 6b. Its configuration corresponds to the geometry of the SNR type reactor having a lower fission gas plenum. The pin consists of a heating element (fuel or electrical heater), and a cladding, separated from the fuel by a gap of given width. The coolant temperature in the cell considered is used as boundary condition for the calculation of the temperature distribution in the pins. For the outermost control volumes the structural material of the hexagonal can is taken into consideration in a similar manner.

In fuel, clad and structure only radial heat conduction is considered. Heat conduction in the coolant is negligible compared to convective heat transfer which affords the coupling between the axial meshes of the channel. Within an axial mesh up to 6 nodes are considered in radial direction in the fuel, 3 nodes in the clad, and 1 for the structural material. The one-dimensional heat conduction equations are solved rigorously for fuel and clad with reference to an axisymmetrical cylindrical coordinate system centred on the fuel pin axis, while the assumption of a linear temperature profile in the structure is made. The structure outer surface can be considered either as adiabatic or as transfering heat to the outer medium, the latter being normally required for the theoretical interpretation of experiments.

The transient calculation of temperature distributions in the pin is carried out for fuel, clad and structure by discretizing the radial heat conduction equations with a half-implicit (Crank-Nicolson) scheme and solving them numerically by means of direct inversion of a three-diagonal matrix. The heat flux beyond the structure outer surface is assumed as boundary condition. The fuel-clad gap conductance, which depends on the gap width and on the composition of the filling gas, influences strongly the fuel temperature distribution, and is calculated in a user written subroutine.

The gradient of the calculated temperature distribution at the clad outer surface is then used to compute the new heat fluxes into the coolant which represent the coupling between the thermal hydraulic calculation and the fuel pin model. These heat fluxes are not updated during the iteration steps necessary for the thermal-hydraulic calculation (see section C 2.4) but are kept constant up to next time step.

Fig. 6a

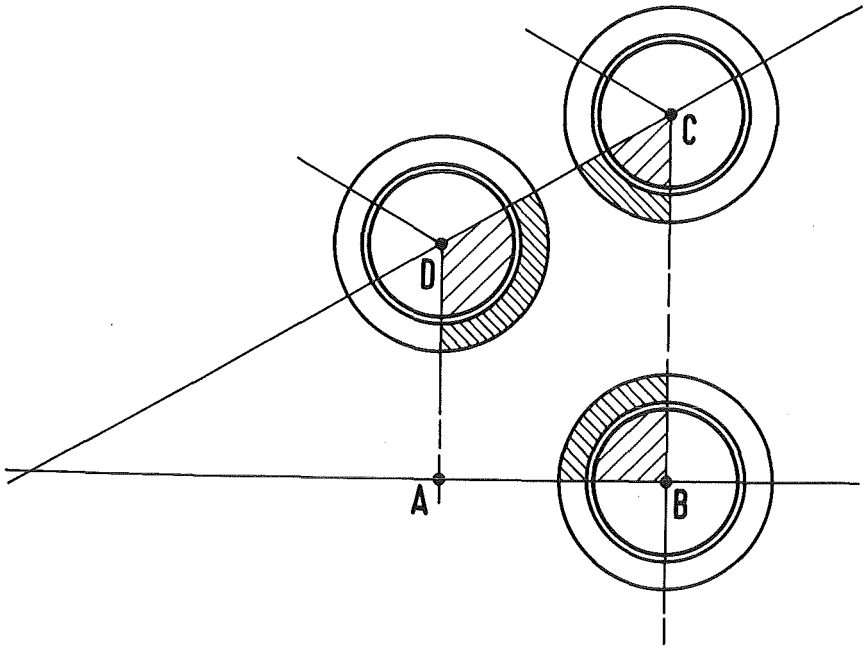

Fig. 6b

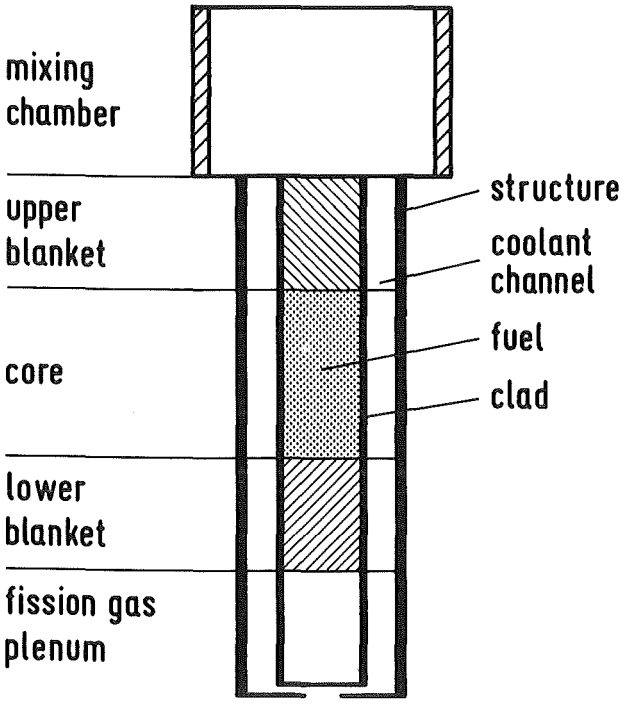

Fig. 6:
Geometrical configuration of an equivalent fuel pin associated to control volumes used for thermal-hydraulic calculation. The structure (hexagonal can) is present only for the outermost control volumes of the bundle.

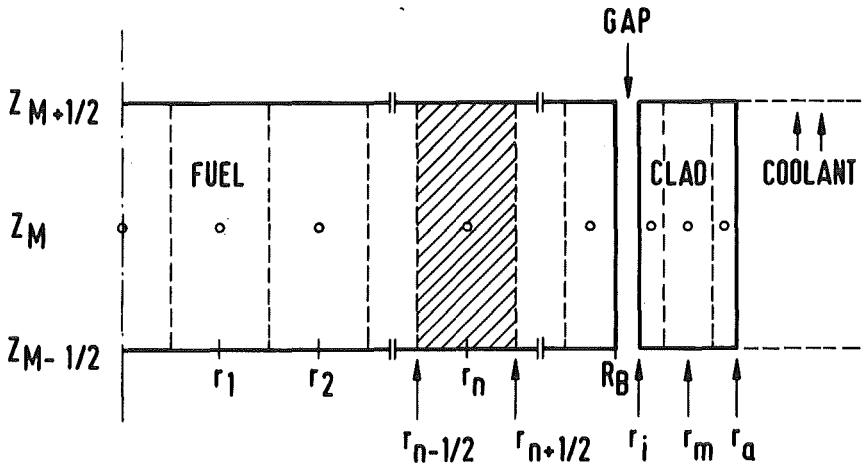

Fig. 7: Definition of radial control volumes in an axial mesh of fuel and cladding.

B) Basic Equations

1) Conservation equations for three-dimensional thermal hydraulic description of single-phase coolant flow

1.1 Conservation equations in local form

The three-dimensional single phase flow of the coolant can be described in the local form by the following equations.

i) Continuity equation

$$\frac{\partial \rho}{\partial t} + \nabla \cdot \rho \vec{V} = 0 \qquad \vec{V} = (u,w,v) \qquad (1)$$

ii) Momentum equation

$$\frac{\partial}{\partial t} (\rho \vec{V}) + \nabla \cdot \rho \vec{V}\vec{V} = \nabla \cdot (\mu \nabla \vec{V}) - \nabla p + \rho \vec{g} - \vec{D}_o \qquad (2)$$

which is equivalent to the three scalar equations for axial, radial and azimuthal directions, respectively:

$$\frac{\partial (\rho w)}{\partial t} + \nabla \cdot (\rho w \vec{V}) = \nabla \cdot (\mu \nabla w) - \frac{\partial p}{\partial z} - \rho g - \vec{D}_o \cdot \vec{n}_z \qquad (2a)$$

$$\frac{\partial}{\partial t} (\rho u) + \nabla \cdot (\rho u \vec{V}) = \nabla \cdot (\mu \nabla u) - \frac{\partial p}{\partial r} - \vec{D}_o \cdot \vec{n}_r \qquad (2b)$$

$$\frac{\partial}{\partial t} (\rho v) + \nabla \cdot (\rho v \vec{V}) = \nabla \cdot (\mu \nabla v) - \frac{\partial p}{\partial s} - \vec{D}_o \cdot \vec{n}_s \qquad (2c)$$

iii) Energy equation

$$\frac{\partial}{\partial t} (\rho h) + \nabla \cdot \rho h \vec{V} = \nabla \cdot \rho \tilde{\alpha} \nabla h + Q \qquad (3)$$

where

D_o = drag force per unit volume at the fluid-solid interface $[kg/m^2s^2]$

g = gravity acceleration $[m/s^2]$

h = specific coolant enthalpy $[J/kg]$

n = unit vector

p = static pressure $[N/m^2]$

Q = source of power supplied to the coolant $[W/m^3]$

r = radial coordinate $[m]$

s = azimuthal coordinate $[m]$

t = time $[s]$

u = radial component of coolant velocity $[m/s]$

v = azimuthal component of coolant velocity $[m/s]$

$\bar{V}$ = coolant velocity (vector) $[m/s]$

w = axial component of coolant velocity $[m/s]$

z = axial coordinate, main flow direction $[m]$

$\tilde{\alpha}$ = effective thermal diffusivity (taking into account both molecular and turbulent diffusivities) $[m^2/s]$

μ = effective dynamic viscosity $[kg/m\ s]$

ρ = coolant density $[kg/m^3]$

Remark:

The "radial" and "azimuthal" components are referred for convenience to a local cartesian coordinate system.
The effective thermal diffusivity $\tilde{\alpha}$ and the effective dynamic viscosity μ are calculated taking into account both the molecular and the turbulent contributions. Details of these calculations are given in sections C 5.2 and C 5.3, respectively.

1.2 Conservation equations averaged over the control volumes

The conservation equations for mass, momentum and energy are integrated over appropriate control volumes and transformed into "volume-averaged" equations using a staggered mesh. The control volumes used are V_I to V_{IV} as defined in section A 1.1.

Volume integrals are transformed into surface integrals by means of the Gauss theorem, time derivatives of volume integrals by means of the Leibniz theorem. The most general form of these theorems for a single phase fluid is reported hereafter. It is derived from the two-phase flow equations given in reference /6/.

Consider a volume of fluid V_f delimited by wall surfaces S_w and interfaces S_i which in the most general case separate the fluid from another medium. In general the positions of the interfaces are time dependent. Their rate of displacement be v_i; $\bar{n}$ be the normal vector of a surface directed outwards.

a) The Leibniz theorem states that for any scalar function f

$$\frac{\partial}{\partial t}\int_{V_f} f \, dV = \int_{V_f} \frac{\partial f}{\partial t} \, dV + \int_{S_i} f \, \bar{v}_i \cdot \bar{n} \, dS \tag{4}$$

b) The Gauss theorem for a vector or tensor $\bar{B}$ is

$$\int_{V_f} \nabla \cdot \bar{B} \, dV = \int_{S_i} \bar{B} \cdot \bar{n} \, dS + \int_{S_w} \bar{B} \cdot \bar{n} \, dS \tag{5}$$

When the interfaces S_i are fixed the Leibniz theorem becomes

$$\frac{\partial}{\partial t}\int_{V_f} f \, dV = \int_{V_f} \frac{\partial f}{\partial t} \, dV \tag{6}$$

In general the interfaces consist of several parts; (e.g. of top and bottom surfaces S_1 and S_2 normal to the z-axis and of side surfaces S_s) therefore the surface integral has to be taken over all parts, i.e.

$$\int_{S_i} \bar{B} \cdot \bar{n} \, dS = \int_{S_1} \bar{B} \cdot \bar{n} \, dS + \int_{S_2} \bar{B} \cdot \bar{n} \, dS + \int_{S_s} \bar{B} \cdot \bar{n} \, dS \tag{7}$$

which can also be written as

$$\int_{S_i} \bar{B} \cdot \bar{n} \, dS = \frac{\partial}{\partial z} \int_{V_f} B_z \, dV + \int_{S_s} \bar{B} \cdot \bar{n} \, dS \qquad (8)$$

where B_z is the z-component of $\bar{B}$.

i) Continuity equation

We refer to the control volume V_I of Fig. 2 and use the indices t, b, e, i, p, m to denote the boundary surfaces (S): top, bottom (z direction), external, internal (r direction) plus, minus (for the positive-clockwise- and negative azimuthals directions) respectively. Let V be the total volume of the control cell and V_f be the volume of the fluid in it (index f refers to the fluid).

It holds

$$\begin{aligned} V = \Delta z \cdot \Delta \vartheta \cdot \Delta z &= S_t \, \Delta z = S_b \, \Delta z \\ &= \Delta z \, (S_i + S_e)/2 = \Delta z \, S_{ie/2} \\ &= S_p \, (\cos\beta)_p \, \Delta \vartheta = S_m \, (\cos\beta)_m \, \Delta \vartheta \end{aligned} \qquad (9)$$

with $S_{ie/2} = (Si+Se)/2$. The angle β is defined as shown in Fig. 5.

Integrating equation (1) over the volume V_f of the fluid in the control cell gives

$$\int_{V_f} \frac{\partial \varrho}{\partial t} \, dV + \int_{V_f} \operatorname{div} (\varrho \bar{V}) \, dV = 0 \qquad (10)$$

Applying the Leibniz and Gauss theorems and introducing the velocity components yields

$$\begin{aligned} &\frac{\partial}{\partial t} \int_{V_f} \varrho \, dV + \int_{S_{ft}} \varrho w \, dS - \int_{S_{fb}} \varrho w \, dS + \\ &+ \int_{S_{fe}} \varrho u \, dS - \int_{S_{fi}} \varrho u \, dS + \int_{S_{fp}} \varrho v \, dS - \int_{S_{fm}} \varrho v \, dS = 0 \end{aligned} \qquad (11)$$

We introduce the following definitions of volume and surface averaged quantities for any scalar function f:

$$\langle f \rangle_3 = \frac{1}{V_f} \int_{V_f} f \, dV \tag{12}$$

$$\langle f \rangle = \frac{1}{S_f} \int_{S_f} f \, dS \tag{13}$$

By means of (9), (12), (13) and the definitions of the porosity and permeability équation (11) becomes:

$$\varepsilon \frac{\partial \langle \rho \rangle_3}{\partial t} + \frac{\varepsilon}{\Delta z} \left[\langle \rho w \rangle_t - \langle \rho w \rangle_b \right] + \frac{1}{\Delta z} \left[\psi_e F_e \langle \rho u \rangle_e - \psi_i F_i \langle \rho u \rangle_i \right] + \\ + \frac{1}{\Delta s} \left[\frac{\varepsilon_p}{(\omega \beta)_p} \langle \rho v \rangle_p - \frac{\varepsilon_m}{(\omega \beta)_m} \langle \rho v \rangle_m \right] = 0 \tag{14}$$

with $F_e = S_e / S_{w/z}$ (14b)

$F_i = S_i / S_{i/z}$ (14c)

This is the volume-averaged continuity equation. It is combined with the volume-averaged momentum equations to derive a discrete Poisson-like equation, as explained in section C. 2.1

ii) Momentum equations

a) Axial momentum equation

Integration of eq. (2a) over the volume V_f of the fluid in the control cell yields

$$\int_{V_f} \frac{\partial \rho w}{\partial t} dV + \int_{V_f} \operatorname{div} (\rho w \bar{v}) \, dV = \int_{V_f} \operatorname{div} (\mu \bar{\nabla} w) \, dV + \\ - \int_{V_f} \frac{\partial p}{\partial z} dV - g \int_{V_f} \rho \, dV - \int_{V_f} \bar{D}_o \cdot \bar{m}_z \, dV \tag{15}$$

By means of the Leibniz and Gauss theorems one has

$$\frac{\partial}{\partial t}\int_{V_f} \rho w \, dV + \int_{S_{ft}} (\rho w) w \, dS - \int_{S_{fb}} (\rho w) w \, dS + \int_{S_{fe}} (\rho w) u \, dS +$$

$$- \int_{S_{fi}} (\rho w) u \, dS + \int_{S_{fp}} (\rho w) v \, dS - \int_{S_{fm}} (\rho w) v \, dS = \qquad (16)$$

$$= \int_{S_{ft}} \mu \frac{\partial w}{\partial z} \, dS - \int_{S_{fb}} \mu \frac{\partial w}{\partial z} \, dS + \int_{S_{fe}} \mu \frac{\partial w}{\partial r} \, dS - \int_{S_{fi}} \mu \frac{\partial w}{\partial r} \, dS +$$

$$+ \int_{S_{fp}} \mu \frac{\partial w}{\partial s} \, dS - \int_{S_{fm}} \mu \frac{\partial w}{\partial s} \, dS +$$

$$- \int_{S_{ft}} p \, dS + \int_{S_{fb}} p \, dS - g \int_{V_f} \rho \, dV - \int_{V_f} \bar{D}_o \cdot \bar{n}_z \, dV$$

Letting $D = D_o \cdot V_f / S_w$, a similar treatment as for the continuity equation leads to

$$\varepsilon \frac{\partial}{\partial t} \langle \rho w \rangle_3 + \frac{\varepsilon}{\Delta z} \left[\langle \rho w^2 \rangle_t - \langle \rho w^2 \rangle_b \right] + \frac{1}{\Delta r} \left[\psi_e F_e \langle \rho w u \rangle_e - \psi_i F_i \langle \rho w u \rangle_i \right] +$$

$$+ \frac{1}{\Delta s} \left[\frac{\varepsilon_p}{(\cos\beta)_p} \langle \rho w v \rangle_p - \frac{\varepsilon_m}{(\cos\beta)_m} \langle \rho w v \rangle_m \right] =$$

$$= \frac{\varepsilon}{\Delta z} \left[\langle \mu \frac{\partial w}{\partial z} \rangle_t - \langle \mu \frac{\partial w}{\partial z} \rangle_b \right] + \frac{1}{\Delta r} \left[\psi_e F_e \langle \mu \frac{\partial w}{\partial r} \rangle_e - \psi_i F_i \langle \mu \frac{\partial w}{\partial r} \rangle_i \right] + \qquad (17)$$

$$+ \frac{1}{\Delta s} \left[\frac{\varepsilon_p}{(\cos\beta)_p} \langle \mu \frac{\partial w}{\partial s} \rangle_p - \frac{\varepsilon_m}{(\cos\beta)_m} \langle \mu \frac{\partial w}{\partial s} \rangle_m \right] +$$

$$+ \frac{\varepsilon}{\Delta z} \left[- \langle p \rangle_t + \langle p \rangle_b \right] - \varepsilon g \langle \rho \rangle_3 - \frac{S_w}{V} \langle \bar{D} \cdot \bar{n}_z \rangle_w$$

Eq. (17) is the volume-averaged axial momentum equation.

b) Radial momentum equation

Integration of eq. (2b) over the volume V_f of the fluid in the control cell yields, with the same procedure as for equations (15) to (17):

$$\varepsilon \frac{\partial}{\partial t}\langle \rho u\rangle_3 + \frac{\varepsilon}{\Delta z}\left[\langle \rho u w\rangle_t - \langle \rho u w\rangle_b\right] + \frac{1}{\Delta r}\left[\psi_e F_e \langle \rho u^2\rangle_e - \psi_i F_i \langle \rho u^2\rangle_i\right] +$$

$$+ \frac{1}{\Delta s}\left[\frac{\varepsilon_p}{(\cos\beta)_p}\langle \rho u v\rangle_p - \frac{\varepsilon_m}{(\cos\beta)_m}\langle \rho u v\rangle_m\right] = \qquad (18)$$

$$= \frac{\varepsilon}{\Delta z}\left[\langle \mu \frac{\partial u}{\partial z}\rangle_t - \langle \mu \frac{\partial u}{\partial z}\rangle_b\right] + \frac{1}{\Delta r}\left[\psi_e F_e \langle \mu \frac{\partial u}{\partial r}\rangle_e - \psi_i F_i \langle \mu \frac{\partial u}{\partial r}\rangle_i\right] +$$

$$+ \frac{1}{\Delta s}\left[\frac{\varepsilon_p}{(\cos\beta)_p}\langle \mu \frac{\partial u}{\partial s}\rangle_p - \frac{\varepsilon_m}{(\cos\beta)_m}\langle \mu \frac{\partial u}{\partial s}\rangle_m\right] +$$

$$+ \frac{1}{\Delta r}\left[-\langle p\rangle_e + \langle p\rangle_i\right] - \frac{S_w}{V}\langle \bar{D}\cdot \bar{n}_r\rangle_w$$

c) Azimuthal momentum equation

Integration of (2c) over the volume V_f gives similarly:

$$\varepsilon \frac{\partial}{\partial t}\langle \rho v\rangle_3 + \frac{\varepsilon}{\Delta z}\left[\langle \rho v w\rangle_t - \langle \rho v w\rangle_b\right] + \frac{1}{\Delta r}\left[\psi_e F_e \langle \rho v u\rangle_e - \psi_i F_i \langle \rho v u\rangle_i\right] +$$

$$+ \frac{1}{\Delta s}\left[\frac{\varepsilon_p}{(\cos\beta)_p}\langle \rho v^2\rangle_p - \frac{\varepsilon_m}{(\cos\beta)_m}\langle \rho v^2\rangle_m\right] =$$

$$= \frac{\varepsilon}{\Delta z}\left[\langle \mu \frac{\partial v}{\partial z}\rangle_t - \langle \mu \frac{\partial v}{\partial z}\rangle_b\right] + \frac{1}{\Delta r}\left[\psi_e F_e \langle \mu \frac{\partial v}{\partial r}\rangle_e - \psi_i F_i \langle \mu \frac{\partial v}{\partial r}\rangle_i\right] + \qquad (19)$$

$$+ \frac{1}{\Delta s}\left[\frac{\varepsilon_p}{(\cos\beta)_p}\langle \mu \frac{\partial v}{\partial s}\rangle_p - \frac{\varepsilon_m}{(\cos\beta)_m}\langle \mu \frac{\partial v}{\partial s}\rangle_m\right] +$$

$$+ \frac{1}{\Delta s}\left[\langle p\rangle_p - \langle p\rangle_m\right] - \frac{S_w}{V}\langle \bar{D}\cdot \bar{n}_s\rangle_w$$

iii) Energy equation

We integrate eq. (3) over the volume V of a control cell. Because the coolant density is not defined outside V_f, this is equivalent to integrate the first three terms over the volume V_f of the fluid:

$$\int_{V_f} \frac{\partial}{\partial t} \rho h \, dV + \int_{V_f} \operatorname{div}(\rho h \bar{V}) \, dV = \int_{V_f} \operatorname{div}(\rho \tilde{\alpha} \nabla h) \, dV + \int_V Q \, dV . \tag{20}$$

Applying the Leibniz and Gauss theorems one has

$$\begin{aligned} &\frac{\partial}{\partial t}\int_{V_f} \rho h \, dV + \int_{S_{ft}} \rho h w \, dS - \int_{S_{fb}} \rho h w \, dS + \int_{S_{fe}} \rho h u \, dS - \int_{S_{fi}} \rho h u \, dS + \\ &\quad + \int_{S_{fp}} \rho h v \, dS - \int_{S_{fm}} \rho h v \, dS = \\ &= \int_{S_{ft}} \rho \tilde{\alpha} \frac{\partial h}{\partial z} \, dS - \int_{S_{fb}} \rho \tilde{\alpha} \frac{\partial h}{\partial z} \, dS + \int_{S_{fe}} \rho \tilde{\alpha} \frac{\partial h}{\partial r} \, dS - \int_{S_{fi}} \rho \tilde{\alpha} \frac{\partial h}{\partial r} \, dS + \\ &\quad + \int_{S_{fp}} \rho \tilde{\alpha} \frac{\partial h}{\partial s} \, dS - \int_{S_{fm}} \rho \tilde{\alpha} \frac{\partial h}{\partial s} \, dS + \int_V Q \, dV . \end{aligned} \tag{21}$$

Introducing the definitions of volume porosity and surface permeabilities and using (12), (13) yields:

$$\begin{aligned} &\varepsilon \frac{\partial}{\partial t} \langle \rho h \rangle_3 + \frac{\varepsilon}{\Delta z}\left[\langle \rho h w \rangle_t - \langle \rho h w \rangle_b\right] + \frac{1}{\Delta r}\left[\psi_e F_e \langle \rho h u \rangle_e - \psi_i F_i \langle \rho h u \rangle_i\right] + \\ &+ \frac{1}{\Delta s}\left[\frac{\xi_p}{(\cos\beta)_p} \langle \rho h v \rangle_p - \frac{\xi_m}{(\cos\beta)_m} \langle \rho h v \rangle_m\right] = \\ &= \frac{\varepsilon}{\Delta z}\left[\langle \rho \tilde{\alpha} \frac{\partial h}{\partial z} \rangle_t - \langle \rho \tilde{\alpha} \frac{\partial h}{\partial z} \rangle_b\right] + \frac{1}{\Delta r}\left[\psi_e F_e \langle \rho \tilde{\alpha} \frac{\partial h}{\partial r} \rangle_e - \psi_i F_i \langle \rho \tilde{\alpha} \frac{\partial h}{\partial r} \rangle_i\right] + \\ &+ \frac{1}{\Delta s}\left[\frac{\xi_p}{(\cos\beta)_p} \langle \rho \tilde{\alpha} \frac{\partial h}{\partial s} \rangle_p - \frac{\xi_m}{(\cos\beta)_m} \langle \rho \tilde{\alpha} \frac{\partial h}{\partial s} \rangle_m\right] + \langle Q \rangle_3 \end{aligned} \tag{22}$$

Eq. (22) is the volume-averaged energy equation.

2) Equations for fuel pin and structural material

i) Fuel

The equations describing the space and time temperature distribution in the fuel are (without taking into account heat conduction in axial direction):

$$\frac{\partial}{\partial r}\left(\lambda_B \frac{\partial T_B}{\partial r}\right) + \frac{1}{r}\lambda_B \frac{\partial T_B}{\partial r} + q_B = \rho_B \, c_{p_B} \frac{\partial T_B}{\partial t} \qquad (r \neq 0) \qquad (1)$$

with the boundary condition

$$-\left(\lambda_B \frac{\partial T_B}{\partial r}\right)_{R_B^-} = \alpha_{BH} \left[T_B(t,R_B) - T_H(t,R_{Hi}) \right] \qquad (2)$$

and the initial condition

$$T_B(o,r) = T_{Bo}(r) \qquad (3)$$

On the fuel axis it holds:

$$2\lambda_B \frac{\partial^2 T_B}{\partial r^2} + q_B = \rho_B \, c_{p_B} \frac{\partial T_B}{\partial t} \qquad (r=0) \qquad (4)$$

with a symmetry condition

$$\left(\frac{\partial T_B}{\partial r}\right)_{r=0} = 0 \qquad (5)$$

In the above equations symbols are defined as follows:

c_{p_B} = fuel specific heat (J/kg°C)

q_B = specific power generated in the fuel (W/m^3)

r = radial coordinate (m)

R_B = fuel outer radius (m)

R_{Hi} = radius of the inner clad surface (m)

t = time (s)

T_B = fuel temperature (°C)

T_H = clad temperature (°C)

α_{BH} = fuel-clad heat transfer coefficient (W/m^2 °C)

λ_B = fuel thermal conductivity (W/m°C)

ρ_B = fuel density (kg/m^3)

ii) Cladding

The equation describing space and time temperature distribution in the clad is

$$\frac{\partial}{\partial r}\left(\lambda_H \frac{\partial T_H}{\partial r}\right) + \frac{1}{r}\lambda_H \frac{\partial T_H}{\partial r} + q_H = \rho_H c_{p_H} \frac{\partial T_H}{\partial t} \qquad (6)$$

with the boundary conditions

$$\alpha_{BH}\left[\bar{T}_B(t,R_B) - T_H(t,R_{Hi})\right] = -\left(\lambda_H \cdot \frac{\partial T_H}{\partial r}\right)_{R_{Hi}} \qquad (7)$$

$$-\left(\lambda_H \cdot \frac{\partial T_H}{\partial r}\right)_{R_{Ha}} = \alpha_{HK}\left[\bar{T}_H(t,R_{Ha}) - T_K(t)\right] \qquad (8)$$

and the initial condition

$$T_H(o,r) = T_{Ho}(r) \qquad (9)$$

Symbols are defined as follows:

c_{p_H} = specific heat of clad material (J/kg°C)

q_H = specific power generated in the clad (W/m^3)

R_B = fuel outer radius (m)

R_{Hi} = radius of inner clad surface (m)

R_{Ha} = radius of outer clad surface (m)

T_B = fuel temperature (°C)

T_H = clad temperature (°C)

T_K = coolant temperature (°C)

α_{BH}, α_{HK} = fuel-clad and clad-coolant heat transfer coefficients ($W/m^{2o}C$)

λ_H = thermal conductivity of clad material (W/m^oC)

ρ_H = density of clad material (kg/m^3)

iii) Structural material

Assuming the structural material of an axial mesh zone concentrated into one node, the equation describing the time dependence of its temperature is

$$\alpha_{KS} \frac{F_S}{V_S} \left[T_K(t) - T_S(t) \right] - \alpha_w \frac{F_w}{V_S} \left[T_S(t) - T_w(t) \right] + q_S(t) = \rho_S c_{pS} \frac{dT_S(t)}{dt} . \qquad (10)$$

The first two terms at the left side represent the boundary conditions, i.e. the energy transfer from coolant to the structure and from the structure surface to a surrounding medium (for instance to a by-pass flow with temperature $T_w(t)$).

In the above equation symbols are defined as follows:

c_{pS} specific heat of structure material (J/kg ^{o}C)

F_S inner surface of structure per unit axial length (m)

F_w outer surface of structure per unit axial length (m)

q_S energy produced in structural material per unit volume and time (W/m^3)

t time (s)

T_K coolant temperature (^{o}C)

T_S structure temperature (^{o}C)

T_w surrounding medium temperature (^{o}C)

V_S volume of structural material per unit axial length (m^2)

α_{KS} heat transfer coefficient coolant-structure (W/m^2 ^{o}C)

α_w heat transfer coefficient structure-surrounding medium (W/m^2 ^{o}C)

ρ_S density of structural material (kg/m^3)

C) Numerical treatment of the basic equations and programming details

1) Steady State Calculation BACCHUS-P

1.1 General

The transient two- or three-dimensional thermal-hydraulic calculations is preceeded by a steady state calculation which is performed in two steps:

a) a real steady state calculation carried out by solving a simplified set of conservation equations in a two-dimensional (r, z) geometry with a loose coupling of subchannels in the radial direction;

b) a transient calculation with constant boundary conditions, which therefore approaches eventually a steady state.

Step a) is considered as an initialization for step b) and allows reaching a convergence to the steady state after only a moderate number of time steps. At the end of step b) time is set to zero, and the real transient calculation with time dependent boundary conditions starts.

Step a) is performed with a programme package called BACCHUS-P which is documented in this section C.1. The basis of the thermal-hydraulic calculation is also reported in reference /1/. The conservation equations for mass, momentum and energy are solved in BACCHUS-P under the simplifying assumptions that

i) heat diffusion in axial direction is negligible

ii) the coolant pressure is uniform at an axial level of the bundle

iii) the radial coupling between control volumes is described by diffusive transport of momentum and enthalpy.

For a two-dimensional ($\mathcal{r}$, $\mathcal{z}$) geometry (see section C.3) the calculation made in BACCHUS-P yields a preliminary field of pressure, enthalpy and velocities (radial and axial) for the full bundle. In three-dimensional (r, z, s) geometry (section C.2) the BACCHUS-P calculation is done for every azimuthal sector; the azimuthal velocity components are initialized to zero.

1.2 Thermal-hydraulic calculation

1.2.1 Basic equations

The steady state calculation is performed by solving numerically the following system of simplified conservation equations:

i) Continuity equation

$$\frac{\partial}{\partial z}(\rho w) = - m' \qquad (1)$$

ii) Momentum equation

$$\frac{\partial}{\partial z}(\rho w^2) + \rho g + \frac{\partial p}{\partial z} = - f_w \frac{\rho w^2}{2 D_h} + \frac{\partial}{\partial r}\left(\mu \frac{\partial w}{\partial r}\right) \qquad (2)$$

iii) Energy equation

$$\frac{\partial}{\partial z}\left(\rho w h\right) - \frac{\partial w p}{\partial z} = q_w + \frac{\partial}{\partial r}\left(\rho \tilde{a} \frac{\partial h}{\partial r}\right) \qquad (3)$$

In equation (1) to (3) symbols are defined as follows

D_h = hydraulic diameter [m]

f_w = wall friction coefficient

g = gravity acceleration [m/s^2]

h = specific enthalpy [J/kg]

m' = mass flux in radial direction per unit length [kg/m^3 s]

p = pressure [N/m^2]

q_w = heat flux from wall to coolant per unit axial length [W/m^3]

$q_f = - \frac{\partial}{\partial r}(\rho \tilde{a} \frac{\partial h}{\partial r})$ = specific enthalpy exchange due to turbulent mixing per unit axial length [W/m^3]

r = radial coordinate [m]

u = radial component of velocity [m/s]

w = axial component of velocity [m/s]

z = axial coordinate [m]

$\tilde{\alpha}$ = $\lambda / \rho c_p$ = thermal diffusivity [m^2/s]

c_p = coolant specific heat at constant pressure [J/kg °C]

λ = coolant thermal conductivity [W/m °C]

μ = dynamic viscosity [kg/m s]

ρ = density [kg/m^3]

1.2.2 Conservation equations averaged over the control volumes

We consider a hexagonal ring-shaped control volume of lengths Δr, Δz in the radial and axial directions, respectively, and let be

S_t the area of the top cross section surface

S_b the area of the bottom cross section suface

S_i the area of the inner surface

S_e the area of the external surface

S_{ft} the cross flow area at the top section

S_{fb} the cross flow area at the bottom section

S_{fi} the cross flow area at the inner surface

S_{fe} the cross flow area at the external surface

ψ_i = S_{fi} /Si the radial permeability at the inner surface

ψ_e = S_{fe} /Se the radial permeability at the external surface

r_i = the distance of the inner surface from the bundle axis

r_e = the distance of the external surface from the bundle axis

V = $\Delta r \cdot \Delta z$ = the cell volume per unit length of the azimuthal direction

V_f = the cell volume occupied by the fluid

$\varepsilon = S_{f_t}/S_t = S_{f_b}/S_b = V_f/V$ the volume porosity.

It holds (for the unit length in the azimuthal direction)

$$V = \Delta r \cdot \Delta z = S_t \cdot \Delta z = S_b \cdot \Delta z \tag{4a}$$

$$\simeq S_i \cdot \Delta r \simeq S_e \cdot \Delta r \tag{4b}$$

i) Continuity equation

Integrating equation (1) over the volume of the fluid V_f and replacing the volume integral of the divergence term by surface integrals yields:

$$\int_{S_{ft}} \rho w \, dS - \int_{S_{fb}} \rho w \, dS = - \int_{S_f(r)} \int_{r_i}^{r_e} \dot{m}' \, dr \, dS \tag{5}$$

when $S_f(r)$ is the area of the hexagonal cylindrical surface parallel to the bundle axis.

Letting

$$\rho u = G_r = \int_{r_i}^{r_e} \dot{m}' \, dr \qquad \left[G_r \right] = \left[\mathrm{kg/m^2 s} \right] \tag{6}$$

and introducing surface averaged values at the top and bottom sections one has

$$S_{ft} \langle \rho w \rangle_t - S_{fb} \langle \rho w \rangle_b = - \int_{S_f(r)} G_r \, dS \tag{7}$$

Dividing by V and using

$$\begin{aligned} V_f = \varepsilon V &= \varepsilon S_t \Delta z = S_{f_t} \Delta z \\ &= \varepsilon S_b \Delta z = S_{f_b} \Delta z \end{aligned} \tag{8}$$

yields

$$\frac{\varepsilon}{\Delta z}\left[\langle \rho w\rangle_t - \langle \rho w\rangle_b\right] = -\frac{1}{V}\int_{S_f(x)} G_x \, dS \tag{9}$$

ii) Momentum equation

Integrating equation (2) over the volume of the fluid V_f and replacing the volume integrals of the divergence terms by surface integrals yields:

$$\int_{S_{ft}} \rho w^2 \, dS - \int_{S_{fb}} \rho w^2 \, dS + g\int_{V_f} \rho \, dV + \int_{S_{ft}} p \, dS - \int_{S_{fb}} p \, dS =$$

$$= -\int_{V_f} f_w \frac{\rho w^2}{2 D_h} \, dV + \frac{\partial}{\partial x}\int_{x_i}^{x_e}\int_{S_f(x)} \mu \frac{\partial w}{\partial x} \, dS \, dx \tag{10}$$

A similar treatment as for the continuity equation gives

$$S_{ft}\langle \rho w^2\rangle_t - S_{fb}\langle \rho w^2\rangle_b + g V_f \langle \rho\rangle_3 + S_{ft}\langle p\rangle_t - S_{fb}\langle p\rangle_b =$$

$$= -V_f\left\langle f_w \frac{\rho w^2}{2 D_h}\right\rangle_3 - S_{fe}\left\langle \mu \frac{\partial w}{\partial x}\right\rangle_e + S_{fi}\left\langle \mu \frac{\partial w}{\partial x}\right\rangle_i \tag{11}$$

when the symbol $\langle\ \rangle_3$ is used for volume averaged quantities.
Dividing by V, taking into account (8) and

$$V = S_e \cdot \Delta x = S_{fe} \cdot \Delta x \,/\, \psi_e$$

$$= S_i \cdot \Delta x = S_{fi} \cdot \Delta x \,/\, \psi_i \tag{12}$$

yields

$$\frac{\varepsilon}{\Delta z}\left[\langle \rho w^2\rangle_t - \langle \rho w^2\rangle_b\right] + \varepsilon g \langle \rho\rangle_3 + \frac{\varepsilon}{\Delta z}\left[\langle p\rangle_t - \langle p\rangle_b\right] =$$

$$= -\varepsilon \langle f_w \frac{\rho w^2}{2D_h}\rangle_3 + \left[\frac{\psi_e}{\Delta x}\langle \mu \frac{\partial w}{\partial x}\rangle_e - \frac{\psi_i}{\Delta x}\langle \mu \frac{\partial w}{\partial x}\rangle_i\right] \qquad (13)$$

iii) Energy equation

Integrating equation (3) over the volume of the fluid (and replacing the volume integrals of the divergence terms with surface integrals) yields:

$$\int_{S_{ft}} \rho w h \, dS - \int_{S_{fb}} \rho w h \, dS - \int_{S_{ft}} w p \, dS + \int_{S_{fb}} w p \, dS =$$

$$= \int_V q_w \, dV + \frac{\partial}{\partial x}\int_{x_i}^{x_e} \int_{S_f(x)} \rho \tilde{\alpha} \frac{\partial h}{\partial x} \, dS \, dx \qquad (14)$$

Using equations (4) and introducing surface and volume averaged values one has

$$S_{ft}\langle \rho w h\rangle_t - S_{fb}\langle \rho w h\rangle_b - S_{ft}\langle w p\rangle_t + S_{fb}\langle w p\rangle_b =$$

$$= V \langle q_w\rangle_3 + S_{fe}\langle \rho \tilde{\alpha} \frac{\partial h}{\partial x}\rangle_e - S_{fi}\langle \rho \tilde{\alpha} \frac{\partial h}{\partial x}\rangle_i \qquad (15)$$

Dividing by V, taking into account (8) and (12) yields

$$\frac{\varepsilon}{\Delta z}\left[\langle \rho w h\rangle_t - \langle \rho w h\rangle_b\right] - \frac{\varepsilon}{\Delta z}\left[\langle wp\rangle_t - \langle wp\rangle_b\right] = \langle q_w\rangle_3 + \left[\frac{\psi_e}{\Delta z}\langle \rho\tilde{\lambda}\frac{\partial h}{\partial z}\rangle_e - \frac{\psi_i}{\Delta z}\langle \rho\tilde{\lambda}\frac{\partial h}{\partial z}\rangle_i\right] \tag{16}$$

Equations (9), (13) and (16) are the basic volume averaged conservation equations which are solved numerically as explained hereafter.

1.2.3 Numerical solution of the volume-averaged conservation equations

i) Continuity equation

Let us refer to the control volume like that shown in Fig. 3, but dropping the azimuthal discretization. Let z_j be the axial level of mesh node (i,j) and $\Delta z_{j+1/2}$ be the distance between two consecutive axial nodes and V_{ij} the volume of the cell. Discretization of equation (9) yields

$$\frac{\varepsilon}{\Delta z_{j+1/2}}\left[\langle \rho w\rangle_{i,j+1} - \langle \rho w\rangle_{ij}\right] = -\frac{1}{V_{ij}}\left[M_{i+1/2,j+1} - M_{i-1/2,j+1}\right] \tag{17}$$

with the definition of mass flow

$$M(z) = S_f(z)\, G_z = S_f(z)\cdot \rho u \qquad [M] = [kg/s] \tag{18}$$

Using $\varepsilon/\Delta z = \frac{S_{ft}}{S_t \Delta z} = \frac{S_{ft}}{V}$ it yields (dropping the symbol $\langle\ \rangle$)

$$M_{i+1/2,j+1} = M_{i-1/2,j+1} - \left[\left(S_f \rho w\right)_{i,j+1} - \left(S_f \rho w\right)_{ij}\right] \tag{19}$$

which is used to calculate the radial mass flow under the simplifying assumption of an uniform radial pressure distribution.

ii) Momentum equation

Introducing the difference operator Δ_z by the definition

$$\Delta_z = \langle \phi \rangle_t - \langle \phi \rangle_b \tag{20}$$

for any scalar quantity ϕ, the first term of equation (13) can be written

$$\frac{\varepsilon}{\Delta z}\left[\langle \rho w^2 \rangle_t - \langle \rho w^2 \rangle_b\right] = \frac{\varepsilon}{\Delta z}\,\Delta_z \langle \rho w^2 \rangle . \tag{21}$$

We assume that for any two scalars ϕ_1, ϕ_2

$$\langle \phi_1 \cdot \phi_2 \rangle = \langle \phi_1 \rangle \cdot \langle \phi_2 \rangle \tag{22}$$

Using (22), applying the chain rule of differentiation to (21) and combining with the discrete continuity equation (9) yields

$$\begin{aligned} \frac{\varepsilon}{\Delta z}\,\Delta_z \langle \rho w^2 \rangle &= \frac{\varepsilon}{\Delta z}\,\Delta_z \langle \rho w \rangle \langle w \rangle = \\ &= \frac{\varepsilon}{\Delta z} \langle \rho w \rangle \Delta_z \langle w \rangle + \frac{\varepsilon}{\Delta z} \langle w \rangle \Delta_z \langle \rho w \rangle \\ &= \frac{\varepsilon}{\Delta z} \langle \rho w \rangle \Delta_z \langle w \rangle - \frac{1}{V} \int_{S_f(z)} G_z \langle w \rangle \, dS \end{aligned} \tag{23}$$

Hence applying (18)

$$\frac{\varepsilon}{\Delta z}\,\Delta_z \langle \rho w^2 \rangle = \frac{\varepsilon}{\Delta z} \langle \rho w \rangle \Delta_z \langle w \rangle - \frac{1}{V}\left(M_e \langle w \rangle_e - M_i \langle w \rangle_i\right). \tag{24}$$

The last term of equation (24) is descretized according to the "donor-cell" technique as follows (dropping the symbol < >):

$$\frac{1}{V}\left(M_e \langle w\rangle_e - M_i \langle w\rangle_i\right) =$$

$$= \frac{1}{V_{ij}}\left\{ M_{i+1/2}\left(w^*_{i+1/2} - \langle w_i\rangle\right) - M_{i-1/2}\left(w^*_{i-1/2} - \langle w\rangle_i\right)\right\} \qquad (24b)$$

with

$$w^*_{i+1/2} = \begin{cases} \langle w\rangle_i & \text{if } M_{i+1/2} > 0 \\ \langle w\rangle_{i+1} & \text{if } M_{i+1/2} < 0 \end{cases}$$

$$w^*_{i-1/2} = \begin{cases} \langle w\rangle_{i-1} & \text{if } M_{i-1/2} > 0 \\ \langle w\rangle_i & \text{if } M_{i-1/2} < 0 \end{cases}$$

Using axial velocities at level j + 1 the above equation can also be written:

$$\frac{1}{V}\left(M_e \langle w\rangle_e - M_i \langle w\rangle_i\right) =$$

$$= \frac{1}{V_{ij}}\frac{1}{2}\left\{\left(\left|M_{i+1/2,j}\right| - M_{i+1/2,j}\right)\left(w_{i+1} - w_i\right)_{j+1} + \right. \qquad (24c)$$

$$\left. + \left(\left|M_{i-1/2,j}\right| + M_{i-1/2,j}\right)\left(w_{i-1} - w_i\right)_{j+1}\right\}$$

Using these conventions eq. (13) is discretized in the following form

$$\left(\varepsilon \rho w\right)_{i,j} \frac{w_{i,j+1} - w_{i,j}}{\Delta z_{j+1/2}} = -g\,\varepsilon_i \frac{\rho_{i,j+1} + \rho_{i,j}}{2} +$$

$$- \varepsilon_i \frac{p_{i,j+1} - p_{i,j}}{\Delta z_{j+1/2}} - \frac{1}{V_{i,j}}\left[\left(\frac{\rho r S_f}{\Delta r}\right)_{i-\frac{1}{2},j}\left(w_i - w_{i-1}\right)_{j+1} - \left(\frac{\rho r S_f}{\Delta r}\right)_{i+\frac{1}{2},j}\left(-w_i + w_{i+1}\right)_{j+1}\right] +$$

$$- \left(\varepsilon f_w \frac{\rho w^2}{2 D_h}\right)_{i,j} + \qquad (25)$$

$$+ \frac{1}{2V_{i,j}}\left\{\left(\left|M_{i+\frac{1}{2},j}\right| - M_{i+\frac{1}{2},j}\right)\left(w_{i+1} - w_i\right)_{j+1} +\right.$$

$$\left. + \left(\left|M_{i-\frac{1}{2},j}\right| + M_{i-1/2,j}\right)\left(w_{i-1} - w_i\right)_{j+1}\right\}$$

Equation (25) can be written in the form

$$w_{i-1,j+1}\left(-B1 - B2\right) + w_{i,j+1}\left(A1 + A2 + B1 + B2 + TR\right) + \qquad (26)$$

$$+ w_{i+1,j+1}\left(-A1 - A2\right) = C1 + C2 - C3 - C4 - C5\, p_{i,j+1}$$

with

$$B1 = \frac{1}{2V_{i,j}}\left(|M| + M\right)_{i-1/2,j} \qquad (26a)$$

$$B2 = \frac{1}{V_{i,j}}\left(\frac{\rho r S_f}{\Delta r}\right)_{i-1/2,j} \qquad (26b)$$

$$A1 = \frac{1}{2V_{i,j}}\left(|M - M\right)_{i+1/2,j} \qquad (26c)$$

$$A2 = \frac{1}{V_{i,j}}\left(\frac{\rho r S_f}{\Delta r}\right)_{i+1/2,j} \qquad (26d)$$

$$TR = \frac{1}{\Delta z_{j+1/2}} \left(\varepsilon \rho w\right)_{i,j} \tag{26e}$$

$$C1 = w_{i,j} \cdot TR \tag{26f}$$

$$C2 = -g \varepsilon_i \frac{\rho_{i,j+1} + \rho_{i,j}}{2} \tag{26g}$$

$$C3 = -\varepsilon_i \frac{p_{i,j}}{\Delta z_{j+1/2}} \tag{26h}$$

$$C4 = \varepsilon_i \left(\rho \frac{\rho w^2}{2 D_h}\right)_{i,j} \tag{26i}$$

$$C5 = \frac{\varepsilon_i}{\Delta z_{j+1/2}} \tag{26j}$$

Letting

$$S = A1 + A2 + B1 + B2 + TR \tag{27a}$$

$$AA = (A1 + A2)/S \tag{27b}$$

$$BB = (B1 + B2)/S \tag{27c}$$

$$CC = (C1 + C2 - C3 - C4)/S \tag{27d}$$

$$DD = -C5/S \tag{27e}$$

equation (26) becomes

$$-BB\ w_{i-1,j+1} + w_{i,j+1} - AA\ w_{i+1,j+1} - DD\ p_{i,j+1} = CC \tag{28}$$

Equation (28) is used to calculate the axial velocities and the coolant pressure at an axial level j + 1. Writing it for every radial node i (i = 2...NC) it supplies a system of equations with a three-diagonal matrix of coefficients for the axial velocities. As eq. (28) contains the unknown pressure term $p_{i,j+1}$ a further condition is necessary for applying the solution algorithm by Thomas /7/.

This condition is supplied by summing eq (19) with respect to i (i = 2, ...NC). It yields the physical constraint that the coolant mass flow remains constant between axial levels j and j + 1.

$$\sum_{i}^{NC} \left(S_f \rho w\right)_{i,j+1} = \sum_{i}^{NC} \left(S_f \rho w\right)_{ij} \qquad (29)$$

According to reference / 8 / the numerical solution method based on eq. (28) is stable as long as the mass flow in axial direction is positive.
A marching technique through all axial levels (j = 2, ... MC) yields the axial velocity distribution.

iii) Energy equation

By analogy with (20) to (24) the first term of equation (16) can be written:

$$\frac{\varepsilon}{\Delta z}\left[\langle \rho w h\rangle_t - \langle \rho w h\rangle_b\right] = \frac{\varepsilon}{\Delta z}\,\Delta_z \langle \rho w h\rangle =$$

$$= \frac{\varepsilon}{\Delta z}\langle \rho w\rangle \Delta_z \langle h\rangle + \frac{\varepsilon}{\Delta z}\langle h\rangle \Delta_z \langle \rho w\rangle = \qquad (30)$$

$$= \frac{\varepsilon}{\Delta z}\langle \rho w\rangle \Delta_z \langle h\rangle - \frac{1}{V}\int_{S_f(z)} G_z \langle h\rangle \, dS =$$

$$= \frac{\varepsilon}{\Delta z}\langle \rho w\rangle \Delta_z \langle h\rangle - \frac{1}{V}\left[M_e \langle h\rangle_e - M_i \langle h\rangle_i\right]$$

According to the "donor-cell" technique, the last term of (30) is discretized as follows:

$$\frac{1}{V}\left[M_e \langle h\rangle_e - M_i \langle h\rangle_i\right] =$$

$$= \frac{1}{V_{ij}}\left\{M_{i+\frac{1}{2}}\left(h^*_{i+\frac{1}{2}} - \langle h\rangle_i\right) - M_{i-1/2}\left(h^*_{i-1/2} - \langle h\rangle_i\right)\right\} \tag{30b}$$

with

$$h^*_{i+1/2} = \begin{cases} \langle h\rangle_i & \text{if } M_{i+1/2} > 0 \\ \langle h\rangle_{i+1} & \text{if } M_{i+1/2} < 0 \end{cases}$$

$$h^*_{i-1/2} = \begin{cases} \langle h\rangle_{i-1} & \text{if } M_{i-1/2} > 0 \\ \langle h\rangle_i & \text{if } M_{i-1/2} < 0 \end{cases}$$

Using enthalpy values at axial level j + 1 the above equation becomes

$$\frac{1}{V}\left[M_e \langle h\rangle_e - M_i \langle h\rangle_i\right] =$$

$$= \frac{1}{2V_{ij}}\left\{\left(\left|M_{i+1/2,j}\right| - M_{i+1/2,j}\right)\left(h_{i+1} - h_i\right)_{j+1} + \right. \tag{30c}$$

$$\left. + \left(\left|M_{i-1/2,j}\right| + M_{i-1/2,j}\right)\left(h_{i-1} - h_i\right)_{j+1}\right\}.$$

The first term at the right hand side of equation (16) can be written:

$$\frac{V_f}{V}\langle q_w\rangle_3 = \frac{Q_{wf}}{V} = \frac{Q_{pin} \cdot V_{pin}}{V} =$$

$$= \frac{Q_{pin}}{V} S_{pin} \cdot \Delta z = \frac{Q_{pin}}{V} \pi R^2_{pin} \Delta z = Q_w \tag{31}$$

where

$Q_{wf} = \frac{V_f}{\varepsilon}\langle q_w\rangle_3$ power delived from the pin walls to the volume V_f of the coolant /W/

Q_{pin} = specific power generated in the pin $[W/m^3]$

Q_w = average specific power in the volume V of the cell $[W/m^3]$

V_{pin} = volume of the pins in the cell $[m^3]$

S_{pin} = pin surface in the cell $[m^2]$

R_{pin} = pin radius $[m]$.

Equation (16) can therefore be discretized as follows

$$(\varepsilon \rho w)_{i,j} \frac{h_{i,j+1} - h_{i,j}}{\Delta z_{j+1/2}} = \varepsilon_i w_i \frac{P_{i,j+1} - P_{i,j}}{\Delta z_{j+1/2}} +$$

$$+ \left(\frac{Q_{pin}}{V}\right)_{i,j} \pi R_{pin}^2 \Delta z_{j+1/2} + \qquad (32)$$

$$- \frac{1}{V_{i,j}} \left[\left(\frac{\rho \tilde{\lambda} S_f}{\Delta z}\right)_{i-1/2,j} \left(h_{i,j} - h_{i-1,j}\right)_{j+1} - \left(\frac{\rho \tilde{\lambda} S_f}{\Delta z}\right)_{i+1/2,j} \left(-h_{i,j} + h_{i+1,j}\right)_{j+1} \right] +$$

$$+ \frac{1}{2V_{i,j}} \left\{ \left(|M_{i+1/2,j}| - M_{i+1/2,j} \right) \left(h_{i+1,j} - h_{i,j}\right)_{j+1} + \right.$$

$$\left. + \left(|M_{i-1/2,j}| + M_{i-1/2,j} \right) \left(h_{i-1,j} - h_{i,j}\right)_{j+1} \right\} .$$

Neglecting the first term at the right hand side, which represents the work done by pressure forces in thermal expansion and is negligible with respect to the energy input, equation (32) can be written in the form

$$h_{i-1,j+1} \left(-B1 - B2\right) + h_{i,j+1} \left(A1 + A2 + B1 + B2 + TR\right) +$$

$$+ h_{i+1,j+1} \left(-A1 - A2\right) = h_{i,j} \cdot TR + SOURCE \qquad (33)$$

with the same symbols defined by (26a) to (26c) but replacing the kinetic viscosity ν by the thermal diffusivity $\tilde{\alpha} = \lambda / \rho c_p$, and

$$\text{SOURCE} = Q_w = \left(\frac{Q_{pin}}{V} \right)_{ij} \cdot \pi \cdot R_{pin}^2 \, \Delta z_{j+1/2} \cdot \qquad (33b)$$

Using again (27a) to (27c) and

$$CC' = (h_{ij} \cdot TR + SOURCE)/S \qquad (34)$$

equation (33) becomes

$$-BB \; h_{i-1,\, j+1} + h_{i,\, j+1} - AA \; h_{i+1,\, j+1} = CC'. \qquad (35)$$

Equation (35) is used to calculate the coolant enthalpy at an axial level j+1. The system of equations obtained writing (35) for every radial node i (i = 2, 3, ...NC) is solved numerically by means of the Thomas algorithm /7/.

The value of $\tilde{\alpha}$ introduced in the above formulas is an equivalent thermal diffusivity which takes into account both contributions from molecular and turbulent diffusivities. (See section C5).

1.2.4 Energy balance

An energy balance is made for every axial mesh of the bundle in the following way.

Letting $\Delta z_j = \Delta z(JC) = z(JZ) - z(JZ-1)$ (See fig. 8)
it should hold:

$$PUCU(JZ) + H(JZ-1) = H(JZ) + VLCU(JZ)$$

or

$$BILH(JZ) + VLCU(JZ) - PUCU(JZ) = 0 \qquad (36)$$

with

BILH (JZ) = H (JZ) - H (JZ-1) = coolant enthalpy balance between levels (JZ-1) and JZ

VLCU (JZ) = power transfered from the coolant to the hexagonal can

PUCU (JZ) = power released to the coolant.

These quantities are calculated as follows:

$$H(\delta z) = \sum_{2}^{NC}{}_{i} \; \gamma_i \, w_i \, S_{fi} \, h_i = \sum_{2}^{NC}{}_{IC} \; R\phi(IC,\delta z) \cdot W(IC,\delta z) \cdot SFC(\delta C) \cdot H(IC,\delta z) \quad [W] \qquad (37)$$

VLCU (JZ) = HKEX (JC) · PEXINT (JC) · (T(NC,JC) -TEX (JC)) · DZC (JC) $\quad /\bar{W}_{-}/$ (38)

PUCU (JZ) = FQ (JZ) · PCH · DZC (JC) $\quad /\bar{W}_{-}/$ (39)

Symbols of the above equations are defined in the list of Part II.

The relative error

ERR = (BILH (JZ) + VLCU (JZ) - PUCU (JZ)) / PUCU (JZ) (40)

can be printed for every axial mesh from Subroutine IMPRIP.

1.2.5 Boundary conditions

Three cases are available for imposing velocity and pressure boundary conditions:

i) Mass flow (coolant velocity) and coolant pressure are imposed at inlet by letting the input parameter MPR = 1. The coolant pressure distribution is then calculated with a marching technique from bundle inlet to the outlet.

ii) Mass flow and outlet coolant pressure are imposed if MPR = 2.

In this case the inlet coolant pressure specified as input is used as a starting value for applying the marching technique from bundle inlet to outlet. When the calculated outlet pressure does not correspond to the boundary value imposed, a new tentative inlet pressure is calculated with the Newton method and the marching technique is applied again. The scheme is repeated till the outlet pressure is approached within a given tolerance or till a maximum number (ITPX) of iterations steps has been attained.

iii) Inlet and outlet coolant pressures are imposed if MPR = 3.

(In case the input parameter LCS = 1, the programme sets MPR = 3).
The inlet mass flow is calculated consistently with the assumed pressure distribution. This third case can be choosen only when the programme

BACCHUS-P is used to initialize the fields for the transient calculation (Subroutine BACCP3).

The BACCHUS-P calculation is always done in two steps. For the first step (IRUN = 1) the hexagonal structure is assumed adiabatic and a preliminary temperature distribution of the coolant is calculated. In the second step (IRUN = 2) the heat transfer from the can outer surface to the outer medium is taken into account to yield a refined coolant temperature distribution.

1.3 Pin model and calculation of hexagonal can temperature

Every centered control volume used for the thermal-hydraulic calculation is associated to the neighbouring pins consisting of the heater element (fuel or electrical heater) and the clad separated from the fuel by a gap. An input heat transfer coefficient from fuel to clad is used for the steady state calculation. Besides that the heat flux from the coolant to the structural material of the hexagonal can is taken into account. The local coolant temperatures are assumed as a boundary condition for the calculation of the temperature distributions in the pin and the structural material. Heat losses from the outer surface of the hexagonal can into the surrounding medium e.g. into a bypass flow, can also be considered.

The calculation of the temperature distribution in the pins is done in a one dimensional (r coordinate) geometry for every axial mesh of the pin. Therefore an azimuthal temperature distribution cannot be obtained and axial heat diffusion is considered negligible in comparison to the radial diffusion. The coupling between axial meshes of the pin is only provided by the coolant.

1.3.1 Steady State equations

The equations for the steady state temperature distribution in fuel, clad and structure are straightly derived from the equations of section: B.2 by setting all time derivatives to zero.

i) Fuel

$$\frac{\partial}{\partial r} \lambda_B \frac{\partial T_B}{\partial r} + \frac{1}{r} \lambda_B \frac{\partial T_B}{\partial r} + q_B = 0 \qquad r \neq 0 \qquad (1)$$

with the boundary condition

$$- \lambda_B \left(\frac{\partial T_B}{\partial r}\right)_{R_B} = \alpha_{BH} \left[\bar{T}_B(0, R_B) - T_H(0, R_{Hi})\right] \qquad (2)$$

and

$$2 \lambda_B \frac{\partial^2 T_B}{\partial r^2} + q_B = 0 \qquad r=0 \qquad (3)$$

with the symmetry condition

$$\left(\frac{\partial T_B}{\partial r}\right)_{r=0} = 0 \qquad (4)$$

ii) Cladding

$$\frac{\partial}{\partial r}\left(\lambda_H \frac{\partial T_H}{\partial r}\right) + \frac{1}{r} \lambda_H \frac{\partial T_H}{\partial r} + q_H = 0 \qquad (5)$$

with the boundary conditions:

$$\alpha_{BH} \left[\bar{T}_B(0,R_B) - T_H(0, R_{Hi})\right] = -\left(\lambda_H \frac{\partial T_H}{\partial r}\right)_{R_{Hi}} \qquad (6)$$

$$- \left(\lambda_H \frac{\partial T_H}{\partial r}\right)_{R_{Ha}} = \alpha_{HK} \left[\bar{T}_H(0, R_a) - T_K(0)\right]$$

(iii) Structure

$$\alpha_{KS} \frac{F_S}{V_S} \left[\bar{T}_K(0) - T_S(0)\right] - \alpha_w \frac{F_w}{V_S} \left[\bar{T}_S(0) - T_w(0)\right] + q_S = 0 \qquad (7)$$

Input data for the stationary calculation are, apart from geometrical data, power generation in fuel, clad and structure material, the latter coming from γ-heating (if any).

1.3.2 Definition of geometrical data for pin model

The following geometrical data are defined for the pin model:

NMO First axial mesh of fuel column (see Input description)

NM1 Last axial mesh of fuel column (see Input description)

NM2 Number of axial zones in the coolant channel (see Input description)

NN Number of radial meshes inside the fuel pellets (see Input description)

HSPALT = Length of lower fission gas section (length of axial mesh zones from 1 to NMO-1)

HKUEKA = Length of the axial breeder zone (section between axial zones NMO and NM1 inclusive)

HTOP = Length of upper coolant mixing section (axial zones from NM1+1 to NM2)

HCORE = HSPALT + HKUEKA = length of test section from inlet to mesh zone NM1 inclusive;

furthermore one has (see Fig. 7)

DRBR = R_B/NN

DRBR2 = DRBR**2

R(N) = r_n (N=1, NN) = radial coordinate of fuel nodes (except fuel axial node)

RMIN(N) = $r_{n-1/2} = r_n$ - DRBR/2

QRMIN(N) = $r_{n-1/2}/r_n$

QRPL(N) = $r_{n+1/2}/r_n$

QRMIV = $(R_B$ - DRBR/4)/R_B

DRC = $r_m - r_i$ = DCAN/2

DRC2 = DRC**2

RCI = r_i

RCM = $r_m = r_i$ + DRC

RCA = $r_a = r_i$ + DCAN

QRPLV = $(r_i$ + DRC/4)/r_i

QRPLH = $(r_i$ + DRC/2)/r_i

QRCA = $(r_a$ - DRC/4)/r_a

QRCH = $(r_a$ - DRC/2)/r_a

QRCMS = $(r_m$ - DRC/2)/r_m

QRCPL = $(r_m$ + DRC/2)/r_m

1.3.3 First evaluation of steady state temperature distributions in fuel and clad

The temperature distribution in the coolant is used as a boundary condition for a first estimation of the temperature in clad and fuel. This occurs by integrating equations (1) and (5) assuming the thermal conductivity to be constant. The integration constants are determined from the boundary condition that for steady state the heat flux through any cylindrical surface in the fuel and clad is equal to the total power generated inside that surface.

Proceeding inwards from the clad outer surface, where the boundary condition given by the coolant temperature is known, one has for the clad outer node temperature

$$\alpha^{o}_{HK} \left(T^{o}_{H_{r_a}} - T^{o}_{K}\right) S_{r_a} = Q^{o}_{B} + Q^{o}_{H} \qquad (8)$$

where S_{r_a} is the clad outer surface per unit axial length and Q^{o}_{b}, Q^{o}_{H} are the powers generated in fuel and clad, respectively. This boundary condition yields $T^{o}_{H,\, r_a}$. Here and in the following the superscript o denotes values at t=o.

Writing equation (5) in the form

$$\frac{1}{r} \frac{d}{dr} \left(r \frac{dT_H}{dr} \right) - \frac{q_H}{\lambda_H} = 0 \qquad (9)$$

under the assumption that the thermal conductivity is constant, and integrating over a hollow cylinder one has

$$T_H(r) = a + b \ln r - \frac{q_H r^2}{4\lambda_H} \qquad (10)$$

where a, b are integration constants.

Assuming that the influence of the power generation in the clad upon the temperature distribution is negligible (hence neglecting the term $q_H r^2/4\lambda_H$), the temperature of the clad middle node is derived from the above equation imposing the boundary conditions

$$T_H(r_a) = T_{Ha} - 2\pi\lambda_H r_a \left(\frac{dT_H}{dr}\right)_{r_a} = Q_B^o + Q_H^o \qquad (11)$$

which gives the constants a, b and yields:

$$T_H^o(r_m) = T_{Hr_a}^o + \frac{Q_B^o + Q_H^o}{2\pi\lambda_H} \ln \frac{r_a}{r_m} \qquad (12)$$

where the thermal conductivity is calculated with reference to the known temperature $T_H(r_a)$.

The temperature of the clad inner node is derived imposing the boundary conditions:

$$- 2\pi\lambda_H r_m \left(\frac{dT_H}{dr}\right)_{r_m} = Q_B^o + Q_{H/2}^o \qquad (13)$$

which yields

$$T_H^o(r_i) = T_{Hm}^o + \frac{Q_B^o + \frac{Q_H^o}{2}}{2\pi\lambda_H} \ln \frac{r_m}{r_i} \qquad (14)$$

The temperature of the outermost fuel node is given by the boundary condition

$$\alpha_{BH}^o \quad (T_{B\ NN} - T_{H\ r_i}^o) = Q_B^o \qquad (15)$$

The temperature distribution in the fuel is described under the assumption of constant thermal conductivity by the equation

$$\frac{1}{r} \frac{d}{dr}\left(r \frac{dT_B}{dr}\right) - \frac{q_B}{\lambda_B} = 0 \qquad (16)$$

Integrating one has

$$T_B(r) = a - \frac{q_B r^2}{4\lambda_B} \qquad (17)$$

The integration constant a represents the fuel axial temperature ($a = T_{BO}$) and is determined from the boundary condition

$$T_B^o(r_{NN}) = T_{B\ NN}^o \tag{18}$$

which yields

$$T_{BO}^{\ o} = T_{B\ NN}^o + \frac{q_B\ r_{NN}^2}{4\lambda_B} \tag{19}$$

The fuel temperature in any internal node N (N = 1,2...,NN-1) is then given by

$$T_B^o(r_n) = T_{BNN}^o + \frac{(T_{BO}^o - T_{BNN}^o)\ (r_{NN}^2 - r_n^2)}{r_{NN}^2} \tag{20}$$

This estimation of the temperature distribution in clad, and fuel is not definite because the thermal conductivities were calculated with reference to a temperature different from the yet unknown temperatures of the respective nodes. The preliminary temperature distributions are therefore only used as first approximations to start the refined calculation performed iteratively by means of the Gauss-Seidel iteration scheme, as explained hereafter.

1.3.4 Refined temperature distributions in fuel and clad with the Gauss-Seidel iteration method and calculation of structure temperature

i) Fuel

Taking for an axial mesh the annulus delimited by the cylindrical surfaces $S_{n-1/2}$, $S_{n+1/2}$ with radii $r_{n\mp1/2}$ as a control volume, and integrating equation (1) over the outer surfaces of this control volume one has

$$- \int_{S_{n-1/2}} \lambda_B^o \frac{\partial T_B^o}{\partial r} \, dS + \int_{S_{n+1/2}} \lambda_B^o \frac{\partial T_B^o}{\partial r} \, dS + q_n^o \, V_n = 0 \qquad (21)$$

or

$$-\lambda_{B,r_{n-1/2}} \left(\frac{\partial T_B^o}{\partial r}\right)_{r_{n-1/2}} S_{n-1/2} + \lambda_{B,r_{n+1/2}} \left(\frac{\partial T_B^o}{\partial r}\right)_{r_{n+1/2}} S_{n+1/2} + q_n^o \, V_n = 0 \qquad (22)$$

where V_n is the volume of the annular section belonging to the considered axial mesh zone. Space discretisation of this equation yields the algebraic equation.

$$A_n^o \, T_{B\,n}^o + B_n^o \, T_{B\,n-1}^o + C_n^o \, T_{B\,n+1}^o = Q_n^o \qquad (23)$$

with

$$A_n^o = \lambda_{B,r_{n-1/2}} \frac{r_{n-1/2}}{r_n} + \lambda_{B,r_{n+1/2}} \frac{r_{n+1/2}}{r_n} \qquad (24a)$$

$$B_n^o = - \lambda_{B,r_{n-1/2}} \frac{r_{n-1/2}}{r_n} \qquad (24b)$$

$$C_n^o = - \lambda_{B,r_{n+1/2}} \frac{r_{n+1/2}}{r_n} \qquad (24c)$$

$$Q_n^o = q_n^o \, \Delta r_B^{\,2} \qquad (24d)$$

and

$$\Delta r_B = r_{n+1/2} - r_{n-1/2} \qquad (24e)$$

The above equation is applicable to all fuel internal nodes (n = 1,2...,NN-1).

For the fuel outermost node, taking as control volume the annulus delimited by the cylindrical surfaces with radii $r_{NN-1/2}$, r_{NN}, one has

$$- \int_{S_{NN-1/2}} \lambda_B \frac{\partial T_B}{\partial r} dS - \alpha_{BH} S_{NN} (T_{B,NN} - T_{Hi}) + q_{NN} V_{NN} = 0 \tag{25}$$

which yields the algebraic equation

$$A^o_{NN} T^o_{B,NN} + B^o_{NN} T^o_{B,NN-1} + C^o_{NN} T^o_{Hi} = Q^o_{NN} \tag{26}$$

with

$$A^o_{NN} = \lambda r_{NN-1/2} \frac{r_{NN-1/2}}{r_{NN}} + \alpha_{BH} \Delta r_B \tag{27a}$$

$$B^o_{NN} = -\lambda r_{NN-1/2} \frac{r_{NN-1/2}}{r_{NN}} \tag{27b}$$

$$C^o_{NN} = -\alpha_{BH} \Delta r_B \tag{27c}$$

$$Q^o_{NN} = \frac{\Delta r_B^2}{2} \frac{r_{NN-1/4}}{r_{NN}} q_{NN} \tag{27d}$$

For the fuel central node, taking as control volume the cylinder of radius $r_{1/2}$, one has

$$- \int_{S_{1/2}} \left(- \frac{\lambda \partial T_B}{\partial r} \right) dS + q_o V_o = 0 \tag{28}$$

which yields the algebraic equation (the superscript "o" refers to the stationary calculation the subscript to the axial fuel node)

$$A_o^{\ o} T^o_{B,o} + C_o^{\ o} T^o_{B,1} = Q_o^{\ o} \tag{29}$$

with:

$$A_o^{\ o} = \lambda_{r1/2} \tag{30a}$$

$$C_o^{\ o} = -\lambda_{r1/2} \tag{30b}$$

$$Q_o^{\ o} = q_o \frac{\Delta r_B^2}{4}. \tag{30c}$$

ii) Cladding

For the clad inner node, taking as control volume the annulus delimited by the cylindrical surfaces with radii r_i, $r_{i+1/2}$, one has

$$\alpha_{BH} (T_{B,NN} - T_{Hi}) S_i - \int_{S_{i+1/2}} \left(-\lambda_H \frac{\partial T_H}{\partial r}\right) dS + q_{Hi} V_{Hi} = 0 \qquad (31)$$

which yields the algebraic equation

$$A^o_{Hi} T^o_{Hi} + B^o_{Hi} T^o_{B,NN} + C^o_{Hi} T^o_{Hm} = Q^o_{Hi} \qquad (32)$$

with

$$A^o_{Hi} = \alpha^o_{BH} \Delta r_H + \lambda^o_{H,r_{i+1/2}} \frac{r_{i+1/2}}{r_i} \qquad (33a)$$

$$B^o_{Hi} = -\alpha^o_{BH} \Delta r_H \qquad (33b)$$

$$C^o_{Hi} = -\lambda^o_{H,r_{1+1/2}} \frac{r_{i+1/2}}{r_i} \qquad (33c)$$

$$Q^o_{Hi} = \frac{r_{i+1/4}}{r_i} \frac{\Delta r_H^2}{2} q_{Hi} \qquad (33d)$$

For the clad middle node, taking as control volume the annulus delimited by the cylindrical surfaces with radii $r_{m-1/2}$, $r_{m+1/2}$ one has

$$- \int_{S_{m-1/2}} \lambda_H \frac{\partial T_H}{\partial r} dS + \int_{S_{m+1/2}} \lambda_H \frac{\partial T_H}{\partial r} dS + q_{H_m} V_{H_m} = 0 \qquad (34)$$

which yields the algebraic equation

$$A^o_{Hm} T^o_{Hm} + B^o_{Hm} T^o_{Hi} + C^o_{Hm} T^o_{Ha} = Q^o_{Hm} \qquad (35)$$

with

$$A^o_{Hm} = \lambda^o_{H,m-1/2} \frac{r_{m-1/2}}{r_m} + \lambda^o_{m+1/2} \frac{r_{m+1/2}}{r_m} \qquad (36a)$$

$$B^o_{Hm} = -\lambda^o_{H,m-1/2} \frac{r_{m-1/2}}{r_m} \qquad (36b)$$

$$C^o_{Hm} = -\lambda_{H,m+1/2} \frac{r_{m+1/2}}{r_m} \qquad (36c)$$

$$Q^o_{Hm} = q^o_{Hm} \Delta r_H^2 \qquad (36d)$$

For the clad outer node, taking as control volume the annulus delimited by the cylindrical surfaces with radii $r_{m+1/2}$, r_a one has

$$-\int_{S_{m+1/2}} \lambda_H \frac{\partial T_H}{\partial r} dS - \alpha_{HK} (T_{Ha} - T_K) S_{ra} + q_{Ha} V_{Ha} = 0 \tag{37}$$

which yields the algebraic equation

$$A_{Ha}^{o} T_{Ha}^{o} + B_{Ha}^{o} T_{Hm}^{o} + C_{Ha}^{o} T_K^{o} = Q_{Ha}^{o} \tag{38}$$

with $$A_{Ha}^{o} = \lambda_{H,r_{a-1/2}} \frac{r_{a-1/2}}{r_a} + \alpha_{HK} \Delta r_H \tag{39a}$$

$$B_{Ha}^{o} = -\lambda_{H,r_{a-1/2}}^{o} \frac{r_{a-1/2}}{r_a} \tag{39b}$$

$$C_{Ha}^{o} = -\alpha_{HK}^{o} \Delta r_H \tag{39c}$$

$$Q_{Ha}^{o} = \frac{\Delta r_H}{2} \frac{r_{a-1/4}}{r_a} q_{Ha}^{o} \tag{39d}$$

iii) Structure

Equation (12) can be straightforward written in the form

$$A_S^{o} T_S^{o} + B_S^{o} T_K^{o} + C_S^{o} T_W^{o} = Q_S^{o} \tag{40}$$

with

$$A_S^{o} = \alpha_{KS}^{o} + \alpha_W^{o} \frac{F_W}{F_S} \tag{41a}$$

$$B_S^{o} = -\alpha_{KS}^{o} \tag{41b}$$

$$C_S^{o} = -\alpha_W^{o} \frac{F_W}{F_S} \tag{41c}$$

$$Q_S^{o} = q_S^{o} \frac{V_S}{F_S} \tag{41d}$$

The above equations form a system of linear algebraic equations which can be written in matrix form as

$$A \cdot T = Q \tag{42}$$

where A is a tridiagonal square matrix, T is a column vector containing the unknown node temperatures and Q a column vector with the power generation terms.
The solution of this linear system yields the steady-state temperature distribution. It is carried out with the iterative Gauss-Seidel method assuming as initial distribution in fuel and clad the one supplied by the analytical solution of the respective equations under the assumption of constant material properties.

1.4 Coupling of BACCUHS-P (steady state) to BACCHUS-T (transient calculation)

The steady state calculation is performed with a marching technique from the bundle inlet to the outlet. Therefore velocity components and coolant physical properties are defined at axial nodes JZ (JZ = 2, MZ).

The coolant radial velocities are defined on the planes parallel to the bundle axis through the pin axes. The other quantities (w, h, physical properties) are defined midway between the above planes.

For the transient calculation (both two- and three-dimensional) physical quantities are defined on staggered meshes. This requires a re-initialization of velocity components and coolant physical properties before the programme control is transfered to the modules for the transient calculation. This is done in the Subroutine BACCHP. The correspondence between the axial nodes used in the steady-state calculation and the axial meshes used in the transient calculation is sketched in Fig. 8.

Before the programme control is transfered to the Subroutine ITER3, which is the driving programme for the 3-D transient calculation, a quasi-stationary calculation is performed in Subroutine PERM3. It is a time-dependent computation with constant inlet and boundary conditions, which is carried out till some convergence criteria are satisfied.
Typically, a few hundred time steps are required for reaching a new steady-state. This calculation is needed because of the different physical modelling in BACCHUS-P and BACCHUS-T. It offers the following advantages with respect to the steady-state calculation of BACCHP

- coolant heat diffusion in axial direction is not neglected
- the radial pressure distribution is calculated

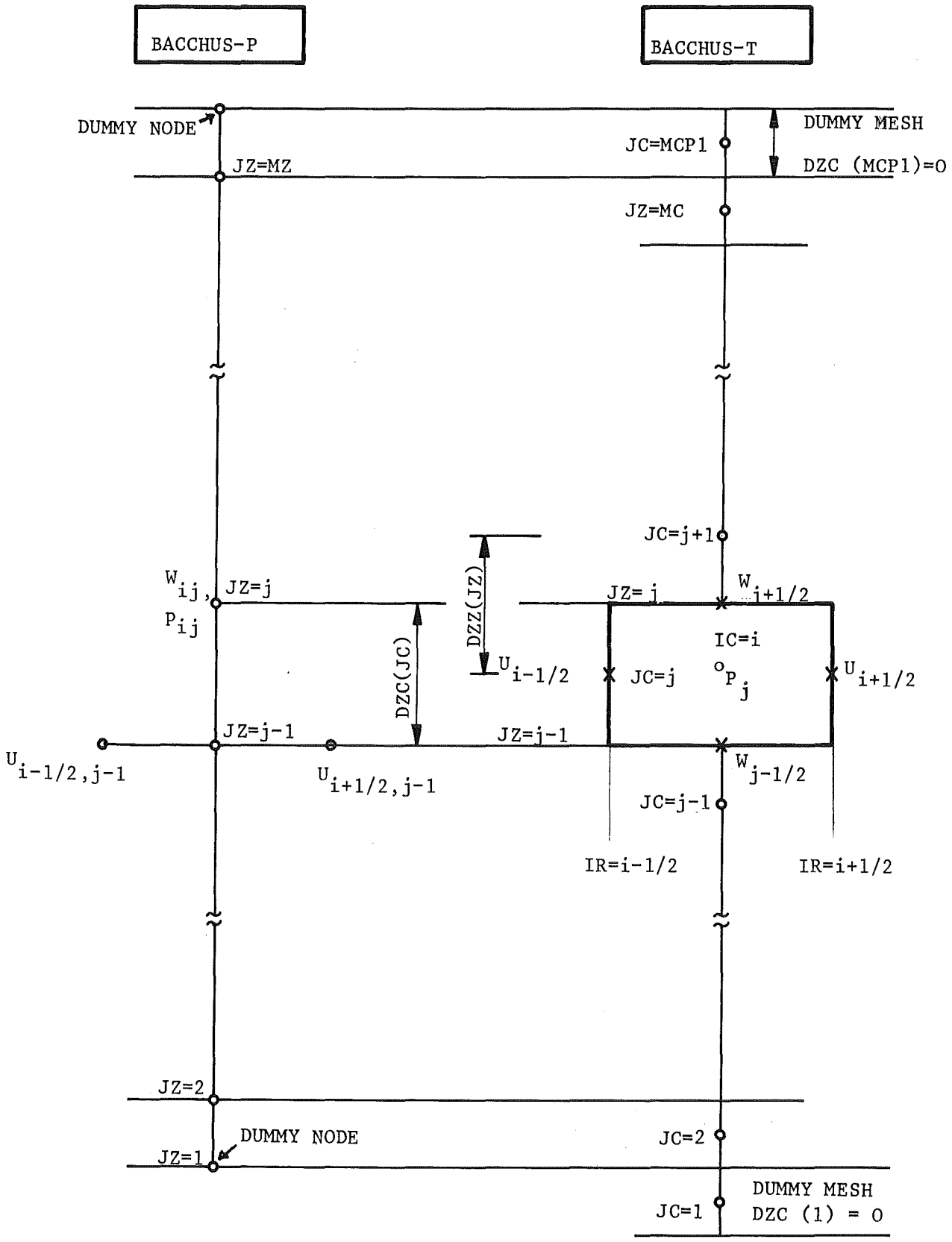

Fig. 8: Indexing of centred and staggered meshes in axial direction.

- in the radial direction, the calculation of convective terms is included in the momentum and the energy equations
- in case of blockages (which cannot be handled in steady-state calculations) completely new flow and temperature fields are calculated by simulating a large pressure drop in the blocked meshes.

1.5 Short description of BACCHUS-P Subroutines

The steady-state calculation is made by transfering the control to the following Subroutines in the sequence:

a_1) MAIN/LECT a_2) BACCP3

b) CHAUF
c) INIT
d) IMPRIP
e) PRESS
f) ITERBP
g) VITAX
h) CFAX
i) TRIDIB
j) ENTH
k) LHTSTX
l) WWSTX
m) TRIDIA
PRESS (2nd run)
IMPRIP (2nd run)
n) FPHU
o) BNDRYP
p) BNDRY3
q) BNDRYH
r) PHYSL
s) TBRO3

The main calculations made in these Subroutines are explained hereafter.

a_1) MAIN Programme / Subroutine LECT

When the BACCHUS-P programme is used as stand-alone or the calculation has to be stopped at the end of the steady-state, a set of input-data (see section 1.6) is read by calling Subroutine LECT. In this case a transient calculation cannot follow.

a_2) Subroutine BACCP3

This is the control programme for the steady-state calculation when BACCHUS-P is used in combination with the transient programme. Besides the transfer from the nodes to the staggered meshes is made for the subsequent quasi-stationary calculations performed in Subroutine PERM.

b) Subroutine CHAUF

The coolant physical properties are calculated according to theinput enthalpy value HZERO, and the axial power distribution is normalized and stored in array FQ (JZ), JZ = 2,...MZ.
The fields containing the fuel power density QVOLL $/\bar{}\ W/m^3\ \bar{}/$ and the steady state heat fluxes at the clad outer surface QQQ1 $/\bar{}\ W/m^2\ \bar{}/$ are initialized.

c) Subroutine INIT

The velocity components and the physical properties of the coolant at the inlet dummy node (JZ = 1) are initialized.

d) Subroutine IMPRIP

i) 1st run. Input and further geometrical data are printed in the following sequence:

- geometrical data of the bundle, including hydraulic diameters
- geometrical data defined at the interface between central meshes and in the central meshes namely
  - number, surface, and perimeter of pins in the control volumes
  - coolant flow area and total area of the displaced control volumes
  - radial porosities
- inlet and outlet boundary conditions
- physical properties of coolant at inlet.

ii) 2nd run. The BACCHUS-P calculation is done with a marching technique from the bundle inlet to the outlet. At the end of the BACCHUS-P calculation following data are printed for every axial level:

- coolant enthalpy, density and temperature,
- axial velocity, axial and radial mass flows
- thermodynamic title and void fraction of two phase fluid (set to zero in case of single phase flow)
- coolant pressure and axial pressure drop
- enthalpy balance between bundle inlet and the axial level considered.

e) Subroutine PRESS

The calculation of coolant pressure axial distribution, coolant enthalpy and velocity is done by calling Subroutine ITERBP. When the coolant pressure at the bundle outlet is given as a boundary condition (MPR = 2), this subroutine checks whether this value has been attained within a given tolerance. If this is not the case a new iteration step from bundle inlet to the outlet is done after modifying the inlet pressure using the Newton method. A maximum number of iteraction sweeps (ITPX) is specified by input.

f) Subroutine ITERBP

The computation of coolant velocity and enthalpy is done for every axial level from bundle inlet to the outlet with the marching technique. For every axial level JZ (JZ = 2, MZ) are computed:

- coolant axial velocity and coolant pressure, by calling subroutine VITAX
- coolant enthalpy, by calling subroutine ENTH
- two-phase flow parameters
- radial mass flow, according to equation C 1.2 (19)
- enthalpy balance from the bundle inlet to the axial level under consideration, according to equation C 1.2 (36)

g) Subroutine VITAX

The coolant pressure and axial velocities at a given axial level JZ are computed by solving numerically the system of equations (28) (Section C 1.2) with the auxiliary condition given by equation (29). The numerical solution

is obtained with the Thomas algorithm / 7 / applied in Subroutine TRIDIB.

h) Subroutine CFAX

The friction coefficient for the coolant flow is calculated.

i) Subroutine TRIDIB

It solves numerically an equation of the form $AY_1 + PY_2 = B$ where A is a three-diagonal matrix, Y_1, Y_2 are unknown vectors, P and B are known vectors. A further condition relating the components of Y_1 and Y_2 is given so that the Thomas algorithm / 7 / can be applied. This Subroutine is called by Subroutine VITAX for solving the system of equations (28) under the restraint represented by equation (29) of section C 1.2.

j) Subroutine ENTH

The coolant enthalpy distribution at an axial level JZ is calculated by solving numerically eq (35). The inversion of the three-diagonal matrix of coefficients is done in Subroutine TRIDIA. It also computes the hexagonal can temperature according to equation (40) of section C 1.2.

k) Subroutine LHTSTX

The coefficient for the heat transfer between coolant to clad (or structure) wall is calculated.

l) Subroutine WWSTX

The heat transfer coefficient form the outer surface of the hexagonal can structure to the outer medium is calculated.

m) Subroutine TRIDIA

A system of linear equations with a three-diagonal matrix of coefficients is solved numerically by means of the Thomas algorithm / 7 /. It is called by Subroutine ENTH for solving the system of equations (35) of section C 1.2.

n) Subroutine FPHU

The boundary conditions for pressure, enthalpy and coolant velocity components are calculated.

o) Subroutine BNDRYP (Entry in BNDRY3)

For all dummy meshes the pressure boundary conditions are imposed according to the input data.

p) Subroutine BNDRY3

The boundary conditions for the coolant velocities and mass flows in the dummy meshes are imposed, according to the input parameters.

q) Subroutine BNDRYH (Entry in BNDRY3)

The boundary conditions for the coolant enthalpy in the dummy meshes are imposed, according to the input parameters.

r) Subroutine PHYSL

The physical properties of the coolant (single phase) corresponding to a given enthalpy are calculated.

s) Subroutine TBRO3

The steady state temperature distributions in the fuel and clad are calculated as explained in section 1.3. A first evaluation of the steady state temperature distribution is made by integrating the heat diffusion equation under the assumption of constant physical properties of the fuel (section 1.3.3). A refined calculation which takes into account the temperature dependence of the physical properties is obtained by solving numerically the discretized Fourier equations by means of the Gauss-Seidel iteration method (section 1.3.4).

1.6 Input description+

The following formats are used for reading input data:

- integers: 18 I 4
- reals : 7 G 10.4

+Corresponds to the stand of the programme as of December 1981.

Card 1	TITRE	Title of up to 80 alpha-numeric digits
Card 2	MD	Dimensions of arrays in COMMON Blocks
	ND	for axial (MD) and radial (ND) discretization.
Card 3	NCAS	Number of cases which can be calculated. All cases assume the same bundle geometry and differ in the boundary conditions.
	ISTØP	= 0 Steady-state calculation only is performed.
Card 4	NC	Number of radial meshes in the bundle.
Card 5	PITCH	Pitch (m)
	DIA	Pin outer diameter (including cladding) (m)
	GAP	Width of external coolant flow surface (m) This surface is bounded externally by the hexagonal can and internally by a plane passing through the axes of the outermost pins.
	DFIL	Diameter of helicoidal spacers (m)
	HELIC	Pitch length of helicoidal spacers (m)
Card 6	NZØ	Number of axial sections
Card 7	ML(I), I=1,NZØ	Number of axial meshes in the NZØ axial sections.
Card 8	ZL(I), I=1,NZØ	Length of axial sections
Card 9	NQ	Number of nodes in which the power profile is given
Card 10	ZQ(I), I=1,NQ	Axial coordinates of the nodes for power profile /m/
Card 11	QZ(I), I=1,NQ	Normalized profile of power density
Card 12	TITRE	Title of up to 72 alpha-numeric digits describing the case being run
Card 13	MPR	= 1 Inlet coolant pressure as boundary condition = 2 Outlet coolant pressure as boundary condition
Card 14	PZERØ	Coolant outlet pressure (N/m^2)
	PKOO	Coolant inlet pressure (N/m^2)
	DHPZO	Axial distance between coolant upper free level and bundle outlet (m)

Card 15 TZERØ Inlet steady state coolant temperature (^{o}C)

WZERØ Inlet steady state coolant axial velocity (m/sec)

PUIS Total power of the bundle (W)

Card 16 CDIFFO, CDIFFI } Coefficients C_o, C_1 for calculating the turbulent momentum diffusivity according to $\nu_{eff} = C_1 + C_o \varepsilon W D_h$

CDIFTO, CDIFT1 } Coefficients C_o, C_1 for calculating the turbulent diffusivity for heat according to $\alpha_{eff} = C_1\alpha + C_o \varepsilon W D_h$.

We suggest $C_1 = 1 - \frac{DIA}{PITCH}$; $C_o = 1$.

Card 17 NITMAX Maximum iteration number for coolant pressure convergence (= 10).

Card 18 EP Tolerance for coolant pressure convergence (1. E-04)

Card 19 CFA, CFB } Coefficients for calculating the friction factor CFO according to the formula CFO = CFA /(REY ** CFB)

Card 20 CFME1, CFME2 } Coefficients for modifying the calculation of the friction coefficient CFO according to the Novendstern relationship:

CF = CFO x CFM

with

CFM = (CFM1 + CFM2 x REY xx CFME1) xx CFME2

and

CFM1 = 1·034 /((PITCH/DIA) xx 0·124)

CFM2 = 29·7 x (PITCH/DIA) x 6·94 / (λ/DIA) xx 2·239

(λ = pitch length of wire wraps (See Subroutine CFAX))

Card 21 EPSEX Thickness of hexagonal can (m)

Card 22 PPSI Coefficient for calculating pressure drops in case of grid spacers Δp = PPSI x D_h/DABST

DABST Distance between grid spacers (m)

Card 23 NMO First axial mesh of fuel column.

(The section JC = 2 ÷ (NMO-1) is regarded as fission gas plenum).

NM1 Last axial mesh of fuel column.

Card 24	CNN1 CNN2 CN1 CN2 CN3	Coefficients to determine the clad-coolant heat transfer coefficient h corresponding to the Nusselt number $N_u = \frac{hD}{\lambda} = CNN1 + CNN3 \cdot RE^{CN1} \cdot Pr^{CN2} \left(\frac{Tw}{T_{bulk}}\right)^{CN3}$ (Tw = wall temperature, T_{bulk} = coolant bulk temperature)
Card 25	RBRR	Fuel radius (m)
	DCANN	Clad thickness (m)
	DBONDD	Gap width (between fuel and clad) (m)
Card 26	ANTBB	Percentage of power produced in the fuel
	ANTCC	Percentage of power produced in the clad
	ANTKK	Percentage of power produced in the coolant
	ANTSS	Percentage of power produced in the structure
Card 27	IS	Steady state results are printed for all axial nodes (IS = 0) or for meshes for which output is desired as specified in next two cards (IS ≠ 0)
Card 28	NDCØUP	Number of axial sections for which a full output is required
Card 29	IDEB	First axial node for which output is desired
	IFIN	Last axial node for which output is desired
	IPAS	Results of every IPAS-th node between IDED and IFIN are printed. Card 29 is repeated NDCØUP times. Cards 28, 29 are not required if IS = 0 (Card 27).

2) Transient three-dimensional (3D) thermal hydraulic calculation

The use of the ICE (Implicit Continuous fluid Eulerian) technique by F.H. Harlow and A.A. Amsden /9/ for the numerical treatment of the thermal hydraulic conservation equations is explained in this section. Emphasis is put on the derivation of a Poisson - like equation for the coolant pressure, which is an essential feature of the ICE technique. In the present programme version the numerical solution of the Poisson equation is obtained with the Alternating Directions Implicit (ADI) method which is used iteratively within one time step. It is based on the well known scheme by Peaceman-Rachford /5/ and Douglas /10/.

2.1 The ICE technique

Referring to reference /9/ for a detailed description, we recall briefly the main features which characterize the Implicit Continuous-fluid Eulerian (ICE) Technique, as applied to the volume averaged conservation equations derived in section B. 1.2. These equations are discretized with respect to time by introducing two weighting parameters ϑ , $1-\vartheta$ $(0 \leq \vartheta \leq 1)$ for quantities referred to time steps t_{n+1} and t_n, respectively. Space discretization is done with reference to "staggered" meshes as shown in fig. 2.

This discretization technique offers the advantage that in the three scalar momentum equations values of the fluid pressure are defined at either side of the velocity components in the respective axis direction. This allows combining momentum and continuity equations to obtain a seven-point formula for pressure-values at time t_{n+1} as it would be generated by space - discretization of a Poisson equation. The main disadvantage consists in the fact that the divergence terms in the continuity equation require the calculation of fluid density at the mesh interfaces, which implies the use of an interpolation formula between known centre values.

As far as time - discretization is concerned, the following ideas form the basis of the ICE technique: a) Convective terms are treated explicitly. b) Terms describing spatial pressure distribution are treated implicitly; divergence terms of the continuity equation, which describe the space distribution of the fluid density, are also treated implicitly. c) Terms describing friction pressure

drops are treated half-implicitly in the BACCHUS programme. It is well known that the implicit treatment of pressure dependent terms removes the very restrictive constraint of time steps smaller than the minimum of $\Delta \ell_\alpha / c$ ($\Delta \ell_\alpha$ = mesh lengths in the z, r, s directions, c = speed of sound).

As shown in detail in the following sections, the application of the ICE technique implies the following steps:

i) Momentum and continuity equations are combined to derive a Poisson equation $\nabla^2 p^{n+1} = G^n$ describing the pressure distribution at time level n+1. The right-hand side G^n of this equation contains convective and diffusivity terms calculated explicitly at time level n as well as pressure terms at the same time t_n.

ii) The Poisson equation is solved numerically, yielding the space distribution of pressure at time t_{n+1}.

iii) The new pressure values are introduced into the scalar momentum equations which are solved explicitly for the mass flows in the respective directions. Velocity fields at time t_{n+1} are hence obtained.

iv) The new velocity values are introduced into the energy equation which is solved for the fluid enthalpy. Physical properties of the fluid are then calculated at time t_{n+1}.

v) Time is updated and the calculation cycle starts again from ii) for the following time step.

2.2 Finite difference form of the volume averaged conservation equations

i) Continuity equation

Let ϑ_c ($0 \leq \vartheta_c \leq 1$) be a time-discretization parameter and n, n+1 be superscripts referring to time levels t_n, t_{n+1} respectively. Space and time discretization of eq. B.1. (14) yields for the control volume V_I shown in Fig.2:

$$\varepsilon_{i,j,\kappa}\,\frac{\rho^{n+1}_{i,j,\kappa}-\rho^{n}_{i,j,\kappa}}{\Delta t_n}+$$

$$+\vartheta_c\,\frac{\varepsilon_{i,j,\kappa}}{\Delta z_j}\left[(\rho w)^{n+1}_{i,j+1/2,\kappa}-(\rho w)^{n+1}_{i,j-1/2,\kappa}\right]+(1-\vartheta_c)\,\frac{\varepsilon_{i,j,\kappa}}{\Delta z_j}\left[(\rho w)^{n}_{i,j+1/2,\kappa}-(\rho w)^{n}_{i,j-1/2,\kappa}\right]+$$

$$+\frac{\vartheta_c}{\Delta x_i}\left[(\psi F\rho u)^{n+1}_{i+1/2,j,\kappa}-(\psi F\rho u)^{n+1}_{i-1/2,j,\kappa}\right]+\frac{(1-\vartheta_c)}{\Delta x_i}\left[(\psi F\rho u)^{n}_{i+1/2,j,\kappa}-(\psi F\rho u)^{n}_{i-1/2,j,\kappa}\right]+$$

$$+\frac{\vartheta_c}{\Delta y_\kappa}\left[\left(\frac{\xi\rho v}{\cos\beta}\right)^{n+1}_{i,j,\kappa+1/2}-\left(\frac{\xi\rho v}{\cos\beta}\right)^{n+1}_{i,j,\kappa-1/2}\right]+ \qquad (1)$$

$$+\frac{1-\vartheta_c}{\Delta y_\kappa}\left[\left(\frac{\xi\rho v}{\cos\beta}\right)^{n}_{i,j,\kappa+1/2}-\left(\frac{\xi\rho v}{\cos\beta}\right)^{n}_{i,j,\kappa-1/2}\right]=0$$

For the reason mentioned in section 2.1, the divergence terms in the continuity equation are treated implicitly. In eq. (1) and in the following ones the symbols $\langle\ \rangle_3, \langle\ \rangle$ denoting volume and surface averaged quantities are dropped for simplicity.

We refer to the list at the end of this section for all new symbols introduced in the following equations.

ii) Momentum equations

a) Axial momentum equation

Space and time discretization of eq. B.1 (17) for the control volume V_{III} shown in fig. 2 yields

$$\varepsilon_{i,j+\frac{1}{2},\kappa}\ \frac{(\rho w)^{m+1}_{i,j+1/2,\kappa}-(\rho w)^{m}_{i,j+1/2,\kappa}}{\Delta t_m}+$$

$$+\frac{\varepsilon_{i,j+1/2,\kappa}}{\Delta z_{j+\frac{1}{2}}}\left[\left(\rho w^2\right)^{m}_{i,j+1,\kappa}-\left(\rho w^2\right)^{m}_{i,j,\kappa}\right]+\frac{1}{\Delta r_i}\left[\left(\psi F \rho w u\right)^{m}_{i+1/2,\,j+1/2,\kappa}-\left(\psi F \rho w u\right)^{m}_{i-1/2,\,j+1/2,\kappa}\right]+$$

$$+\frac{1}{\Delta \vartheta_\kappa}\left[\left(\frac{\xi \rho w v}{\cos\beta}\right)^{m}_{i,j+1/2,\,\kappa+1/2}-\left(\frac{\xi \rho w v}{\cos\beta}\right)^{m}_{i,j+1/2,\,\kappa-1/2}\right]+$$

$$-\frac{\varepsilon_{i,j+1/2,\kappa}}{\Delta z_{j+1/2}}\left[\left(\mu\frac{\partial w}{\partial z}\right)^{m}_{i,j+1,\kappa}-\left(\mu\frac{\partial w}{\partial z}\right)^{m}_{i,j,\kappa}\right]-\frac{1}{\Delta r_i}\left[\left(\psi F \mu\frac{\partial w}{\partial r}\right)^{m}_{i+1/2,\,j+1/2,\kappa}-\left(\psi F \mu\frac{\partial w}{\partial r}\right)^{m}_{i-1/2,\,j+1/2,\kappa}\right]+$$

$$-\frac{1}{\Delta \vartheta_\kappa}\left[\left(\frac{\xi \mu\frac{\partial w}{\partial \vartheta}}{\cos\beta}\right)^{m}_{i,j+1/2,\,\kappa+1/2}-\left(\frac{\xi \mu\frac{\partial w}{\partial \vartheta}}{\cos\beta}\right)^{m}_{i,j+1/2,\,\kappa-1/2}\right]+ \qquad (2)$$

$$+\vartheta_m\frac{\varepsilon_{i,j+1/2,\kappa}}{\Delta z_{j+1/2}}\left[p^{m+1}_{i,j+1,\kappa}-p^{m+1}_{i,j,\kappa}\right]+(1-\vartheta_m)\frac{\varepsilon_{i,j+\frac{1}{2},\kappa}}{\Delta z_{j+\frac{1}{2}}}\left[p^{m}_{i,j+1,\kappa}-p^{m}_{i,j,\kappa}\right]+$$

$$+g\left(\varepsilon\rho\right)^{m}_{i,j+1/2,\kappa}+\frac{1}{2}\left(\frac{\varepsilon f}{D_h}\left|w^m\right|(\rho w)^{m+1}\right)_{i,j+1/2,\kappa}=0$$

As remarked before, convective and diffusive terms are treated explicitly with respect to time, pressure terms implicitly and the term representing friction pressure drops is treated half-implicitly. ϑ_m $(0\leq\vartheta_m\leq 1)$ is a time-discretization parameter for the pressure terms in the momentum equations. The last term of eq. B.1 (17) has been rewritten taking into account that

$$\frac{S_w}{V}=\varepsilon\frac{S_w}{V_f}=\frac{\varepsilon P_w}{S_f}=\varepsilon\frac{4}{D_h} \qquad (3)$$

$$f=4\chi \qquad (4)$$

where

D_h = hydraulic diameter [m]

S_f = cross flow area for the fluid [m^2]

ρ_w = wetted wall perimeter [m]

f, χ = friction coefficients.

Letting

$$FC\emptyset Z = \frac{f|W^n|}{2\,D_h} \tag{5}$$

$$FWZ = \frac{1}{1+\Delta t_n \cdot \frac{f|W^n|}{2D_h}} = \frac{1}{1+\Delta t_n \cdot FC\emptyset Z} \tag{6}$$

eq. (2) can be rewritten

$$\left(\rho W\right)^{n+1}_{i,j+1/2,K} =$$

$$= \left\{ \left(\rho W\right)^{n}_{i,j+1/2,K} - \frac{\theta_m \Delta t_m}{\Delta z_{j+1/2}} \left[P^{n+1}_{i,j+1,K} - P^{n+1}_{i,j,K} \right] + \right.$$

$$- \frac{(1-\theta_m)\,\Delta t_m}{\Delta z_{j+1/2}} \left[P^{n}_{i,j+1,K} - P^{n}_{i,j,K} \right] + \tag{7}$$

$$\left. - \frac{\Delta t_m}{\rho_{i,j+1/2,K}} \left(CVZZ + CVZR + CVZT - FZZ - FZR - FZT - GVZ \right)^{n}_{i,j+1/2,K} \right\} FWZ^{n}_{i,j+\frac{1}{2},K}.$$

b) Radial momentum equation

Space and time discretization of eq. B.1 (18) for control volume V_{II} shown in fig. 2 yields

$$\varepsilon_{i+1/2,j,K}\ \frac{(\rho u)^{n+1}_{i+1/2,j,K} - (\rho u)^{n}_{i+1/2,j,K}}{\Delta t_m} +$$

$$+ \frac{\varepsilon_{i+\frac{1}{2},jK}}{\Delta z_j}\left[(\rho u w)^{n}_{i+1/2,\ j+1/2,K} - (\rho u w)^{n}_{i+1/2,\ j-1/2,K}\right] +$$

$$+ \frac{1}{\Delta r_{i+1/2}}\left[(\psi F \rho u^2)^{n}_{i+1,\ jK} - (\psi F \rho u^2)^{n}_{ijK}\right] + \frac{1}{\Delta \vartheta_K}\left[\left(\frac{\xi \rho u v}{\cos\beta}\right)^{n}_{i+\frac{1}{2},j,\ K+1/2} - \left(\frac{\xi \rho u v}{\cos\beta}\right)^{n}_{i+\frac{1}{2},j,\ K-1/2}\right] +$$

$$- \frac{\varepsilon_{i+\frac{1}{2},jK}}{\Delta z_j}\left[\left(\mu \frac{\partial u}{\partial z}\right)^{n}_{i+1/2,\ j+1/2,K} - \left(\mu \frac{\partial u}{\partial z}\right)^{n}_{i+1/2,\ j-1/2,K}\right] - \frac{1}{\Delta r_{i+\frac{1}{2}}}\left[\left(\psi F \mu \frac{\partial u}{\partial r}\right)^{n}_{i+1,\ jK} - \left(\psi F \mu \frac{\partial u}{\partial r}\right)^{n}_{ijK}\right] +$$

$$- \frac{1}{\Delta \vartheta_K}\left[\left(\frac{\xi \mu \frac{\partial u}{\partial \vartheta}}{\cos\beta}\right)^{n}_{i+1/2,j,\ K+1/2} - \left(\frac{\xi \mu \frac{\partial u}{\partial \vartheta}}{\cos\beta}\right)^{n}_{i+1/2,j,\ K-1/2}\right] +$$

$$+ \frac{\vartheta_m}{\Delta r_{i+\frac{1}{2}}}\left[P^{m+1}_{i+1,jK} - P^{m+1}_{ijK}\right] + \frac{(1-\vartheta_m)}{\Delta r_{i+1/2}}\left[P^{m}_{i+1,jK} - P^{m}_{ijK}\right] +$$

$$+ \frac{1}{2}\left(\varepsilon \frac{\rho w}{S_f} f \left|u^{*m}\right| (\rho u^{m+1})\right)_{i+\frac{1}{2},j,K} = 0 \qquad (8)$$

The velocity u^* in last term of ep. (8) is defined by

$$u^* = u\left[\frac{4P - \pi D}{4(P-D)}\right]^2 \qquad (9)$$

where D is the pin diameter and P the pitch.

Letting

$$FC\emptyset R = \frac{\rho_w}{S_f}\,\frac{f}{2}\,|u^{*m}| \tag{10}$$

$$FWR = \frac{1}{1+\Delta t_m \frac{\rho_w}{S_f}\frac{f}{2}|u^{*m}|} = \frac{1}{1+\Delta t_m \cdot FC\emptyset R} \tag{11}$$

eq. (8) can be rewritten

$$(\rho u)^{m+1}_{i+1/2,j,k} = \tag{12}$$

$$= \Bigg\{ (\rho u)^{m}_{i+1/2,j,k} - \frac{\vartheta_m \Delta t_m}{\varepsilon_{i+\frac{1}{2},j,k}\cdot \Delta\eta_{i+\frac{1}{2}}}\left[p^{m+1}_{i+1,j,k} - p^{m+1}_{i,j,k}\right] +$$

$$- \frac{(1-\vartheta_m)\,\Delta t_m}{\varepsilon_{i+\frac{1}{2},j,k}\cdot \Delta\eta_{i+\frac{1}{2}}}\left[p^{m}_{i+1,j,k} - p^{m}_{i,j,k}\right] +$$

$$- \frac{\Delta t_m}{\varepsilon_{i+\frac{1}{2},j,k}}\Big(CVRz + CVRR + CVRT - FRz - FRR - FRT\Big)^{m}_{i+\frac{1}{2},j,k} \Bigg\} FWR^{m}_{i+\frac{1}{2},j,k}$$

c) Azimuthal momentum equation

Space and time discretization of eq. B.1 (19) for the control volume V_{IV} of fig. 2 yields

$$\varepsilon_{i,j,k+\frac{1}{2}} \frac{(\rho v)^{n+1}_{i,j,k+1/2} - (\rho v)^{n}_{i,j,k+1/2}}{\Delta t_n} + \tag{13}$$

$$+ \frac{\varepsilon_{i,j,k+\frac{1}{2}}}{\Delta z_j}\left[(\rho v w)^{n}_{i,j+\frac{1}{2}} - (\rho v w)^{n}_{i,j-\frac{1}{2}}\right]_{k+1/2} + \frac{1}{\Delta x_i}\left[(\psi F \rho v u)^{n}_{i+\frac{1}{2},j} - (\psi F \rho v u)^{n}_{i-1/2,j}\right]_{k+1/2} +$$

$$+ \frac{1}{(\Delta s \cdot \cos\beta)_{i,j}}\left[(\xi \rho v^2)^{n}_{i,j,k+1} - (\xi \rho v^2)^{n}_{i,j,k}\right]_{k+1/2} +$$

$$- \frac{\varepsilon_{i,j,k+1/2}}{\Delta z_j}\left[\left(\mu \frac{\partial v}{\partial z}\right)^{n}_{i,j+1/2} - \left(\mu \frac{\partial v}{\partial z}\right)^{n}_{i,j-1/2}\right]_{k+1/2} - \frac{1}{\Delta x_i}\left[\left(\psi F \mu \frac{\partial v}{\partial x}\right)^{n}_{i+\frac{1}{2},j} - \left(\psi F \mu \frac{\partial v}{\partial x}\right)^{n}_{i-\frac{1}{2},j}\right]_{k+1/2} +$$

$$- \frac{1}{(\Delta s \cdot \cos\beta)_{i,j,k+1/2}}\left[\left(\xi \mu \frac{\partial v}{\partial s}\right)^{n}_{i,j,k+1} - \left(\xi \mu \frac{\partial v}{\partial s}\right)^{n}_{i,j,k}\right] +$$

$$+ \frac{\theta_m}{(\Delta s)_{i,j,k+1/2}}\left[p^{m+1}_{i,j,k+1} - p^{m+1}_{i,j,k}\right] + \frac{(1-\theta_m)}{(\Delta s)_{i,j,k+1/2}}\left[p^{n}_{i,j,k+1} - p^{n}_{i,j,k}\right] +$$

$$+ \frac{1}{2}\left(\varepsilon \frac{\rho_w}{S_f} f \left|v^{*n}\right| \left(\rho v^{n+1}\right)\right)_{i,j,k+1/2} = 0$$

The velocity v^* in last term of eq. (13) is defined by a formula equivalent to (9).

Letting

$$FC\phi T = \frac{\rho_w}{S_f} \frac{f}{2} \left|v^{*n}\right| \tag{14}$$

$$FWT = \frac{1}{1 + \Delta t_n \frac{\rho_w}{S_f} \frac{f}{2} \left|v^{*n}\right|} = \frac{1}{1 + \Delta t_n \cdot FC\phi T} \tag{15}$$

eq. (13) can be written

$$\left(\rho v\right)^{m+1}_{i,j,k+1/2} = \tag{16}$$

$$= \left\{ \left(\rho v\right)^{m}_{i,j,k+1/2} - \frac{\vartheta_m \Delta t_m}{\varepsilon_{i,j,k+\frac{1}{2}} \left(\Delta y\right)_{i,j,k+1/2}} \cdot \left[p^{m+1}_{i,j,k+1} - p^{m+1}_{i,j,k} \right] + \right.$$

$$- \frac{(1-\vartheta_m)\,\Delta t_m}{\varepsilon_{i,j,k+\frac{1}{2}} \left(\Delta y\right)_{i,j,k+1/2}} \cdot \left[p^{m}_{i,j,k+1} - p^{m}_{i,j,k} \right] +$$

$$\left. - \frac{\Delta t_m}{\varepsilon_{i,j,k+1/2}} \left(CVTZ + CVTR + CVTT - FTZ - FTR - FTT \right)^{m}_{\substack{i,j \\ k+1/2}} \right\} FWT^{m}_{\substack{i,j \\ k+1/2}}$$

Equations (7), (12), (16) are the basic equations for the calculation of the mass flows, when the updated pressure field has been obtained (see section 2.5).

iii) Energy equation

The volume-averaged energy equation B.1. (22) is discretized with reference to the control volume V_I shown in fig. 2 . All terms are treated explicitly with respect to time. The discretized equation is as follows:

(17)

$$\varepsilon_{i,j,k}\frac{(\rho h)^{n+1}_{i,j,k}-(\rho h)^{n}_{i,j,k}}{\Delta t_m}+\frac{\varepsilon_{i,j,k}}{\Delta z_j}\left[(\rho h w)^{n}_{i,j+\frac{1}{2},k}-(\rho h w)^{n}_{i,j-\frac{1}{2},k}\right]+$$

$$+\frac{1}{\Delta x_i}\left[(\psi F \rho h u)^{n}_{i+1/2,\,j,k}-(\psi F \rho h u)^{n}_{i-1/2,\,j,k}\right]+\frac{1}{\Delta y_k}\left[\left(\frac{\xi \rho h v}{\cos\beta}\right)^{n}_{i,j,\,k+1/2}-\left(\frac{\xi \rho h v}{\cos\beta}\right)^{n}_{i,j,\,k-1/2}\right]+$$

$$-\frac{\varepsilon_{i,j,k}}{\Delta z_j}\left[\left(\rho\tilde{\alpha}\frac{\partial h}{\partial t}\right)^{n}_{i,j+1/2,\,k}-\left(\rho\tilde{\alpha}\frac{\partial h}{\partial t}\right)^{n}_{i,j-1/2,\,k}\right]-\frac{1}{\Delta x_i}\left[\left(\psi F\tilde{\alpha}\frac{\partial h}{\partial x}\right)^{n}_{i+1/2,\,j,k}-\left(\psi F d\rho\frac{\partial h}{\partial x}\right)^{n}_{i-1/2,\,j,k}\right]+$$

$$-\frac{1}{\Delta y_k}\left[\left(\frac{\xi\tilde{\alpha}\frac{\partial h}{\partial y}}{\cos\beta}\right)^{n}_{i,j,\,k+1/2}-\left(\frac{\xi\tilde{\alpha}\frac{\partial h}{\partial y}}{\cos\beta}\right)^{n}_{i,j,\,k-1/2}\right]-\qquad Q^{n}_{i,j,k}=0$$

2.3 Derivation of a Poisson - like equation for the coolant pressure distribution

The ICE technique allows to derive a difference equation for pressure values from the continuity and momentum equations as it would be obtained discretizing a Poisson equation. From the practical viewpoint the procedure is as follows:

Consider the finite differences form of the volume averaged continuity equation (1). Replace the values of the mass flows at time level n+1 by using the momentum equations (7), (12), (16) written for the nodes i, j±1/2, k/ i±1/2, j,k/ i, j, k±1/2 respectively. From the equation of state replace the time-difference of coolant density in (1) by

$$\rho^{n+1}_{i,j,k}-\rho^{n}_{i,j,k}=\frac{1}{c^2_{i,j,k}}\left(p^{n+1}_{i,j,k}-p^{n}_{i,j,k}\right) \tag{18}$$

with

$$c^2=dp/d\rho. \tag{19}$$

Rearranging one derives a linear algebraic equation for the unkowns

$$p^{n+1}_{i,j,k},\quad p^{n+1}_{i+1,j,k},\quad p^{n+1}_{i-1,j,k},\quad p^{n+1}_{i,j+1,k},\quad p^{n+1}_{i,j-1,k},\quad p^{n+1}_{i,j,k+1},\quad p^{n+1}_{i,j,k-1}$$

which can be written

$$
\begin{aligned}
&- p^{m+1}_{i,j+1,k}\left[\frac{\varepsilon_{i,j,k}}{\Delta z_j \cdot \Delta z_{j+1/2}}\right] \cdot FWZ^{m}_{i,j+1/2,k} \cdot \vartheta_c \vartheta_m \Delta t_m^2 + \\
&- p^{m+1}_{i,j-1,k}\left[\frac{\varepsilon_{i,j,k}}{\Delta z_j \cdot \Delta z_{j-1/2}}\right] \cdot FWZ^{m}_{i,j-1/2,k} \cdot \vartheta_c \vartheta_m \Delta t_m^2 + \\
&- p^{m+1}_{i+1,j,k}\left[\frac{\psi_{i+1/2,j,k} \cdot FACCP_i}{\varepsilon_{i+1/2,j,k} \cdot \Delta r_i \cdot \Delta r_{i+1/2}}\right] \cdot FWR^{m}_{i+1/2,j,k} \cdot \vartheta_c \vartheta_m \Delta t_m^2 + \\
&- p^{m+1}_{i-1,j,k}\left[\frac{\psi_{i-1/2,j,k} \cdot FACCM_i}{\varepsilon_{i-1/2,j,k} \cdot \Delta r_i \cdot \Delta r_{i-1/2}}\right] \cdot FWR^{m}_{i-1/2,j,k} \cdot \vartheta_c \vartheta_m \Delta t_m^2 + \\
&- p^{m+1}_{i,j,k+1}\left[\frac{\xi_{i,j,k+1/2}}{\varepsilon_{i,j,k+1/2} \cdot \Delta \vartheta_k \cdot \Delta \vartheta_{k+1/2} \cdot \cos\beta^2_{k+1/2}}\right] \cdot FWT^{m}_{i,j,k+1/2} \cdot \vartheta_c \vartheta_m \Delta t_m^2 + \\
&- p^{m+1}_{i,j,k-1}\left[\frac{\xi_{i,j,k-1/2}}{\varepsilon_{i,j,k-1/2} \cdot \Delta \vartheta_k \cdot \Delta \vartheta_{k-1/2} \cdot \cos\beta^2_{k-1/2}}\right] \cdot FWT^{m}_{i,j,k-1/2} \cdot \vartheta_c \vartheta_m \Delta t_m^2 + \\
&+ p^{m+1}_{i,j,k}\left\{\left[\frac{\varepsilon_{i,j,k}}{\Delta z_j \cdot \Delta z_{j+1/2}} \cdot FWZ^{m}_{i,j+1/2,k} + \frac{\varepsilon_{i,j,k}}{\Delta z_j \cdot \Delta z_{j-1/2}} \cdot FWZ^{m}_{i,j-1/2,k} + \right.\right. \\
&\quad + \frac{\psi_{i+1/2,j,k} \cdot FACCP_i}{\varepsilon_{i+1/2,j,k} \cdot \Delta r_i \cdot \Delta r_{i+1/2}} \cdot FWR^{m}_{i+1/2,j,k} + \frac{\psi_{i-1/2,j,k} \cdot FACCM_i}{\varepsilon_{i-1/2,j,k} \cdot \Delta r_i \cdot \Delta r_{i-1/2}} \cdot FWR^{m}_{i-1/2,j,k} + \\
&\quad \left.\left. + \frac{\xi_{i,j,k+1/2}}{\varepsilon_{i,j,k+1/2} \cdot \Delta \vartheta_k \cdot \Delta \vartheta_{k+1/2} \cdot \cos\beta^2_{k+1/2}} \cdot FWT^{m}_{i,j,k+1/2} + \frac{\xi_{i,j,k-1/2}}{\varepsilon_{i,j,k-1/2} \cdot \Delta \vartheta_k \cdot \Delta \vartheta_{k-1/2} \cdot \cos\beta^2_{k-1/2}} \cdot FWT^{m}_{i,j,k-1/2}\right] \cdot \right. \\
&\quad \left. \cdot \vartheta_c \vartheta_m \Delta t_m^2 + \frac{\varepsilon_{i,j,k}}{c^2{}^{m}_{i,j,k}}\right\} = G^{m}_{i,j,k} \cdot
\end{aligned}
\tag{20}
$$

The right-hand side G^n_{ijk} is given fully in the next equation. We introduce the coefficients CKN, CKS, CKW, CKE, CKTP, CKTM (defined in the list at the end of this section) which depend only on the bundle geometry and discretization. Dropping the subscripts ijk for these geometry coefficients, eq. (20) can be written:

$$
\begin{aligned}
&\Big\{ -\rho^{m+1}_{i,j+1,k} \cdot CKN \cdot FWZ^{m}_{i,j+\frac{1}{2},k} - \rho^{m+1}_{i,j-1,k} \cdot CKS \cdot FWZ^{m}_{i,j-\frac{1}{2},k} + \\
&- \rho^{m+1}_{i+1,jk} \cdot CKE \cdot FWR^{m}_{i+\frac{1}{2},jk} - \rho^{m+1}_{i-1,jk} \cdot CKW \cdot FWR^{m}_{i-\frac{1}{2},jk} + \\
&- \rho^{m+1}_{ij,k+1} \cdot CKTP \cdot FWT^{m}_{\substack{ij \\ k+\frac{1}{2}}} - \rho^{m+1}_{ij,k-1} \cdot CKTM \cdot FWT^{m}_{\substack{ij \\ k-\frac{1}{2}}} \Big\} \vartheta_c \vartheta_m \Delta t_m^2 + \\
&+ \rho^{m+1}_{ijk} \Big\{ \Big[CKN \cdot FWZ^{m}_{i,j+\frac{1}{2},k} + CKS \cdot FWZ^{m}_{i,j-\frac{1}{2},k} + \\
&\qquad + CKE \cdot FWR^{m}_{\substack{i+\frac{1}{2} \\ jk}} + CKW \cdot FWR^{m}_{i-\frac{1}{2},jk} + \\
&\qquad + CKTP \cdot FWT^{m}_{\substack{ij \\ k+\frac{1}{2}}} + CKTM \cdot FWT^{m}_{\substack{ij \\ k-\frac{1}{2}}} \Big] \vartheta_c \vartheta_m \Delta t_m^2 + \\
&\qquad + \varepsilon_{ijk} / c^2 {}^{m}_{ijk} \Big\} = \qquad (21)
\end{aligned}
$$

$$
\begin{aligned}
= \Big\{ &\rho^{m}_{i,j+1,k} \cdot CKN \cdot FWZ^{m}_{i,j+\frac{1}{2},k} + \rho^{m}_{i,j-1,k} \cdot CKS \cdot FWZ^{m}_{i,j-\frac{1}{2},k} + \\
&+ \rho^{m}_{i+1,jk} \cdot CKE \cdot FWR^{m}_{i+\frac{1}{2},jk} + \rho^{m}_{i-1,jk} \cdot CKW \cdot FWR^{m}_{i-\frac{1}{2},jk} + \\
&+ \rho^{m}_{ij,k+1} \cdot CKTP \cdot FWT^{m}_{\substack{ij \\ k+\frac{1}{2}}} + \rho^{m}_{\substack{ij \\ k-1}} \cdot CKTM \cdot FWT^{m}_{\substack{ij \\ k-\frac{1}{2}}} \Big\} \vartheta_c (1-\vartheta_m) \Delta t_m^2 +
\end{aligned}
$$

$$
\begin{aligned}
&- P^{m}_{i,j,k}\Big[CKN \cdot FWZ^{m}_{i,j+1/2,k} + CKS \cdot FWZ^{m}_{i,j-1/2,k} + \\
&\quad + CKE \cdot FWR^{m}_{i+1/2,j,k} + CKW \cdot FWR^{m}_{i-1/2,j,k} + \\
&\quad + CKTP \cdot FWT^{m}_{\substack{i,j\\ k+1/2}} + CKTM \cdot FWT^{m}_{\substack{i,j\\ k-1/2}} \Big] \vartheta_c (1-\vartheta_m)\,\Delta t_m^2 + \\
&- \frac{\vartheta_c \Delta t_m\, \varepsilon_{i,j,k}}{\Delta z_j}\Big[(\rho w \cdot FWZ)^{m}_{i,j+1/2,k} - (\rho w \cdot FWZ)^{m}_{i,j-1/2,k} \Big] + \\
&- \frac{(1-\vartheta_c)\,\Delta t_m\, \varepsilon_{i,j,k}}{\Delta z_j}\Big[(\rho w)^{m}_{i,j+1/2,k} - (\rho w)^{m}_{i,j-1/2,k} \Big] + \\
&- \frac{\vartheta_c \Delta t_m}{\Delta r_i}\Big[(\psi \rho u \cdot FWR)^{m}_{i+1/2,j,k} \cdot FACCP_i - (\psi \rho u \cdot FWR)^{m}_{i-1/2,j,k} \cdot FACCM_i \Big] + \qquad (21) \\
&- \frac{(1-\vartheta_c)\,\Delta t_m}{\Delta r_i}\Big[(\psi \rho u)^{m}_{i+1/2,j,k} \cdot FACCP_i - (\psi \rho u)^{m}_{i-1/2,j,k} \cdot FACCM_i \Big] + \\
&- \frac{\vartheta_c \Delta t_m}{\Delta s_k}\Big[\left(\frac{\xi \rho v \cdot FWT}{\cos\beta} \right)^{m}_{i,j,k+1/2} - \left(\frac{\xi \rho v \cdot FWT}{\cos\beta} \right)^{m}_{i,j,k-1/2} \Big] + \\
&- \frac{(1-\vartheta_c)\,\Delta t_m}{\Delta s_k}\Big[\left(\frac{\xi \rho v}{\cos\beta} \right)^{m}_{i,j,k+1/2} - \left(\frac{\xi \rho v}{\cos\beta} \right)^{m}_{i,j,k-1/2} \Big] + \\
&+ \frac{\vartheta_c \Delta t_m^2}{\Delta z_j} \cdot \frac{\varepsilon_{i,j,k}}{\varepsilon_{i,j+1/2,k}} \Big(CVZZ + CVZR + CVZT - FZZ - FZR - FZT - GVZ \Big)^{m}_{\substack{i,j+\frac{1}{2}\\ k}} \cdot FWZ^{m}_{\substack{i,j+\frac{1}{2}\\ k}} + \\
&- \frac{\vartheta_c \Delta t_m^2}{\Delta z_j} \cdot \frac{\varepsilon_{i,j,k}}{\varepsilon_{i,j-1/2,k}} \Big(CVZZ + CVZR + CVZT - FZZ - FZR - FZT - GVZ \Big)^{m}_{\substack{i,j-\frac{1}{2}\\ k}} \cdot FWZ^{m}_{\substack{i,j-1/2\\ k}} + \\
&+ \frac{\vartheta_c \Delta t_m^2}{\Delta r_i} \cdot \frac{\psi_{i+1/2} \cdot FACCP_i}{\varepsilon_{i+1/2,j,k}} \Big(CVRZ + CVRR + CVRT - FRZ - FRR - FRT \Big)^{m}_{\substack{i+1/2\\ j,k}} \cdot FWR^{m}_{\substack{i+1/2\\ j,k}} + \\
&- \frac{\vartheta_c \Delta t_m^2}{\Delta r_i} \cdot \frac{\psi_{i-1/2} \cdot FACCM_i}{\varepsilon_{i-1/2,j,k}} \Big(CVRZ + CVRR + CVRT - FRZ - FRR - FRT \Big)^{m}_{\substack{i-1/2\\ j,k}} \cdot FWR^{m}_{\substack{i-1/2\\ j,k}} +
\end{aligned}
$$

(21)

$$+\frac{\vartheta_c \Delta t_m^2 \cdot \varepsilon_{i,j,k+1/2}}{\Delta z_k \cdot \cos\beta_{k+1/2} \cdot \varepsilon_{i,j,k+1/2}} \left(CVTZ + CVTR + CVTT - FTZ - FTR - FTT \right)^{m}_{\substack{i,j \\ k+1/2}} \cdot FWT^{m}_{\substack{i,j \\ k+1/2}} +$$

$$-\frac{\vartheta_c \Delta t_m^2 \cdot \varepsilon_{i,j,k-1/2}}{\Delta z_k \cdot \cos\beta_{k-1/2} \cdot \varepsilon_{i,j,k-1/2}} \left(CVTZ + CVTR + CVTT - FTZ - FTR - FTT \right)^{m}_{\substack{i,j \\ k-1/2}} \cdot FWT^{m}_{\substack{i,j \\ k-1/2}} +$$

$$+ \varepsilon_{i,j,k} \frac{p^{m}_{i,j,k}}{c^{2\,m}_{i,j,k}} .$$

Equation (21) can be written in the following compact form (ratios of volume porosities at different axial locations are equal to one in undisturbed geometry and are therefore dropped as multiplying factor):

$$\left\{ - p^{m+1}_{i,j+1,k} \cdot CKN^* - p^{m+1}_{i,j-1,k} \cdot CKS^* - p^{m+1}_{i+1,j,k} \cdot CKE^* - p^{m+1}_{i-1,j,k} \cdot CKW^* + \right.$$

$$\left. - p^{m+1}_{i,j,k+1} \cdot CKTP^* - p^{m+1}_{i,j,k-1} \cdot CKTM^* \right\} \vartheta_c \vartheta_m \Delta t_m^2 +$$

$$+ p^{m+1}_{i,j,k} \left\{ CKC^* \vartheta_c \vartheta_m \Delta t_m^2 + \varepsilon_{i,j,k} / c^{2\,m}_{i,j,k} \right\} = \qquad (22)$$

$$= PRS^{m}_{i,j,k} + PRC^{m}_{i,j,k} - FLUZ^{m}_{i,j,k} - FLUR^{m}_{i,j,k} - FLUT^{m}_{i,j,k} +$$

$$+ \frac{\vartheta_c \Delta t_m^2}{\Delta z_j} \left[\left(SZ \cdot FWZ \right)^{m}_{i,j+1/2,k} - \left(SZ \cdot FWZ \right)^{m}_{i,j-1/2,k} \right] +$$

$$+ \frac{\vartheta_c \Delta t_m^2}{\Delta r_i} \left[\frac{\psi_{i+1/2,j,k}}{\varepsilon_{i+1/2,j,k}} \left(SR \cdot FWR \right)^{m}_{i+1/2,j,k} \cdot FACCP_i - \frac{\psi_{i-1/2,j,k}}{\varepsilon_{i-1/2,j,k}} \left(SR \cdot FWR \right)^{m}_{i-1/2,j,k} \cdot FACCM_i \right] +$$

$$+ \frac{\vartheta_c \Delta t_m^2}{\Delta z_k} \left[\frac{\varepsilon_{i,j,k+1/2}}{(\cos\beta \cdot \varepsilon)_{i,j,k+1/2}} \left(ST \cdot FWT \right)^{m}_{i,j,k+1/2} - \frac{\varepsilon_{i,j,k-1/2}}{(\cos\beta \cdot \varepsilon)_{\substack{i,j \\ k-1/2}}} \left(ST \cdot FWT \right)^{m}_{\substack{i,j \\ k-1/2}} \right] +$$

$$+ \varepsilon_{i,j,k} \frac{p^{m}_{i,j,k}}{c^{2\,m}_{i,j,k}} .$$

The numerical solution of the discrete Poisson - like equation (22) is explained in the next section.

List of Symbols used in the previous equations.

$$CKN_{i,j,k} = \frac{\varepsilon_{i,j,k}}{\Delta z_j \cdot \Delta z_{j+1/2}} \tag{23}$$

$$CKS_{i,j,k} = \frac{\varepsilon_{i,j,k}}{\Delta z_j \cdot \Delta z_{j-1/2}} \tag{24}$$

$$CKE_{i,j,k} = \frac{\psi_{i+1/2,j,k} \cdot FACCP_i}{\varepsilon_{i+1/2,j,k} \cdot \Delta r_i \cdot \Delta r_{i+1/2}} \tag{25}$$

$$CKW_{i,j,k} = \frac{\psi_{i-1/2,j,k} \cdot FACCM_i}{\varepsilon_{i-1/2,j,k} \cdot \Delta r_i \cdot \Delta r_{i-1/2}} \tag{26}$$

$$CKTP_{i,j,k} = \frac{\varepsilon_{i,j,k+1/2}}{\varepsilon_{i,j,k+1/2} \cdot \Delta \vartheta_k \cdot \Delta \vartheta_{k+1/2} \cdot \cos\beta^2_{k+1/2}} \tag{27}$$

$$CKTM_{i,j,k} = \frac{\varepsilon_{i,j,k-1/2}}{\varepsilon_{i,j,k-1/2} \cdot \Delta \vartheta_k \cdot \Delta \vartheta_{k-1/2} \cdot \cos\beta^2_{k-1/2}} \tag{28}$$

$$CKC_{i,j,k} = \left(CKN + CKS + CKE + CKW + CKTP + CKTM\right)_{i,j,k} \tag{29}$$

$$CKN^*_{i,j,k} = CKN_{i,j,k} \cdot \overset{\sim}{FWZ}_{i,j+1/2,k} \tag{30}$$

$$CKS^*_{i,j,k} = CKS_{i,j,k} \cdot \overset{\sim}{FWZ}_{i,j-1/2,k} \tag{31}$$

$$CKE^*_{i,j,k} = CKE_{i,j,k} \cdot \overset{\sim}{FWR}_{i+1/2,j,k} \tag{32}$$

$$CKW^*_{i,j,k} = CKW_{i,j,k} \cdot \overset{\sim}{FWR}_{i-1/2,j,k} \tag{33}$$

$$CKTP^*_{i,j,k} = CKTP_{i,j,k} \cdot \overset{\sim}{FWT}_{i,j,k+1/2} \tag{34}$$

$$CKTM^*_{i,j,k} = CKTM_{i,j,k} \cdot \overset{\sim}{FWT}_{i,j,k-1/2} \tag{35}$$

$$CKC^{*}_{i,j,k} = CKN^{*}_{i,j,k} + CKS^{*}_{i,j,k} + CKE^{*}_{i,j,k} + CKW^{*}_{i,j,k} + CKTP^{*}_{i,j,k} + CKTM^{*}_{i,j,k} \quad (36)$$

$$FWZ^{m}_{i,j\pm 1/2,k} = 1/\left(1 + \Delta t_m \cdot FCOZ^{m}_{j\pm 1/2}\right) \quad (37)$$

$$FWR^{m}_{i\pm 1/2,j,k} = 1/\left(1 + \Delta t_m \cdot FCOR^{m}_{i\pm 1/2}\right) \quad (38)$$

$$FWT^{m}_{i,j,k\pm 1/2} = 1/\left(1 + \Delta t_m \cdot FCOT^{m}_{k\pm 1/2}\right) \quad (39)$$

$$FCOZ^{m}_{j\pm 1/2} = \frac{f \cdot \left| W^{m}_{i,j\pm 1/2,k} \right|}{2 D_R} \quad (40)$$

$$FCOR^{m}_{i\pm 1/2} = \frac{1}{2}\left(\frac{\rho_w}{S_f}\right)_{i\pm 1/2} \cdot f \left| u^{*m}_{i\pm 1/2,j,k} \right| \quad (41)$$

$$FCOT^{m}_{k\pm 1/2} = \frac{1}{2}\left(\frac{\rho_w}{S_f}\right)_{k\pm 1/2} \cdot f \left| v^{*m}_{i,j,k\pm 1/2} \right| \quad (42)$$

$$CVZZ^{m}_{i,j+1/2,k} = \frac{\varepsilon_{i,j+1/2,k}}{\Delta z_{j+1/2}} \left[\left(\rho w^2\right)^{m}_{i,j+1,k} - \left(\rho w^2\right)^{m}_{i,j,k} \right] \quad (43)$$

$$CVZR^{m}_{i,j+1/2,k} = \frac{1}{\Delta r_i} \left[\left(\psi \rho w u\right)^{m}_{\substack{i+1/2 \\ j+1/2,k}} \cdot FACCP_i - \left(\psi \rho w u\right)^{m}_{\substack{i-1/2 \\ j+1/2,k}} \cdot FACCM_i \right] \quad (44)$$

$$CVZT^{m}_{i,j+\frac{1}{2},k} = \frac{1}{\Delta \vartheta_k} \left[\left(\frac{\xi \rho w v}{\cos\beta} \right)^{m}_{i,j+1/2,k+1/2} - \left(\frac{\xi \rho w v}{\cos\beta} \right)^{m}_{\substack{i,j+1/2, \\ k-1/2}} \right] \quad (45)$$

$$FZZ^{m}_{i,j+1/2,k} = \frac{\varepsilon_{i,j+1/2,k}}{\Delta z_{j+1/2}} \left[\left(\mu \frac{\partial w}{\partial z}\right)^{m}_{i,j+1,k} - \left(\mu \frac{\partial w}{\partial z}\right)^{m}_{i,j,k} \right] \quad (46)$$

$$FZR^{m}_{i,j+\frac{1}{2},k} = \frac{1}{\Delta x_i}\left[\left(\psi\mu\frac{\partial w}{\partial x}\right)^{m}_{i+1/2,\,j+1/2,k}\cdot FACCP_i - \left(\psi\mu\frac{\partial w}{\partial x}\right)^{m}_{i-1/2,\,j+1/2,k}\cdot FACCM_i\right] \tag{47}$$

$$FZT^{m}_{i,j+1/2,k} = \frac{1}{\Delta s_k}\left[\left(\frac{\xi\mu\frac{\partial w}{\partial s}}{\cos\beta}\right)^{m}_{i,\,j+1/2,\,k+1/2} - \left(\frac{\xi\mu\frac{\partial w}{\partial s}}{\cos\beta}\right)^{m}_{i,\,j+1/2,\,k-1/2}\right] \tag{48}$$

$$GVZ^{m}_{i,j+1/2,k} = g\,(\xi\varrho)^{m}_{i,j+1/2,k} \tag{49}$$

$$CVRZ^{m}_{i+1/2,j,k} = \frac{\xi_{i+1/2,j,k}}{\Delta z_j}\left[(\varrho u w)^{m}_{i+1/2,j+1/2,k} - (\varrho u w)^{m}_{i+1/2,j-1/2,k}\right] \tag{50}$$

$$CVRR^{m}_{i+1/2,j,k} = \frac{1}{\Delta x_{i+1/2}}\left[(\psi\varrho u^2)^{m}_{i+1,j,k}\cdot FACRP_{i+1/2} - (\psi\varrho u^2)^{m}_{i,j,k}\cdot FACRM_{i+1/2}\right] \tag{51}$$

$$CVRT^{m}_{i+1/2,j,k} = \frac{1}{\Delta s_k}\left[\left(\frac{\xi\varrho u v}{\cos\beta}\right)^{m}_{i+1/2,\,j,\,k+1/2} - \left(\frac{\xi\varrho u v}{\cos\beta}\right)^{m}_{i+1/2,\,j,\,k-1/2}\right] \tag{52}$$

$$FRZ^{m}_{i+1/2,j,k} = \frac{\xi_{i+1/2,j,k}}{\Delta z_j}\left[\left(\mu\frac{\partial u}{\partial z}\right)^{m}_{i+1/2,\,j+1/2,k} - \left(\mu\frac{\partial u}{\partial z}\right)^{m}_{i+1/2,\,j-1/2,k}\right] \tag{53}$$

$$FRR^{m}_{i+1/2,j,k} = \frac{1}{\Delta x_{i+1/2}}\left[\left(\psi\mu\frac{\partial u}{\partial x}\right)^{m}_{i+1,\,j,k}\cdot FACRP_{i+1/2} - \left(\psi\mu\frac{\partial u}{\partial x}\right)_{i,j,k}\cdot FACRM_{i+1/2}\right] \tag{54}$$

$$FRT^{m}_{i+1/2,j,k} = \frac{1}{\Delta s_k}\left[\left(\frac{\xi\mu\frac{\partial u}{\partial s}}{\cos\beta}\right)^{m}_{i+1/2,\,j,\,k+1/2} - \left(\frac{\xi\mu\frac{\partial u}{\partial s}}{\cos\beta}\right)^{m}_{i+1/2,\,j,\,k-1/2}\right] \tag{55}$$

$$CVTZ^{m}_{i,j,k+1/2} = \frac{\xi_{i,j,k+1/2}}{\Delta z_j}\left[(\varrho v w)^{m}_{i,\,j+1/2,\,k+1/2} - (\varrho v w)^{m}_{i,\,j-1/2,\,k+1/2}\right] \tag{56}$$

$$CVTR^{m}_{i,j,k+\frac{1}{2}} = \frac{1}{\Delta r_i}\left[\left(\psi \varrho v u\right)^{m}_{i+1/2,j,\,k+1/2} \cdot FACCP_i - \left(\psi \varrho v u\right)^{m}_{i-1/2,j,\,k+1/2} \cdot FACCM_i\right] \quad (57)$$

$$CVTT^{m}_{i,j,k+1/2} = \frac{1}{(\Delta s \cdot \cos\beta)_{i,j,\,k+1/2}}\left[\left(\xi \varrho v^2\right)^{m}_{i,j,k+1} - \left(\xi \varrho v^2\right)^{m}_{i,j,k}\right] \quad (58)$$

$$FTZ^{m}_{i,j,k+1/2} = \frac{\varepsilon_{i,j,k+1/2}}{\Delta z_j}\left[\left(\mu \frac{\partial v}{\partial z}\right)^{m}_{i,j+1/2,\,k+1/2} - \left(\mu \frac{\partial v}{\partial z}\right)^{m}_{i,j-1/2,\,k+1/2}\right] \quad (59)$$

$$FTR^{m}_{i,j,k+1/2} = \frac{1}{\Delta r_i}\left[\left(\psi \mu \frac{\partial v}{\partial r}\right)^{m}_{i+1/2,j,\,k+1/2} \cdot FACCP_i - \left(\psi \mu \frac{\partial v}{\partial r}\right)^{m}_{i-1/2,j,\,k+1/2} \cdot FACCM_i\right] \quad (60)$$

$$FTT^{m}_{i,j,k+1/2} = \frac{1}{(\Delta s \cdot \cos\beta)_{i,j,k+1/2}}\left[\left(\xi \mu \frac{\partial v}{\partial s}\right)^{m}_{i,j,\,k+1} - \left(\xi \mu \frac{\partial v}{\partial s}\right)^{m}_{i,j,k}\right] \quad (61)$$

$$FLUZ^{m}_{i,j,k} = \frac{\vartheta_c \Delta t_m \varepsilon_{i,j,k}}{\Delta z_j}\left[\left(\varrho w \cdot FWZ\right)^{m}_{i,j+1/2,k} - \left(\varrho w \cdot FWZ\right)^{m}_{i,j-1/2,k}\right] + \quad (62)$$

$$- \frac{(1-\vartheta_c)\,\Delta t_m\, \varepsilon_{i,j,k}}{\Delta z_j}\left[\left(\varrho w\right)^{m}_{i,j+1/2,k} - \left(\varrho w\right)^{m}_{i,j-1/2,k}\right]$$

$$FLUR^{m}_{i,j,k} = \frac{\vartheta_c \Delta t_m}{\Delta r_i}\left[\left(\psi \varrho u \cdot FWR\right)^{m}_{i+1/2,\,j,k} \cdot FACCP_i - \left(\psi \varrho u \cdot FWR\right)^{m}_{i-1/2,\,j,k} \cdot FACCM_i\right] + \quad (63)$$

$$- \frac{(1-\vartheta_c)\,\Delta t_m}{\Delta r_i}\left[\left(\psi \varrho u\right)_{i+1/2,\,j,k} \cdot FACCP_i - \left(\psi \varrho u\right)_{i-1/2,\,j,k} \cdot FACCM_i\right]$$

$$FLUT^{m}_{i,j,k} = \frac{\vartheta_c \Delta t_m}{\Delta s_k}\left[\left(\frac{\xi \varrho v \cdot FWT}{\cos\beta}\right)^{m}_{i,j,k+1/2} - \left(\frac{\xi \varrho v \cdot FWT}{\cos\beta}\right)^{m}_{i,j,k-1/2}\right] + \quad (64)$$

$$- \frac{(1-\vartheta_c)\,\Delta t_m}{\Delta s_k}\left[\left(\frac{\xi \varrho v}{\cos\beta}\right)^{m}_{i,j,k+1/2} - \left(\frac{\xi \varrho v}{\cos\beta}\right)^{m}_{i,j,k-1/2}\right]$$

$$PRS^{m}_{i,j,k} = \Big\{ p^{m}_{i,j+1,k} \cdot CKN^{*}_{i,j,k} + p^{m}_{i,j-1,k} \cdot CKS^{*}_{i,j,k} + p^{m}_{i+1,j,k} \cdot CKE^{*}_{i,j,k} + p^{m}_{i-1,j,k} \cdot CKW^{*}_{i,j,k} + p^{m}_{i,j,k+1} \cdot CKTP^{*}_{i,j,k} + p^{m}_{i,j,k-1} \cdot CKTM^{*}_{i,j,k} \Big\} \vartheta_c (1-\vartheta_m) \Delta t_m^2 \tag{65}$$

$$PRC^{m}_{i,j,k} = - p^{m}_{i,j,k} \cdot CKC^{*}_{i,j,k} \cdot \vartheta_c (1-\vartheta_m) \Delta t_m^2 =$$

$$= - p^{m}_{i,j,k} \Big\{ CKN^{*}_{i,j,k} + CKS^{*}_{i,j,k} + CKE^{*} + CKW^{*} + CKTP^{*}_{i,j,k} + CKTM^{*}_{i,j,k} \Big\} \vartheta_c (1-\vartheta_m) \Delta t_m^2 \tag{66}$$

$$SZ^{m}_{i,j+1/2,k} = \Big(CVZZ + CVZR + CVZT - GVZ - FZZ - FZR - FZT \Big)^{m}_{i,j+1/2,k} \tag{67}$$

$$SR^{m}_{i+1/2,j,k} = \Big(CVRZ + CVRR + CVRT - FRZ - FRR - FRT \Big)^{m}_{i+1/2,j,k} \tag{68}$$

$$ST^{m}_{i,j,k+1/2} = \Big(CVTZ + CVTR + CVTT - FTZ - FTR - FTT \Big)^{m}_{i,j,k+1/2} \tag{69}$$

$$CMPR^{m}_{i,j,k} = \Big(\varepsilon_{i,j,k} \; / \; C^{2\,m}_{i,j,k} \Big) \; p^{m}_{i,j,k} \tag{70}$$

$$G^{m}_{i,j,k} = \text{Right-hand side of equation (22).} \tag{71}$$

Furthermore, the following symbols are used in the programme:

F1	=	ϑ_c
F9	=	$1 - \vartheta_c$
F2	=	ϑ_m
F8	=	$1 - \vartheta_m$
DZC (JC)	=	Δz_j
DZZ (JZ)	=	$\Delta z_{j+1/2}$
DRC (IC)	=	$\Delta \eta_i$
DRR (IR)	=	$\Delta \eta_{i+1/2}$
PFC (IC)	=	Δs_i
EPS (IC)	=	ε_i
EPR (IR)	=	$\varepsilon_{i+1/2}$
EPT (IT)	=	$\varepsilon_{k+1/2}$
PSI (IC)	=	ψ_i
GSIT (IC,IT)	=	$\varphi_{i,k}$
GSITR (IC,ITR)	=	$\varphi_{i,k+1/2}$
CØSB12 (ITR)	=	$\cos\beta_{k+1/2}$
SFR (IR)	=	$S_{f\,i+1/2}$
SFTR (IC, ITR)	=	$S_{f\,i,k+1/2}$
PAR (IR)	=	$\rho_{w\,i+1/2}$
PATR (IC, ITR)	=	$\rho_{w\,i,k+1/2}$
CF	=	f
SCSQ	=	$c^2_{i,j,k}$
PSIR (IR)	=	$\psi_{i+1/2}$
FACCM(IC)	=	$1 - \frac{\sqrt{3}}{6} \frac{\Delta \eta_i}{\Delta s_k}$
FACCP(IC)	=	$1 + \frac{\sqrt{3}}{6} \Delta \eta_i / \Delta s_k$
FACRM(IR)	=	$1 - 6 \cdot DRR(IR) / (\sqrt{3} \cdot PFC(IC) + 6 \cdot DRR(IR))$
FACRP(IR)	=	$1 + 6 \cdot DRR(IR) / (\sqrt{3} \cdot PFC(IC) + 6 \cdot DRR(IR))$

The following symbols are introduced for saving computing time:

CUC = $\dfrac{4 \cdot PITCH - \pi \cdot DIA}{4\,(PITCH - DIA)}$

UCØL = CUC $\cdot\ \mu$

UCØLT = CUC $\cdot\ \nu$

GUCØL (IR) = $\dfrac{\rho}{2}\left(\dfrac{P_w}{S_f}\right)_{i+1/2}$

GUCØT (IC, ITR) = $\dfrac{\rho}{2}\left(\dfrac{P_w}{S_f}\right)_{i,k+1/2}$

EPDD (IC, JC) = $\varepsilon_i / \Delta z_j$

EPDZ (IC, JZ) = $\varepsilon_i / \Delta z_{j+1/2}$

ERDD (IR, JC) = $\varepsilon_{i+1/2} / \Delta z_j$

PFCØS (IC, ITR) = $\Delta y_i \cdot \cos\beta_{k+1/2}$

CGEP (IC) = $g\,\varepsilon_i$

GSCØS (IC,ITR) = $\varphi_{i,k+1/2} / \cos\beta_{k+1/2}$

GCCØSE (IC, ITR) = $\varphi_{i,k+1/2} / (\varepsilon_i \cdot \cos\beta_{k+1/2})$

PSER (IR) = $\psi_{i+1/2} / \varepsilon_{i+1/2}$

PSFARM (IC) = PSI (IR) · FACRM (IR) = ψ_i^*

PSFARP (IC) = PSI (IC+1) · FACRP (IR) = ψ_{i+1}^*

PSFACM (IR) = PSIR (IR-1) · FACCM (IC) = $\psi^*_{i-1/2}$

PSFACP (IR) = PSIR (IR) · FACCP (IC) = $\psi^*_{i+1/2}$

PSMDP (IR) = PSIRM (IR) / PSIRP (IR) = ψ_i / ψ_{i+1}

PSPDM (IR) = PSIRP (IR-1)/ PSIRM (IR-1) = ψ_i / ψ_{i-1}

PSERP (IC) = $\psi^*_{i+1/2} / \varepsilon_{i+1/2}$

PSERM (IC) = $\psi^*_{i-1/2} / \varepsilon_{i-1/2}$

GSIDP (IC,IT) = $\varphi_k / \varphi_{k+1}$

GSIDM (IC,IT) = $\varphi_k / \varphi_{k-1}$

and the following time step - dependent symbols

DTSQ = Δt_m^2

DTSQ1 = $\vartheta_c \cdot \Delta t_m^2$

DTSQ18 = $\vartheta_c (1-\vartheta_m) \Delta t_m^2$

CFDT = $\vartheta_c \cdot \vartheta_m \Delta t_m^2$

DTEP1 (IC, JC) = $\vartheta_c \varepsilon_i \Delta t_m / \Delta z_j$

DTEP9 (IC, JC) = $(1-\vartheta_c) \varepsilon_i \Delta t_m / \Delta z_j$

DTDR1 (IC) = $\vartheta_c \Delta t_m / \Delta \eta_i$

DTDR9 (IC) = $(1-\vartheta_c) \Delta t_m / \Delta \eta_i$

DTPF1 (IC) = $\vartheta_c \Delta t_m / \Delta \vartheta_i$

DTPF9 (IC) = $(1-\vartheta_c) \Delta t_m / \Delta \vartheta_i$

DTSZ1 (JC) = $\vartheta_c \Delta t_m^2 / \Delta z_j$

DTSR1 (IC) = $\vartheta_c \Delta t_m^2 / \Delta \eta_i$

DTSP1 (IC) = $\vartheta_c \Delta t_m^2 / \Delta \vartheta_i$

AA (IC, JC, IT) = $\vartheta_c \vartheta_m \Delta t_m^2 \cdot CKC^*_{ijk} + \varepsilon_{ijk} / c^2{}^m_{ijk}$

BB (IC, JC, IT) = $-\vartheta_c \vartheta_m \Delta t_m^2 \cdot CKS^*_{ijk}$

CC (IC, JC, IT) = $-\vartheta_c \vartheta_m \Delta t_m^2 \cdot CKN^*_{ijk}$

DD (IC, JC, IT) = $-\vartheta_c \vartheta_m \Delta t_m^2 \cdot CKW^*_{ijk}$

EE (IC, JC, IT) = $-\vartheta_c \vartheta_m \Delta t_m^2 \cdot CKE^*_{ijk}$

ATM (IC, JC, IT) = $-\vartheta_c \vartheta_m \Delta t_m^2 \cdot CK\bar{T}M^*_{ijk}$

ATP (IC, JC, IT) = $-\vartheta_c \vartheta_m \Delta t_m^2 \cdot CK\bar{T}P^*_{ijk}$.

2.4 Numerical Solution of the Poisson-equation. The Alternating Direction Implicit (ADI) method.

Write the Poisson equation (22) in the form

$$A_{ijk} \cdot p^{n+1}_{ijk} + B_{ijk} \cdot p^{n+1}_{i,j-1,k} + C_{ijk} \cdot p^{n+1}_{i,j+1,k} + D_{ijk} \cdot p^{n+1}_{i-1,j,k} +$$

$$E_{ijk} \cdot p^{n+1}_{i+1,j,k} + ATM_{ijk} \cdot p^{n+1}_{i,j,k-1} + ATP_{ijk} \cdot p^{n+1}_{i,j,k+1} = G^{n}_{ijk} \qquad (72)$$

where G^{n}_{ijk} collects all convective, diffusive and pressure terms at time level t_n.

According to the Alternating Direction Implicit (ADI) technique we integrate equation (72) in each of the three coordinate directions separately. We reduce therefore the solution of a three dimensional problem to the simpler solution of three one-dimensional ones. After every integration in one direction the fully updated pressure field is used for the subsequent integration. The three integration steps are as follows:

- Step 1. Integration along the axial z coordinate (j=2,3,...MC) for every radial and azimuthal (i,k) mesh. Equation (72) is written in the form

$$A_{ijk} \cdot p^{(1)}_{ijk} + B_{ijk} \cdot p^{(1)}_{i,j-1,k} + C_{ijk} \cdot p^{(1)}_{i,j+1,k} =$$

$$= G^{n}_{ijk} - D_{ijk} \cdot p^{n}_{i-1,j,k} - E_{ijk} \cdot p^{n}_{i+1,j,k} + \qquad (73)$$

$$- ATM_{ijk} \cdot p^{n}_{i,j,k-1} - ATP_{ijk} \cdot p^{n}_{i,j,k+1}$$

where pressure values at the right-hand side, provisionally considered as known, are taken first from the previous time step. Equation (73) yields for every (i,k) a system of equations with three-diagonal matrix of coefficients. Its solution is direct and gives a new pressure field $p^{(1)}_{ijk}$ which is used for next integration step.

- Step 2. Integration along the radial r coordinate (i=2,3,...NC) for every axial and azimuthal mesh (j,k). Equation (72) is written in the form

$$A_{ijk} \cdot p^{(2)}_{ijk} + D_{ijk} \cdot p^{(2)}_{i-1,j,k} + E_{ijk} \cdot p^{(2)}_{i+1,j,k} =$$

$$= G^{n}_{ijk} - B_{ijk} \cdot p^{(1)}_{i,j-1,k} - C_{ijk} \cdot p^{(1)}_{i,j+1,k} + \qquad (74)$$

$$- ATM_{ijk} \cdot p^{(1)}_{i,j,k-1} - ATP_{ijk} \cdot p^{(1)}_{i,j,k+1}$$

The pressure field $p^{(1)}_{ijk}$ from previous step is used at the right-hand side. Solution of the system of equations (74) yields the updated pressure field $p^{(2)}_{ijk}$.

- Step 3. Integration along the azimuthal s coordinate (k=2,3,...NTH) for every axial and radial mesh (i,j). Equation (72) is written in the form:

$$A_{ijk} \cdot p^{(r+1)}_{ijk} + ATM_{ijk} \cdot p^{(r+1)}_{i,j,k-1} + ATP_{ijk} \cdot p^{(r+1)}_{i,j,k+1} =$$

$$= G^{n}_{ijk} - B_{ijk} \cdot p^{(2)}_{i,j-1,k} - C_{ijk} \cdot p^{(2)}_{i,j+1,k} + \qquad (75)$$

$$- D_{ijk} \cdot p^{(2)}_{i-1,jk} - E_{ijk} \cdot p^{(2)}_{i+1,jk}.$$

Equation (75) yields the updated pressure field $p^{(r+1)}_{ijk}$, where r represents an iteration index. This pressure field is used for next iteration which consists in applying again equations (73) to (75). The iteration is terminated when two subsequent solutions of the pressure field differ by less than a given tolerance. On an average, 10 to 20 iteration steps are necessary for reaching a tolerance of 10^{-5}.

Future programme developments may involve the implementation of accelerating convergence procedures in the ADI method as suggested for instance in references /11/, /12/ or, as an alternative to time-consuming iteration schemes, direct methods can be taken into consideration for instance: a) methods based on cyclic reductions (a review of such methods is given in reference /13/); b) application of Fast Fourier Transform /14/; c) direct inversion of the block-tridiagonal matrix of coefficients /15/, /16/, /17/.

2.5 Numerical solution of the momentum equations

Once the numerical solution of the Poisson-equation (72) has given the coolant pressure field at time level t_{n+1}, the discretized momentum equations (7), (12), (16) yield directly the mass flows in the three coordinate directions at the same time level. The stability of the numerical solution of the coupled continuity and momentum equations is favoured by the half-implicit treatment of the terms representing friction pressure drops in equations (2), (8), (13).

2.6 Numerical solution of the energy equation

The discretized energy equation is solved explicitly with respect to $(h)^{n+1}_{ijk}$ using the mass flows at time level t_{n+1} and enthalpies at time level t_n . From (17) one derives:

$$(\varrho h)^{n+1}_{ijk} = (\varrho h)^{n}_{ijk} +$$

$$+ \frac{\Delta t_n}{\varepsilon_{ijk}} \left[-CVEZ - CVER - CVET + QZ + QR + QT \right]^{n}_{ijk} + \tag{76}$$

$$+ \Delta t_n \, Q^{n}_{ijk}$$

where the convective and diffusive terms are given by

$$(CVEZ)^{n}_{ijk} = \frac{\varepsilon_{ijk}}{\Delta z_j} \left[\left(h^m (\varrho w)^{m+1} \right)_{\substack{i,j+1/2 \\ k}} - \left(h^m (\varrho w)^{m+1} \right)_{\substack{i,j-1/2 \\ k}} \right] \tag{77}$$

$$(CVER)^{n}_{ijk} = \frac{1}{\Delta r_i} \left[\left(\psi_F h^m (\varrho u)^{m+1} \right)_{\substack{i+1/2 \\ jk}} - \left(\psi_F h^m (\varrho u)^{m+1} \right)_{\substack{i-1/2 \\ jk}} \right] \tag{78}$$

$$(CVET)^{n}_{ijk} = \frac{1}{\Delta \vartheta_k} \left[\left(\frac{\xi h^m (\varrho v)^{m+1}}{\cos\beta} \right)_{\substack{ij \\ k+1/2}} - \left(\frac{\xi h^m (\varrho v)^{m+1}}{\cos\beta} \right)_{\substack{ij \\ k-1/2}} \right] \tag{79}$$

$$(QZ)^{n}_{ijk} = \frac{\varepsilon_{ijk}}{\Delta z_j} \left[\left(\tilde{\varrho a} \frac{\partial h}{\partial t} \right)^{m}_{i,j+1/2,k} - \left(\tilde{\varrho a} \frac{\partial h}{\partial t} \right)^{m}_{i,j-1/2,k} \right] \tag{80}$$

$$(QR)^{n}_{ijk} = \frac{1}{\Delta r_i} \left[\left(\psi_F \tilde{\varrho a} \frac{\partial h}{\partial r} \right)^{m}_{i+1/2,jk} - \left(\psi_F \tilde{\varrho a} \frac{\partial h}{\partial r} \right)^{m}_{i-1/2,jk} \right] \tag{81}$$

$$(QT)^{n}_{ijk} = \frac{1}{\Delta \vartheta_k} \left[\left(\frac{\xi \tilde{\varrho a} \frac{\partial h}{\partial \vartheta}}{\cos\beta} \right)^{m}_{i,j,k+1/2} - \left(\frac{\xi \tilde{\varrho a} \frac{\partial h}{\partial \vartheta}}{\cos\beta} \right)^{m}_{i,j,k-1/2} \right] \tag{82}$$

Further programme details regarding the finite differences schemes used for calculating convective and diffusive terms in the above equations are given in section 6.2.

2.7 Calculation of the pressure gradient terms in the momentum equations.

We refer to Fig. 9 for the definition of the control volumes in the three coordinate directions. Let us recall Green's theorems with reference to the coordinate axes (r, s)

$$\iint_S \frac{\partial f(r,s)}{\partial r}\, dr\, ds = \int_\Gamma f(r,s)\, \bar{m} \times \bar{r}\, d\gamma \tag{83a}$$

$$\iint_S \frac{\partial f(r,s)}{\partial s}\, dr\, ds = \int_\Gamma f(r,s)\, \bar{m} \times \bar{s}\, d\gamma \tag{83b}$$

where S is a surface in the (r, s) plane bounded by a curve Γ, $\bar{m}$ is the outward normal to Γ and r, s are unit vectors of the coordinate axes.

The basic equations B.1 (1) to B.1. (3) are integrated over the volume V of a cell. Taking into account that the physical properties of the coolant are defined only in the volume V_f this is equivalent to integrate over the volume V_f of the fluid. The calculation of pressure gradient terms requires a different treatment for the coordinate directions. In the z direction the pressure forces act only on the fluid cross flow sections normal to the bundle axis, thus the pressure gradient term can be integrated on V_f. For the radial (and azimuthal) direction the pressure forces act also on the pin surfaces. The component of the forces acting on the pin surfaces is the same which would act on the cell boundaries in absence of the pins. The pressure gradient term requires therefore to be integrated over the volume V of the cell.

i) Axial direction. We refer to the control volume TGLV displaced by $\Delta z/2$ in axial direction. The pressure gradient term in the momentum equation B.1.15 is calculated as follows:

$$\frac{1}{V}\int_{V_f}\frac{\partial p}{\partial z}\,dV = \frac{1}{V}\frac{\partial}{\partial z}\int_{V_f} p\,dV = \frac{1}{V}\frac{\partial}{\partial z}\int_{z-\Delta z/2}^{z+\Delta z/2}\int_{S_f(z)} p\,dS\cdot dz =$$

$$= \frac{1}{V}\left[\int_{S_{ft}} p\,dS - \int_{S_{fb}} p\,dS\right] = \frac{1}{S\cdot\Delta z}\left[\langle p\rangle_t S_{ft} - \langle p\rangle_b S_{fb}\right] =$$

$$= \frac{\varepsilon}{\Delta z}\left[\langle p\rangle_t - \langle p\rangle_b\right]. \qquad (84)$$

ii) Radial direction. We refer to a control volume like TGLV but displaced by $\Delta r/2$ in radial direction. The pressure gradient term in the radial momentum equation is calculated by applying (83a) as follows

$$\frac{1}{V}\int_V \frac{\partial p}{\partial r}\,dV = \frac{1}{V}\int_{\Delta z}\int_S \frac{\partial p}{\partial r}\,dS\cdot dr = \frac{1}{V}\int_{\Delta z}\int_\Gamma p\,\bar{n}\times\bar{r}\,d\gamma\cdot dz =$$

$$= \frac{1}{V}\Delta z\left[\int_{\bar{TG}} p\,\bar{n}\times\bar{r}\,d\gamma + \int_{\bar{GL}} p\,\bar{n}\times\bar{r}\,d\gamma + \int_{\bar{LV}} p\,\bar{n}\times\bar{r}\,d\gamma + \int_{\widehat{VT}} p\,\bar{n}\times\bar{r}\,d\gamma\right]. \qquad (85)$$

The contribution from the last integral is zero. Hence

$$\frac{1}{V}\int_V \frac{\partial p}{\partial r}\,dV = \frac{\Delta z}{V}\left[-\langle p\rangle_i\,\bar{TG} - \frac{\langle p\rangle_i + \langle p\rangle_e}{2}\,\bar{GL}\cos\beta + \langle p\rangle_e\cdot\bar{VL}\right] =$$

$$= \frac{\Delta z}{V}\left[-\langle p\rangle_i\cdot\bar{TG} - \frac{1}{2}\left(\langle p\rangle_i + \langle p\rangle_e\right)\bar{zL} + \langle p\rangle_e\cdot\bar{VL}\right] =$$

$$= \frac{\Delta z}{V}\left[-\langle p\rangle_i\left(\bar{TG} + \frac{\bar{zL}}{2}\right) + \langle p\rangle_e\left(\bar{VL} - \frac{\bar{zL}}{2}\right)\right] =$$

$$= \frac{\Delta z}{V}\,\Delta s\left(\langle p\rangle_i - \langle p\rangle_e\right) = \frac{1}{\Delta r}\left(\langle p\rangle_i - \langle p\rangle_e\right) \qquad (86)$$

The assumption made in deriving (86) is that the pressure varies linearly along Δr.

iii) Azimuthal direction. The control volumes for the azimuthal direction are defined by splitting a 30 degree azimuthal sector into two halves having equal volumes. The angle β_R in Fig. 9 is chosen so that $\overline{TB} = \overline{BG}$ thus giving $tg\beta_R = 1/2\sqrt{3}$. We must consider two different control volumes:

a) Control volume ABCD centred around an axial plane normal to the hexagonal can. Applying (83b) one derives

$$\frac{1}{V}\int_V \frac{\partial p}{\partial s}\,dV = \frac{1}{V}\int_{\Delta z}\int_S \frac{\partial p}{\partial s}\,dS\cdot dz = \frac{\Delta z}{V}\int_\Gamma p\,\bar{n}\times\bar{s}\,d\gamma = \tag{87}$$

$$= \frac{\Delta z}{V}\left[\int_{\overline{AB}} p\,\bar{n}\times\bar{s}\,d\gamma + \int_{\overline{BC}} p\,\bar{n}\times\bar{s}\,d\gamma + \int_{CD} p\,\bar{n}\times\bar{s}\,d\gamma + \int_{\overline{DA}} p\,\bar{n}\times\bar{s}\,d\gamma\right]$$

The contributions of the first and third integrals are zero, hence

$$\frac{1}{V}\int_V \frac{\partial f}{\partial s}\,dV = \frac{\Delta z}{V}\left[\langle p\rangle_p\,\overline{BC}\,(\cos\alpha)_p - \langle p\rangle_m\,\overline{DA}\,(\cos\alpha)_m\right] = \tag{88}$$

$$= \frac{\Delta z\cdot\Delta z}{V}\left[\langle p\rangle_p - \langle p\rangle_m\right] = \frac{1}{\Delta s}\left[\langle p\rangle_p - \langle p\rangle_m\right].$$

b) Control volume BGHILC centred about an axial plane passing though the corner of the hecagonal can. Applying (83b) one derives

$$\frac{1}{V}\int_V \frac{\partial p}{\partial s}\,dV = \frac{1}{V}\int_{\Delta z}\int_S \frac{\partial p}{\partial s}\,dS\cdot dz = \frac{\Delta z}{V}\int_\Gamma p\,\bar{n}\times\bar{s}\,d\gamma = \tag{89}$$

$$= \frac{\Delta z}{V}\left[\int_{\overline{BGH}} p\,\bar{n}\times\bar{s}\,d\gamma + \int_{\overline{HI}} p\,\bar{n}\times\bar{s}\,d\gamma + \int_{\overline{ILC}} p\,\bar{n}\times\bar{s}\,d\gamma + \int_{\overline{CB}} p\,\bar{n}\times\bar{s}\,d\gamma\right].$$

Because of the symmetriy with respect to the GL plane we assume

$$\int_{\overline{BGH}} p\,\bar{n}\times\bar{s}\,d\gamma \simeq 2\int_{\overline{BG}} p\,\bar{n}\times\bar{s}\,d\gamma = 0 \tag{90}$$

$$\int_{\overline{ILC}} p\,\bar{n}\times\bar{s}\,d\gamma \simeq 2\int_{\overline{LC}} p\,\bar{n}\times\bar{s}\,d\gamma = 0 \tag{91}$$

Hence

$$\frac{1}{V}\int_V \frac{\partial p}{\partial s}\,dV = \frac{\Delta z}{V}\left[\overline{HI}\cos\beta_R\langle p\rangle_p - \overline{BC}\cos\beta_R\langle p\rangle_m\right] = \tag{92}$$

$$= \frac{\Delta z\cdot\Delta r}{V}\left[\langle p\rangle_p - \langle p\rangle_m\right] = \frac{1}{\Delta s}\left[\langle p\rangle_p - \langle p\rangle_m\right].$$

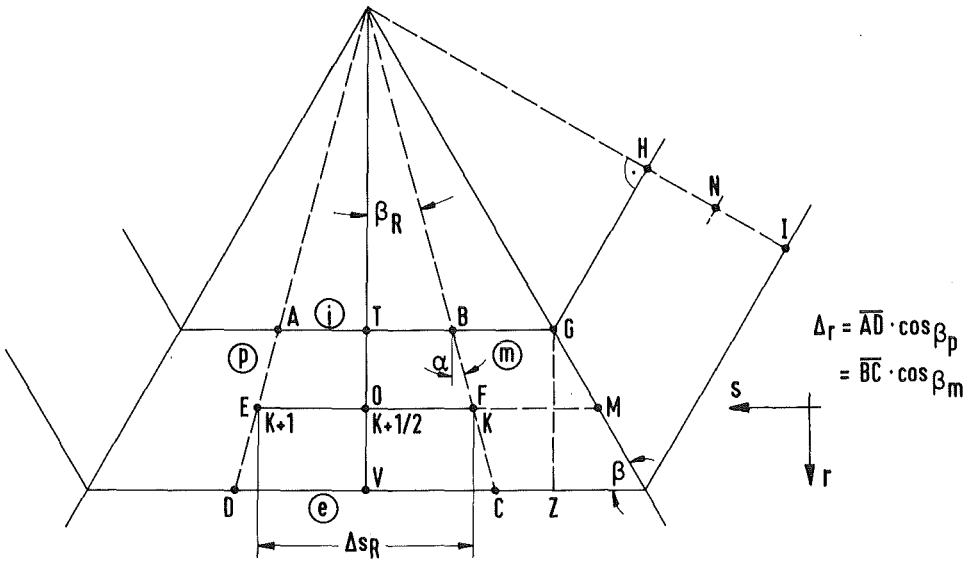

Fig. 9: Definition of control volumes for the azimuthal direction

3. Transient two-dimensional (2 D) thermal hydraulic calculation

In this section the two-dimensional transient single-phase flow version of the BACCHUS programme (BACCHUS-2D/SP) is documented with respect to the thermal hydraulic calculation. The equations are similar to those of the three dimensional case but the azimuthal component is suppressed. The transient calculation is preceeded by a steady-state calculation with the BACCHUS-P programme, as explained in section C 1. The link between the steady-state and the transient programmes is explained in section C 1.4. The calculation of the temperature distributions in fuel, cladding and structure materials, which determines the heat fluxes into the coolant, is done as explained in section C 4 for both the 2D and 3D programmes.

3.1 Conservation equations in local form

The two dimensional single phase flow of the coolant can be described in the local form by the following equations.

i) Continuity equation

$$\frac{\partial \rho}{\partial t} + \nabla \cdot \rho \bar{V} = 0 \qquad \bar{V} = (u, w) \tag{1}$$

ii) Momentum equation

$$\frac{\partial}{\partial t}(\rho \bar{V}) + \nabla \cdot \rho \bar{V} \bar{V} = \nabla \cdot (\mu \nabla \bar{V}) - \nabla p - \rho \bar{g} - \bar{D} \tag{2}$$

which is equivalent to the two scalar equations for axial and radial directions, respectively:

$$\frac{\partial}{\partial t}(\rho w) + \nabla \cdot (\rho w \bar{V}) = \nabla \cdot (\mu \nabla w) - \frac{\partial p}{\partial z} - \rho g - \bar{D} \cdot \bar{n}_z \tag{2a}$$

$$\frac{\partial}{\partial t}(\rho u) + \nabla \cdot (\rho u \bar{V}) = \nabla \cdot (\mu \nabla u) - \frac{\partial p}{\partial r} - \bar{D} \cdot \bar{n}_r \tag{2b}$$

iii) Energy equation

$$\frac{\partial}{\partial t}(\rho h) + \nabla \cdot \rho h \bar{V} = \nabla \cdot \rho \tilde{\alpha} \nabla h + Q \qquad (3)$$

The symbols are the same as in section 2. For convenience the "radial" velocity component is referred to a local cartesian coordinate system.

3.2 Conservation equations averaged over the control volumes

The conservation equations for mass, momentum and energy are integrated over appropriate control volumes and transformed into a "volume-averaged" equation using a staggered mesh. The following control volumes are defined for the volume averaging procedure (see Fig. 2) in analogy to the 3D case.

- V_I is used for the continuity and the energy equation. It consists of a control cell bounded radially by vertical planes through the pin axes, and axially by horizontal planes located a distance Δz apart.

- Volume V_{II} is used for the radial components of the momentum equation. It consists of a hexagonal ring bounded radially by vertical planes midway between the axes of the pins.

- Volume V_{III} is used for the axial component of the momentum equation. It is obtained by translating the control volume V_I by $\Delta z/2$ in axial direction.

Contrary to the 3D case, the control volumes form rings instead of sectors. Volume integrals are transformed into surface integrals by means of the Gauss theorem, time derivatives of volume integrals by means of the Leibniz theorem (see section B 1.2).

i) Continuity equation

We refer to the control volume V_I of Fig. 2 and use the indices t, b, e, i, to denote the boundary surfaces (S): top, bottom (z direction), external, internal (r direction) respectively. Let V be the total volume of the control cell and V_f be the volume of the fluid in it (index f refers to the fluid). The following definitions of volume porosity and surface permeability are introduced, as in the 3D case:

$\varepsilon = V_f/V$ = volume porosity

$\varepsilon_t = S_{ft}/S_t$
$\varepsilon_b = S_{fb}/S_b$
} surface permeabilities for the axial direction. In case of undisturbed geometry these ratios are equal to the volume porosity

$\Psi_e = S_{fe}/S_e$ = surface permeability at the outer radial surface

$\Psi_i = S_{fi}/S_i$ = surface permeability at the inner radial surface.

It holds

$$V = \Delta r \cdot \Delta \vartheta \cdot \Delta z = S_t \cdot \Delta z = S_b \cdot \Delta z \qquad (4)$$
$$= \Delta r \, (S_i + S_e)/2 = \Delta r \cdot S_m$$

where S_m is the surface midway between S_i and S_e.

Integrating equation (1) over the volume V_f of the fluid in the control cell gives

$$\int_{V_f} \frac{\partial \varrho}{\partial t} \, dV + \int_{V_f} \operatorname{div}(\varrho \bar{v}) \, dV = 0. \qquad (5)$$

Applying the Leibniz and Gauss theorems and introducing the velocity components yields

$$\frac{\partial}{\partial t} \int_{V_f} \varrho \, dV + \int_{S_{ft}} \varrho w \, dS - \int_{S_{fb}} \varrho w \, dS + \qquad (6)$$
$$+ \int_{S_{fe}} \varrho u \, dS - \int_{S_{fi}} \varrho u \, dS = 0.$$

We introduce the following definitions of volume and surface averaged quantities for any scalar function f:

$$\langle f \rangle_3 = \frac{1}{V_f} \int_{V_f} f \, dV \qquad (7)$$

$$\langle f \rangle = \frac{1}{S_f} \int_{S_f} f \, dS \qquad (8)$$

By means of (4), (7), (8) and using the definitions of the porosities and permeabilities, equation (6) becomes:

$$\varepsilon \frac{\partial \langle s \rangle_s}{\partial t} + \frac{\varepsilon}{\Delta z}\left[\langle \rho w \rangle_t - \langle \rho w \rangle_b\right] + \frac{1}{\Delta x}\left[\psi_e F_e \langle \rho u \rangle_e - \psi_i F_i \langle \rho u \rangle_i\right] = 0 \qquad (9)$$

with

$$F_e = S_e / S_m$$

$$F_i = S_i / S_m . \qquad (10)$$

This is the volume-averaged continuity equation. It is combined with the volume-averaged momentum equations to derive a discrete Poisson-like equation.

ii) Momentum equations

a) Axial momentum equation

Integration of eq. (2a) over the volume V_f of the fluid in the control cell yields

$$\int_{V_f} \frac{\partial \rho w}{\partial t} dV + \int_{V_f} div\left(\rho w \bar{v}\right) dV =$$

$$= \int_{V_f} div\left(\mu \nabla w\right) dV - \int_{V_f} \frac{\partial p}{\partial z} dV - g \int_{V_f} \rho dV - \int_{V_f} \bar{D} \cdot \bar{n}_z \, dV \qquad (11)$$

By means of the Leibniz and Gauss theorems one has

$$\frac{\partial}{\partial t}\int_{V_f} \rho w \, dV + \int_{S_{ft}} (\rho w) w \, dS - \int_{S_{fb}} (\rho w) w \, dS +$$

$$+ \int_{S_{fe}} (\rho w) u \, dS - \int_{S_{fi}} (\rho w) u \, dS = \tag{12}$$

$$= \int_{S_{ft}} \mu \frac{\partial w}{\partial z} \, dS - \int_{S_{fb}} \mu \frac{\partial w}{\partial z} \, dS + \int_{S_{fe}} \mu \frac{\partial w}{\partial x} \, dS - \int_{S_{fi}} \mu \frac{\partial w}{\partial x} \, dS +$$

$$- \int_{S_{ft}} p \, dS + \int_{S_{fb}} p \, dS - g \int_{V_f} \rho \, dV - \int_{S_w} \bar{\sigma} \cdot \bar{n}_z \, dS .$$

A similar treatment as for the continuity equation leads to

$$\varepsilon \frac{\partial}{\partial t} \langle \rho w \rangle_3 + \frac{\varepsilon}{\Delta z} \left[\langle \rho w^2 \rangle_t - \langle \rho w^2 \rangle_b \right] + \frac{1}{\Delta x} \left[\psi_e F_e \langle \rho w u \rangle_e - \psi_i F_i \langle \rho w u \rangle_i \right] =$$

$$= \frac{\varepsilon}{\Delta z} \left[\langle \mu \frac{\partial w}{\partial z} \rangle_t - \langle \mu \frac{\partial w}{\partial z} \rangle_b \right] + \frac{1}{\Delta x} \left[\psi_e F_e \langle \mu \frac{\partial w}{\partial x} \rangle_e - \psi_i F_i \langle \mu \frac{\partial w}{\partial x} \rangle_i \right] +$$

$$+ \frac{\varepsilon}{\Delta z} \left[- \langle p \rangle_t + \langle p \rangle_b \right] - \varepsilon g \langle \rho \rangle_3 - \frac{S_w}{V} \langle \bar{\sigma} \cdot \bar{n}_z \rangle_w . \tag{13}$$

b) Radial momentum equation

Integration of eq. (2b) over the volume V_f of the fluid in the control cell yields, with the same procedure as for equations (11) to (13):

$$\varepsilon \frac{\partial}{\partial t}\langle \rho u\rangle_3 + \frac{\varepsilon}{\Delta z}\left[\langle \rho u w\rangle_t - \langle \rho u w\rangle_b\right] + \frac{1}{\Delta r}\left[\psi_e F_e \langle \rho u^2\rangle_e - \psi_i F_i \langle \rho u^2\rangle_i\right] =$$

$$= \frac{\varepsilon}{\Delta z}\left[\langle \mu \frac{\partial u}{\partial z}\rangle_t - \langle \mu \frac{\partial u}{\partial z}\rangle_b\right] + \frac{1}{\Delta r}\left[\psi_e F_e \langle \mu \frac{\partial u}{\partial r}\rangle_e - \psi_i F_i \langle \mu \frac{\partial u}{\partial r}\rangle_i\right] + \tag{14}$$

$$+ \frac{1}{\Delta r}\left[-\langle p\rangle_e + \langle p\rangle_i\right] - \frac{S_w}{V}\langle \vec{D}\cdot\vec{n}_r\rangle_w .$$

iii) Energy equation

Integration of eq. (3) over the volume V_f of the fluid in the control cell yields

$$\int_{V_f} \frac{\partial(\rho h)}{\partial t}\,dV + \int_{V_f} \operatorname{div}(\rho h \vec{v})\,dV = \int_{V_f} \operatorname{div}(\tilde{\rho\alpha}\,\nabla h)\,dV + \int_V Q\,dV. \tag{15}$$

Applying the Leibniz and Gauss theorems one has

$$\frac{\partial}{\partial t}\int_{V_f} \rho h\,dV + \int_{S_{ft}} \rho h w\,dS - \int_{S_{fb}} \rho h w\,dS + \int_{S_{fe}} \rho h u\,dS - \int_{S_{fi}} \rho h u\,dS = \tag{16}$$

$$= \int_{S_{ft}} \tilde{\rho\alpha}\frac{\partial h}{\partial z}\,dS - \int_{S_{fb}} \tilde{\rho\alpha}\frac{\partial h}{\partial z}\,dS + \int_{S_{fe}} \tilde{\rho\alpha}\frac{\partial h}{\partial r}\,dS - \int_{S_{fi}} \tilde{\rho\alpha}\frac{\partial h}{\partial r}\,dS + \int_V Q\,dV.$$

Introducing the definitions of volume porosity and surface permeabilities and using (7), (8) yields:

$$\varepsilon \frac{\partial}{\partial t}\langle \rho h\rangle_3 + \frac{\varepsilon}{\Delta z}\left[\langle \rho h w\rangle_t - \langle \rho h w\rangle_b\right] + \frac{1}{\Delta r}\left[\psi_e F_e \langle \rho h u\rangle_e - \psi_i F_i \langle \rho h u\rangle_i\right] =$$

$$= \frac{\varepsilon}{\Delta z}\left[\langle \tilde{\rho\alpha}\frac{\partial h}{\partial t}\rangle_t - \langle \tilde{\rho\alpha}\frac{\partial h}{\partial z}\rangle_b\right] + \frac{1}{\Delta r}\left[\psi_e F_e \langle \tilde{\rho\alpha}\frac{\partial h}{\partial r}\rangle_e - \psi_i F_i \langle \tilde{\rho\alpha}\frac{\partial h}{\partial r}\rangle_i\right] + \tag{17}$$

$$+ \langle Q\rangle_3 .$$

Eq. (17) is the volume-averaged energy equation.

3.3 Finite difference form of the volume averaged conservation equations

i) Continuity equation

Let Θ_c ($0 \leq \Theta_c \leq 1$) be a time-discretization parameter and n, n+1 be superscripts referring to time levels t_n, t_{n+1} respectively. Space and time discretization of eq. (9) yields for the control volume V_I shown in Fig. 2:

$$\varepsilon_{i,j}\,\frac{\rho^{n+1}_{i,j}-\rho^{n}_{i,j}}{\Delta t_n}+ \tag{18}$$

$$+\Theta_c\,\frac{\varepsilon_{i,j}}{\Delta z_j}\left[(\rho w)^{n+1}_{i,j+1/2}-(\rho w)^{n+1}_{i,j-1/2}\right]+(1-\Theta_c)\,\frac{\varepsilon_{i,j}}{\Delta z_j}\left[(\rho w)^{n}_{i,j+1/2}-(\rho w)^{n}_{i,j-1/2}\right]+$$

$$+\Theta_c\,\frac{1}{\Delta r_i}\left[(\psi F \rho u)^{n+1}_{i+1/2,j}-(\psi F \rho u)^{n+1}_{i-1/2,j}\right]+\frac{1-\Theta_c}{\Delta r_i}\left[(\psi F \rho u)^{n}_{i+\frac{1}{2},j}-(\psi F \rho u)^{n}_{i-1/2,j}\right]=0$$

In eq. (18) and in the following ones the symbols $\langle\rangle_s$, $\langle\rangle$ denoting volume and surface averaged quantities are dropped for simplicity.
We refer to the list at the end of this section for all new symbols introduced in the following equations.

ii) Momentum equations

a) Axial momentum equation

Space and time discretization of eq. (13) yields for the control volume V_{III} shown in Fig. 2:

$$\varepsilon_{i,j+1/2}\,\frac{(\rho w)^{n+1}_{i,j+1/2}-(\rho w)^{n}_{i,j+1/2}}{\Delta t_n}+\frac{\varepsilon_{i,j+1/2}}{\Delta z_{j+1/2}}\left[(\rho w^2)^{n}_{i,j+1}-(\rho w^2)^{n}_{i,j}\right]+ \tag{19}$$

$$+\frac{1}{\Delta r_i}\left[(\psi F \rho w u)^{n}_{\substack{i+1/2\\ j+1/2}}-(\psi F \rho w u)^{n}_{\substack{i-1/2\\ j+1/2}}\right]-\frac{\varepsilon_{i,j+1/2}}{\Delta z_{j+1/2}}\left[\left(\mu\frac{\partial w}{\partial z}\right)^{n}_{i,j+1}-\left(\mu\frac{\partial w}{\partial z}\right)^{n}_{i,j}\right]+$$

$$-\frac{1}{\Delta r_i}\left[\left(\psi F \mu\frac{\partial w}{\partial r}\right)^{n}_{\substack{i+1/2\\ j+1/2}}-\left(\psi F \mu\frac{\partial w}{\partial r}\right)^{n}_{\substack{i-1/2\\ j+1/2}}\right]+\Theta_n\,\frac{\varepsilon_{i,j+1/2}}{\Delta z_{j+1/2}}\left[p^{n+1}_{i,j+1}-p^{n+1}_{i,j}\right]+$$

$$+(1-\Theta_n)\,\frac{\varepsilon_{i,j+1/2}}{\Delta z_{j+1/2}}\left[p^{n}_{i,j+1}-p^{n}_{i,j}\right]+g(\varepsilon\rho)^{n}_{i,j+1/2}+\frac{1}{2}\left(\frac{\varepsilon f}{D_h}\,|w^n|\,(\rho w)^{n+1}\right)_{i,j+1/2}=0$$

Convective and diffusive terms are treated explicitly with respect to time, pressure terms implicitly and the term representing friction pressure drops is treated half-implicitly. ϑ_m ($o \leq \vartheta_m \leq 1$) is a time-discretization parameter for the pressure terms in the momentum equations. The last term of eq. (13) has been rewritten taking into account that

$$\frac{S_w}{V} = \varepsilon \frac{S_w}{V_f} = \varepsilon \frac{P_w}{S_f} = \varepsilon \frac{4}{D_h} \tag{20}$$

$$f = 4\chi \tag{21}$$

where

D_h = hydraulic diameter [m]

S_f = cross flow area for the fluid [m^2]

p_w = wetted wall perimeter [m]

f, χ = friction coefficients .

Letting

$$FC\emptyset Z = \frac{f|W^n|}{2 D_h} \tag{22}$$

$$FWZ = \frac{1}{1+\Delta t_n \frac{f|W^n|}{2D_h}} = \frac{1}{1+\Delta t_n \; FC\emptyset Z} \tag{23}$$

eq.(19) can be rewritten

$$\left(\rho w\right)^{m+1}_{i,j+1/2} = \left\{ \left(\rho w\right)^{m}_{i,j+1/2} - \frac{\vartheta_m \Delta t_m}{\Delta z_{j+1/2}} \left[p^{m+1}_{i,j+1} - p^{m+1}_{i,j} \right] + \right. \tag{24}$$

$$\left. - \frac{(1-\vartheta_m)\Delta t_m}{\Delta z_{j+1/2}} \left[p^{m}_{i,j+1} - p^{m}_{i,j} \right] - \frac{\Delta t_m}{\varepsilon_{i,j+1/2}} \left(CVZZ + CVZR - FZZ - FZR - GVZ \right)^{m}_{i,j+1/2} \right\} FWZ^{m}_{i,j+\frac{1}{2}} .$$

b) Radial momentum equation

Space and time discretization of eq. (14) yields for control volume V_{II} shown in Fig. 2

$$\varepsilon_{i+1/2,j}\,\frac{(\rho u)^{m+1}_{i+1/2,j}-(\rho u)^{m}_{i+1/2,j}}{\Delta t_m}+$$

$$+\frac{\varepsilon_{i+1/2,j}}{\Delta z_j}\left[(\rho u w)^{m}_{\substack{i+1/2\\ j+1/2}}-(\rho u w)^{m}_{\substack{i+1/2\\ j-1/2}}\right]+\frac{1}{\Delta r_{i+1/2}}\left[(\psi_F \rho u^2)^{m}_{\substack{i+1\\ j}}-(\psi_F \rho u^2)^{m}_{i,j}\right]+$$

$$-\frac{\varepsilon_{i+1/2,j}}{\Delta z_j}\left[\left(\mu\frac{\partial u}{\partial z}\right)^{m}_{\substack{i+1/2\\ j+1/2}}-\left(\mu\frac{\partial u}{\partial z}\right)^{m}_{\substack{i+1/2\\ j-1/2}}\right]+ \qquad (25)$$

$$-\frac{1}{\Delta r_{i+1/2}}\left[\left(\psi_F\mu\frac{\partial u}{\partial r}\right)^{m}_{i+1,j}-\left(\psi_F\mu\frac{\partial u}{\partial r}\right)^{m}_{i,j}\right]+$$

$$+\frac{\vartheta_m}{\Delta r_{i+1/2}}\left[p^{m+1}_{i+1,j}-p^{m+1}_{i,j}\right]+\frac{1-\vartheta_m}{\Delta r_{i+1/2}}\left[p^{m}_{i+1,j}-p^{m}_{i,j}\right]+$$

$$+\frac{1}{2}\left(\varepsilon\,\frac{\rho_w}{s_f}\,f\,|u^{*m}|\,(\rho u^{m+1})\right)_{i+1/2,j}=0.$$

The velocity u^* in last term of eq. (25) is defined by

$$u^* = u\left[\frac{4P-\pi D}{4(P-D)}\right]^2 \qquad (26)$$

where D is the pin diameter and P the pitch.

Letting

$$FC\emptyset R = \frac{\rho_w}{S_f} \frac{f}{2} |u^{*m}| \tag{27}$$

$$FWR = \frac{1}{1 + \Delta t_m \frac{\rho_w}{S_f} \frac{f}{2} |u^{*m}|} = \frac{1}{1 + \Delta t_m \cdot FC\emptyset R} \tag{28}$$

eq.(25) can be rewritten

$$\begin{aligned}
&(\rho u)^{m+1}_{i+1/2,j} = \\
&= \left\{ (\rho u)^{m}_{i+1/2,j} - \frac{\vartheta_m \Delta t_m}{\varepsilon_{i+1/2,j} \cdot \Delta x_{i+1/2}} \left[p^{m+1}_{i+1,j} - p^{m+1}_{ij} \right] + \right. \\
&- \frac{(1-\vartheta_m) \Delta t_m}{\varepsilon_{i+1/2,j} \cdot \Delta x_{i+1/2}} \left[p^{m}_{i+1,j} - p^{m}_{ij} \right] + \\
&\left. - \frac{\Delta t_m}{\varepsilon_{i+1/2,j}} \left(CVRZ + CVRR - FRZ - FRR \right)^{m}_{i+1/2,j} \right\} \cdot FWR^{m}_{i+1/2,j} \cdot
\end{aligned} \tag{29}$$

Equations (24), (29) are the basic equations for the calculation of the mass flows when the updated pressure field has been obtained.

iii) Energy equation

The volume-averaged energy equation (17) is discretized with reference to the control volume V_I shown in fig. 2. All terms are treated explicitly with respect to time. The discretized equation is as follows:

$$\varepsilon_{i,j}\,\frac{(\rho h)^{n+1}_{i,j}-(\rho h)^{n}_{i,j}}{\Delta t_n}+\frac{\varepsilon_{i,j}}{\Delta z_j}\left[(\rho h w)^{n}_{i,j+1/2}-(\rho h w)^{n}_{i,j-1/2}\right]+$$

$$+\frac{1}{\Delta r_i}\left[(\psi F \rho h u)^{n}_{i+1/2,j}-(\psi F \rho h u)^{n}_{i-1/2,j}\right]+ \qquad (30)$$

$$-\frac{\varepsilon_{i,j}}{\Delta z_j}\left[\tilde{\beta}\frac{\partial h}{\partial z}\right)^{n}_{i,j+\frac{1}{2}}-\left(\tilde{\beta}\frac{\partial h}{\partial z}\right)^{n}_{i,j-1/2}\Big]-\frac{1}{\Delta r_i}\left[\left(\psi F\tilde{\beta}\frac{\partial h}{\partial r}\right)^{n}_{i+1/2,j}-\left(\psi F\tilde{\beta}\frac{\partial h}{\partial r}\right)^{n}_{i-1/2,j}\right]+$$

$$-\quad Q^{n}_{i,j}=0.$$

3.4 The Poisson equation for the coolant pressure distribution

The ICE technique allows to derive a difference equation for pressure values from the continuity and momentum equations as it would be obtained discretizing a Poisson equation. From the practical viewpoint the procedure is as follows:

Consider the finite differences form of the volume averaged continuity equation (18). Replace the values of the mass flows at time level n+1 by using the momentum equations (24), (29) written for the nodes $j\pm 1/2$ and $i\pm 1/2$, respectively. From the equation of state replace the time-difference of coolant density in (18) by

$$\rho^{n+1}_{i,j}-\rho^{n}_{i,j}=\frac{1}{c^2_{i,j}}\left(p^{n+1}_{i,j}-p^{n}_{i,j}\right) \qquad (31)$$

with

$$c^2=dp/d\rho. \qquad (32)$$

Rearranging one derives a linear algebraic equation for the unknowns

$$p^{n+1}_{i,j},\ p^{n+1}_{i+1,j},\ p^{n+1}_{i-1,j},\ p^{n+1}_{i,j+1},\ p^{n+1}_{i,j-1},$$

which can be written

$$
\begin{aligned}
&- p^{n+1}_{i,j+1}\left[\frac{\varepsilon_{i,j}}{\Delta z_j \cdot \Delta z_{j+1/2}}\right] \cdot FWZ^{m}_{i,j+1/2} \cdot \vartheta_c \vartheta_m \Delta t_m^2 + \\
&- p^{n+1}_{i,j-1}\left[\frac{\varepsilon_{i,j}}{\Delta z_j \cdot \Delta z_{j-1/2}}\right] \cdot FWZ^{m}_{i,j-1/2} \cdot \vartheta_c \vartheta_m \Delta t_m^2 + \\
&- p^{n+1}_{i+1,j}\left[\frac{\Psi_{i+1/2,j} \cdot FACCP_i}{\varepsilon_{i+1/2,j} \cdot \Delta r_i \cdot \Delta r_{i+1/2}}\right] \cdot FWR^{m}_{i+1/2,j} \cdot \vartheta_c \vartheta_m \Delta t_m^2 + \qquad (33) \\
&- p^{n+1}_{i-1,j}\left[\frac{\Psi_{i-1/2,j} \cdot FACCM_i}{\varepsilon_{i-1/2,j} \cdot \Delta r_i \cdot \Delta r_{i-1/2}}\right] \cdot FWR^{m}_{i-1/2,j} \cdot \vartheta_c \vartheta_m \Delta t_m^2 + \\
&+ p^{n+1}_{i,j}\left\{\left[\frac{\varepsilon_{i,j}}{\Delta z_j \cdot \Delta z_{j+1/2}} \cdot FWZ^{m}_{i,j+1/2} + \frac{\varepsilon_{i,j}}{\Delta z_j \cdot \Delta z_{j-1/2}} \cdot FWZ^{m}_{i,j-1/2} + \right.\right. \\
&\qquad \left.\left. + \frac{\Psi_{i+1/2,j} \cdot FACCP_i}{\varepsilon_{i+1/2,j} \cdot \Delta r_i \cdot \Delta r_{i+1/2}} \cdot FWR^{m}_{i+1/2,j} + \frac{\Psi_{i-1/2} \cdot FACCM_i}{\varepsilon_{i-\frac{1}{2},j} \cdot \Delta r_i \cdot \Delta r_{i-1/2}} \cdot FWR^{m}_{i-1/2,j}\right] \cdot \right. \\
&\qquad \left. \cdot \vartheta_c \vartheta_m \Delta t_m^2 + \frac{\varepsilon_{i,j}}{c^2_{i,j}}\right\} = G^{m}_{i,j} \cdot
\end{aligned}
$$

The right-hand side G^{n}_{ijk} is given fully in the next equation . We introduce the coefficients CKN, CKS, CKW, CKE, (defined in the list at the end of this section) which depend only on the bundle geometry and discretization. Dropping the subscripts ij for these geometry coefficients, eq. (33) can be written:

$$
\begin{aligned}
&\Big\{ - p^{n+1}_{i,j+1} \cdot CKN \cdot FWZ^{m}_{i,j+1/2} - p^{n+1}_{i,j-1} \cdot CKS \cdot FWZ^{m}_{i,j-1/2} + \\
&- p^{n+1}_{i+1,j} \cdot CKE \cdot FWR^{m}_{i+1/2,j} - p^{n+1}_{i-1,j} \cdot CKW \cdot FWR^{m}_{i-\frac{1}{2},j} \Big\} \vartheta_c \vartheta_m \Delta t_m^2 + \\
&+ p^{n+1}_{ij} \Big\{ \Big[CKN \cdot FWZ^{m}_{i,j+\frac{1}{2}} + CKS \cdot FWZ^{m}_{i,j-1/2} + CKE \cdot FWR^{m}_{i+\frac{1}{2},j} + \\
&\quad + CKW \cdot FWR^{m}_{i-1/2,j} \Big] \vartheta_c \vartheta_m \Delta t_m^2 + \frac{\varepsilon_{ij}}{c^2_{ij}} \Big\} = \qquad (34) \\
&= \Big\{ p^{m}_{i,j+1} \cdot CKN \cdot FWZ^{m}_{i,j+1/2} + p^{m}_{i,j-1} \cdot CKS \cdot FWZ^{m}_{i,j-1/2} + \\
&\quad + p^{m}_{i+1,j} \cdot CKE \cdot FWR^{m}_{i+1/2,j} + p^{m}_{i-1,j} \cdot CKW \cdot FWR^{m}_{i-\frac{1}{2},j} \Big\} \vartheta_c (1-\vartheta_m) \Delta t_m^2 + \\
&- p^{m}_{ij} \Big\{ CKN \cdot FWZ^{m}_{i,j+\frac{1}{2}} + CKS \cdot FWZ^{m}_{i,j-1/2} + CKE \cdot FWR^{m}_{i+\frac{1}{2},j} + CKW \cdot FWR^{m}_{i-\frac{1}{2},j} \Big\} \vartheta_c (1-\vartheta_m) \Delta t_m^2 + \\
&- \frac{\vartheta_c \Delta t_m \, \varepsilon_{ij}}{\Delta z_j} \Big[(\rho w \cdot FWZ)^{m}_{i,j+\frac{1}{2}} - (\rho w \cdot FWZ)^{m}_{i,j-\frac{1}{2}} \Big] + \frac{(1-\vartheta_c) \Delta t_m \, \varepsilon_{ij}}{\Delta z_j} \Big[(\rho w)^{m}_{i,j+\frac{1}{2}} - (\rho w)^{m}_{i,j-\frac{1}{2}} \Big] + \\
&- \frac{\vartheta_c \Delta t_m}{\Delta r_i} \Big[(\psi \rho u \cdot FWR)^{m}_{i+1/2,j} \cdot FACCP_i - (\psi \rho u \cdot FWR)^{m}_{i-1/2,j} \cdot FACCM_i \Big] + \\
&- \frac{(1-\vartheta_c) \Delta t_m}{\Delta r_i} \Big[(\psi \rho u)^{m}_{i+1/2,j} \cdot FACCP_i - (\psi \rho u)^{m}_{i-1/2,j} \cdot FACCM_i \Big] + \\
&+ \frac{\vartheta_c \Delta t_m^2}{\Delta t_j} \cdot \frac{\varepsilon_{ij}}{\varepsilon_{i,j+1/2}} \Big(CVZZ + CVZR - FZZ - FZR - GVZ \Big)^{m}_{i,j+1/2} \cdot FWZ^{m}_{i,j+1/2} + \\
&- \frac{\vartheta_c \Delta t_m^2}{\Delta t_j} \cdot \frac{\varepsilon_{ij}}{\varepsilon_{i,j-1/2}} \Big(CVZZ + CVZR - FZZ - FZR - GVZ \Big)^{m}_{i,j-1/2} \cdot FWZ^{m}_{i,j-1/2} + \\
&+ \frac{\vartheta_c \Delta t_m^2}{\Delta r_i} \cdot \frac{\psi_{i+1/2,j}}{\varepsilon_{i+1/2,j}} \cdot FACCP_i \cdot \Big(CVRZ + CVRR - FRZ - FRR \Big)^{m}_{i+\frac{1}{2},j} \cdot FWR^{m}_{i+\frac{1}{2},j} + \\
&- \frac{\vartheta_c \Delta t_m^2}{\Delta r_i} \cdot \frac{\psi_{i-1/2,j}}{\varepsilon_{i-1/2,j}} \cdot FACCM_i \cdot \Big(CVRZ + CVRR - FRZ - FRR \Big)^{m}_{i-\frac{1}{2},j} \cdot FWR^{m}_{i-1/2,j} + \\
&+ \varepsilon_{ij} \frac{p^{m}_{ij}}{c^2_{ij}} \cdot
\end{aligned}
$$

Equation (34) can be written in the following compact form (ratios of volume porosities at different axial locations are equal to one in undisturbed geometry and are therefore dropped as multiplying factor):

$$\left\{ - P^{m+1}_{i,j+1} \cdot CKN^* - P^{m+1}_{i,j-1} \cdot CKS^* - P^{m+1}_{i+1,j} \cdot CKE^* - P^{m+1}_{i-1,j} \cdot CKW^* \right\} \vartheta_c \vartheta_m \Delta t_m^2 +$$

$$+ P^{m+1}_{i,j} \left\{ CKC^* \cdot \vartheta_c \vartheta_m \Delta t_m^2 + \varepsilon_{i,j} / c^2_{i,j} \right\} =$$

$$= PRS^m_{i,j} + PRC^m_{i,j} - FLUZ^m_{i,j} - FLUR^m_{i,j} + \qquad (35)$$

$$+ \frac{\vartheta_c \cdot \Delta t_m^2}{\Delta z_j} \left[\left(SZ \cdot FWZ \right)^m_{i,j+1/2} - \left(SZ \cdot FWZ \right)^m_{i,j-1/2} \right] +$$

$$+ \frac{\vartheta_c \cdot \Delta t_m^2}{\Delta r_i} \left[\frac{\psi_{i+\frac{1}{2},j}}{\varepsilon_{i+\frac{1}{2},j}} \left(SR \cdot FWR \right)^m_{i+\frac{1}{2},j} \cdot FACCP_i + \right.$$

$$\left. - \frac{\psi_{i-\frac{1}{2},j}}{\varepsilon_{i-\frac{1}{2},j}} \left(SR \cdot FWR \right)^m_{i-1/2,j} \cdot FACCM_i \right] +$$

$$+ \varepsilon_{i,j} \frac{P^m_{i,j}}{c^{2\,m}_{i,j}} \cdot$$

The numerical solution of the discrete Poisson - like equation (35) is explained in the next section.

List of Symbols used in the previous equations.

$$CKN_{i,j} = \frac{\varepsilon_{i,j}}{\Delta z_j \cdot \Delta z_{j+1/2}}$$

$$CKS_{i,j} = \frac{\varepsilon_{i,j}}{\Delta z_j \cdot \Delta z_{j-1/2}}$$

$$CKE_{i,j} = \frac{\psi_{i+1/2,j} \cdot FACCP_i}{\varepsilon_{i+1/2,j} \cdot \Delta x_i \cdot \Delta x_{i+1/2}}$$

$$CKW_{i,j} = \frac{\psi_{i-1/2,j} \cdot FACCM_i}{\varepsilon_{i-1/2,j} \cdot \Delta x_i \cdot \Delta x_{i-1/2}}$$

$$CKN^*_{i,j} = CKN_{i,j} \cdot FWZ^m_{i,j+1/2}$$

$$CKS^*_{i,j} = CKS_{i,j} \cdot FWZ^m_{i,j-1/2}$$

$$CKE^*_{i,j} = CKE_{i,j} \cdot FWR^m_{i+1/2,j}$$

$$CKW^*_{i,j} = CKW_{i,j} \cdot FWR^m_{i-1/2,j}$$

$$CKC^*_{i,j} = CKN^*_{i,j} + CKS^*_{i,j} + CKE^*_{i,j} + CKW^*_{i,j} \,.$$

$$FWZ^m_{i,j\pm1/2} = 1 \Big/ \left(1 + \Delta t_m \cdot FC\phi Z^m_{j\pm1/2}\right)$$

$$FWR^m_{i\pm1/2,j} = 1 \Big/ \left(1 + \Delta t_m \cdot FC\phi R^m_{i\pm1/2}\right)$$

$$FC\phi Z^m_{j\pm1/2} = \frac{f\,|W^m_{i,j\pm1/2}|}{2\,D_h}$$

$$FC\phi R^m_{i\pm1/2} = \frac{1}{2}\left(\frac{P_w}{S_f}\right)_{i\pm\frac{1}{2}} \cdot f\,|u^{*m}_{i\pm\frac{1}{2},j}|$$

$$CVZZ^{m}_{i,j+\frac{1}{2}} = \frac{\varepsilon_{i,j+\frac{1}{2}}}{\Delta z_{j+1/2}} \left[\left(\rho w^2\right)^{m}_{i,j+1} - \left(\rho w^2\right)^{m}_{i,j} \right]$$

$$CVZR^{m}_{i,j+1/2} = \frac{1}{\Delta r_i} \left[\left(\psi \rho w u\right)^{m}_{\substack{i+1/2 \\ j+1/2}} \cdot FACCP_i - \left(\psi \rho w u\right)^{m}_{\substack{i-1/2 \\ j+1/2}} \cdot FACCM_i \right]$$

$$FZZ^{m}_{i,j+1/2} = \frac{\varepsilon_{i,j+1/2}}{\Delta z_{j+1/2}} \left[\left(\mu \frac{\partial w}{\partial z}\right)^{m}_{i,j+1} - \left(\mu \frac{\partial w}{\partial z}\right)^{m}_{i,j} \right]$$

$$FZR^{m}_{i,j+1/2} = \frac{1}{\Delta r_i} \left[\left(\psi \mu \frac{\partial w}{\partial r}\right)^{m}_{\substack{i+1/2 \\ j+1/2}} \cdot FACCP_i - \left(\psi \mu \frac{\partial w}{\partial r}\right)^{m}_{\substack{i-1/2 \\ j+1/2}} \cdot FACCM_i \right]$$

$$GVZ^{m}_{i,j+1/2} = g \left(\varepsilon \rho\right)^{m}_{i,j+1/2}$$

$$CVRZ^{m}_{i+\frac{1}{2},j} = \frac{\varepsilon_{i+1/2,j}}{\Delta z_j} \left[\left(\rho u w\right)^{m}_{i+\frac{1}{2},j+1/2} - \left(\rho u w\right)^{m}_{i+\frac{1}{2},j-1/2} \right]$$

$$CVRR^{m}_{i+1/2,j} = \frac{1}{\Delta r_{i+\frac{1}{2}}} \left[\left(\psi \rho u^2\right)^{m}_{i+1,j} \cdot FACRP_{i+\frac{1}{2}} - \left(\psi \rho u^2\right)^{m}_{i,j} \cdot FACRM_{i+\frac{1}{2}} \right]$$

$$FRZ^{m}_{i+1/2,j} = \frac{\varepsilon_{i+1/2,j}}{\Delta z_j} \left[\left(\mu \frac{\partial u}{\partial z}\right)^{m}_{\substack{i+1/2 \\ j+1/2}} - \left(\mu \frac{\partial u}{\partial z}\right)^{m}_{\substack{i+1/2 \\ j-1/2}} \right]$$

$$FRR^{m}_{i+1/2,j} = \frac{1}{\Delta r_{i+1/2}} \left[\left(\psi \mu \frac{\partial u}{\partial r}\right)^{m}_{i+1,j} \cdot FACRP_{i+\frac{1}{2}} - \left(\psi \mu \frac{\partial u}{\partial r}\right)^{m}_{i,j} \cdot FACRM_{i+\frac{1}{2}} \right]$$

$$FLUZ^{m}_{i,j} = \frac{\vartheta_c \, \Delta t_m \, \varepsilon_{i,j}}{\Delta z_j} \left[\left(\rho w \cdot FWZ\right)^{m}_{i,j+1/2} - \left(\rho w \cdot FWZ\right)^{m}_{i,j-1/2} \right] +$$

$$- \frac{(1-\vartheta_c) \, \Delta t_m \, \varepsilon_{i,j}}{\Delta z_j} \left[\left(\rho w\right)^{m}_{i,j+1/2} - \left(\rho w\right)^{m}_{i,j-1/2} \right]$$

$$FLUR^{m}_{i,j} = \frac{\vartheta_c \, \Delta t_m}{\Delta r_i} \left[\left(\psi \rho u \cdot FWR\right)^{m}_{i+1/2,j} \cdot FACCP_i - \left(\psi \rho u \cdot FWR\right)^{m}_{\substack{i-1/2 \\ j}} \cdot FACCM_i \right] +$$

$$- \frac{(1-\vartheta_c) \cdot \Delta t_m}{\Delta r_i} \left[\left(\psi \rho u\right)^{m}_{i+1/2,j} \cdot FACCP_i - \left(\psi \rho u\right)^{m}_{i-\frac{1}{2},j} \cdot FACCM_i \right]$$

$$PRS^{m}_{i,j} = \left\{ \rho^{m}_{i,j+1} \cdot CKN^{*}_{i,j} + \rho^{m}_{i,j-1} \cdot CKS^{*}_{i,j} + \right.$$

$$\left. + \rho^{m}_{i+1,j} \cdot CKE^{*}_{i,j} + \rho^{m}_{i-1,j} \cdot CKW^{*}_{i,j} \right\} \vartheta_c (1-\vartheta_m) \Delta t^{2}_{m}$$

$$PRC^{m}_{i,j} = - \rho^{m}_{i,j} \cdot CKC^{*}_{i,j} \cdot \vartheta_c (1-\vartheta_m) \Delta t^{2}_{m} =$$

$$= - \rho^{m}_{i,j} \left\{ CKN^{*}_{i,j} + CKS^{*}_{i,j} + CKE^{*}_{i,j} + CKW^{*}_{i,j} \right\} \vartheta_c (1-\vartheta_m) \Delta t^{2}_{m}$$

$$SZ^{m}_{i,j+\frac{1}{2}} = \left(CVZZ + CVZR - GVZ - FZZ - FZR \right)^{m}_{i,j+1/2}$$

$$SR^{m}_{i+\frac{1}{2},j} = \left(CVRZ + CVRR - FRZ - FRR \right)^{m}_{i+1/2,j}$$

$$CMPR^{m}_{i,j} = \left(\varepsilon_{i,j} / c^{2\,m}_{i,j} \right) \rho^{m}_{i,j}$$

$G^{m}_{i,j}$ = right hand side of equation (35).

Furthermore, the following symbols are used in the programme:

F1 = ϑ_c

F2 = ϑ_m

DD12(JC) = $\Delta z_j + \Delta z_{j+1}$

DZC (JC) = Δz_j

DZZ (JZ) = $\Delta z_{j+1/2}$

DRC (IC) = Δr_i

DRR (IR) = $\Delta r_{i+1/2}$

EPS (IC) = ε_{ij}

EPR (IR) = $\varepsilon_{i+1/2,j}$

PSI (IC) = ψ_i

PSIR (IR) = $\psi_{i+1/2}$

SFR (IR) = $s_{fi+1/2}$

PAR (IR) = $\rho_{w\,i+1/2}$

CF = f

SCSQ = c^2_{ij}

The following symbols are introduced for saving computing time

CUC = $\dfrac{4 \cdot PITCH - \pi \cdot DIA}{4\,(PITCH - DIA)}$

UCØL = CUC · u

DTSQ = Δt_m^2

CFDT = $\vartheta_c \vartheta_m \Delta t_m^2$

AA (IC,JC) = $A_{ij} = \vartheta_c \vartheta_m \Delta t_m^2 \cdot CKC^*_{ij} + \varepsilon_{ij} / c^2_{ij}$

BB (IC,JC) = $B_{ij} = -\vartheta_c \vartheta_m \Delta t_m^2 \cdot CKS^*_{ij}$

CC (IC,JC) = $C_{ij} = -\vartheta_c \vartheta_m \Delta t_m^2 \cdot CKN^*_{ij}$

DD (IC,JC) = $D_{ij} = -\vartheta_c \vartheta_m \Delta t_m^2 \cdot CKW^*_{ij}$

EE (IC,JC) = $E_{ij} = -\vartheta_c \vartheta_m \Delta t_m^2 \cdot CKE^*_{ij}$

3.5 Numerical solution of the Poisson equation

The numerical solution of the Poisson equation for the coolant pressure distribution can be performed either with iterative methods or by means of a direct matrix inversion technique. The iterative methods are

i) Successive Overrelaxation (SOR) with or without the automatic search of the optimum relaxation parameter.

ii) Alternating Direction Implicit (ADI) method.

The matrix inversion method is based on a factorization technique which takes advantage of the block-three-diagonal structure of the matrix of coefficients of the Poisson equation.

In the following sections these methods are explained in detail in the order in which they were developed and linked to the main programme. Their advantages or drawbacks with respect to each other will be discussed briefly at the end of the section.

3.5.1 The SOR Method

The mathematical foundations of the Successive Overrelaxation (SOR) method are given in references /11/, /12/, /15/. The programme user can choose between the following varieties of the SOR method by specifying the input parameter NPN (see input description):

a) SOR method with an input specified (optimum) relaxation parameter (Subroutine SLØR).

b) Automatic search of the optimum relaxation parameter for every time step by means of the so-called "basic iterative method" (Subroutine SLØMX) and subsequent call for Subroutine SLØR.

c) Search of the optimum relaxation parameter by means of the "First Method" of reference /11/ (Iteration with Simultaneous or Successive Relaxation) (Subroutine SLØM) and subsequent call for Subroutine SLØR.

d) Search of the optimum relaxation parameter by means of the "Third Method" of reference /11/ (Subroutine SLØR2) with subsequent call for Subroutine SLØR.

In the following methods a) to d) are analyzed in detail.

a) Subroutine SLØR. The SOR method by input specified (optimum) relaxation parameter ω.

The discrete form of the Poisson equation (35) is solved iteratively by means of a line-method, a line consisting of the axial meshes (j = 2, ...MC) parallel to the bundle axis for a fixed radial mesh index i. Letting r be an iteration index within the time step $t_n \div t_{n+1}$, equation (35) yields

$$A_{i,j}\, p^{r+1}_{i,j} + B_{i,j}\, p^{r+1}_{i,j-1} + C_{i,j}\, p^{r+1}_{i,j+1} = G_{i,j} - D_{i,j}\, p^{r+1}_{i-1,j} - E_{i,j}\, p^{r}_{i+1,j} \qquad (36)$$

$$= Q^{*}_{i,j} \qquad (j = 2,3...MC)$$

When eq. (36) is written for a radial mesh i, the last available value $p^{r+1}_{i-1,j}$ is used at the right-hand side. Equations (36) (j = 2, ...MC) form a system of algebraic equations with three-diagonal matrix A of coefficients

$$A \cdot Y = Q^{*} \qquad A = \begin{vmatrix} a_1 & c_1 & & \\ b_1 & a_2 & c_2 & \\ & \ddots & \ddots & \ddots \end{vmatrix} \qquad (37)$$

where Y represents the vector of unknown pressure values ($y_1 = p_{i2}, y_2 = p_{i3} \cdots y_N = p_{i,MC}$ (N = MC-1)).

The matrix equation (37) is solved by means of the Thomas algorithm /7/. In a first sweep (j = 2 ... MC) it is reduced to the equation

$$A^{*} \cdot Y = D^{*} \qquad A^{*} = \begin{vmatrix} 1 & c_1 & & \\ o & 1 & c_2 & \\ & \ddots & \ddots & \ddots \end{vmatrix} \qquad (38)$$

where the matrix A^{*} is upper bi-diagonal with $a_{jj} = 1$ (j = 1, ...N) and the upper diagonal is defined by

$$c^{*}_{1} = c_1 / a_1 \qquad (j = 1,2 \ldots N-1)$$

$$c^{*}_{j+1} = \frac{c_{j+1}}{a_{j+1} - b_{j+1}\, c^{*}_{j}} \qquad (N = MC-1) \qquad (39)$$

The vector D^* is defined by

$$d_1^* = d_1/a_1$$

$$d_{j+1}^* = \frac{d_{j+1} - b_{j+1}\, d_j^*}{a_{j+1} - b_{j+1}\, c_j^*} \qquad (j = 1,2...N-1) \qquad (40)$$

The second sweep yields the solution vector $\tilde{Y}$

$$\tilde{y}_N = d_N^*$$

$$\tilde{y}_j = d_j^* - c_j^*\, y_{j+1}. \qquad (j = N-1,\ N-2,...1) \qquad (41)$$

$\tilde{Y}$ is the exact solution of eq. (36) but only a first approximation to the solution Y of eq. (35), which is then obtained by means of the iterative scheme

$$Y^{r+1} = Y^r + \omega\left(\tilde{Y}^{r+1} - Y^r\right) \qquad 0 \leq \omega \leq 2 \qquad (42)$$

where the vector $\tilde{Y}^{r+1} - Y^r$ has been determined by an exact displacement (ω=1). The scheme is then applied to the other lines i (i = 2, ... NC). The iteration is carried on till a convergence criterion is satisfied:

$$\max\left\{\left|P_{i,j}^{r+1} - P_{i,j}^{r}\right|_{\substack{i=2,..NC \\ j=2,..MC}}\right\} \leq \varepsilon \qquad (43)$$

where ε is an input value.

b) Subroutine SLØMX. Search of optimum relaxation parameter by the "basic iterative method".

The subroutine SLØMX works basically with the same iterative scheme explained previously for the subroutine SLØR but at the same time it performs a search of the optimum relaxation parameter. The principles of the relaxation theory by Young and Frankel /18/, /19/ which form the basis of this part of the programme are summarized in the following.

The successive overrelaxation method (SOR) for the matrix equation

$$A \cdot Y = b \qquad (44)$$

is expressed by the iterative scheme /12/

$$Y^{n+1} = \mathcal{L}_\omega Y^n + (\mathcal{J} - \omega L)^{-1} \omega c \qquad (1 < \omega < 2) \tag{45}$$

where

$$\mathcal{L}_\omega = (I-\omega L)^{-1} (\omega U + (1-\omega) I) \tag{46a}$$

$$c = D^{-1} b \tag{46b}$$

$$D = \text{diag } A \tag{46c}$$

$$C = D-A \tag{46d}$$

$$B = D^{-1} C = L + U \tag{46e}$$

$$L = \text{strictly lower triangular matrix} \tag{46f}$$

$$U = \text{strictly upper triangular matrix} \tag{46g}$$

$$I = \text{unity matrix} \tag{46h}$$

For $\omega = 1$, the Gauss-Seidel (G-S) method, it holds

$$Y^{n+1} = \mathcal{L} Y^n + (\mathcal{J} - L)^{-1} c \tag{47}$$

with

$$\mathcal{L} = (\mathcal{J} - L)^{-1} U. \tag{48}$$

For the Jacobi (J) method one would use

$$Y^{n+1} = B Y^n + c. \tag{49}$$

The convergence of the iteration scheme (45) is controlled by the maximum modulus of the eigenvalues of $\mathcal{L}_\omega$. Hence arises the exigence of searching the value of the overrelaxation parameter ω for which the maximum modulus is minimized. Let λ_i denote the eigenvalues of $\mathcal{L}_\omega$.
They satisfy the equation

$$\begin{aligned} &\det [\mathcal{L}_\omega - \lambda \mathcal{J}] = 0 \\ &Q(\lambda) = 0. \end{aligned} \tag{50}$$

The relaxation theory shows that there is a relationship between the eigenvalues λ_i of the matrix $\mathcal{L}_\omega$ and the eigenvalues μ_i of the iteration matrix B of the Jacobi method which satisfy the equation

$$\begin{aligned} &\det [B - \mu \mathcal{J}] = 0 \\ &P(\mu) = 0. \end{aligned} \tag{51}$$

The relation between the roots of the characteristic equations (50) and (51) is

$$\frac{(\lambda+\omega-1)^2}{\lambda} = \omega^2\mu^2 \tag{52}$$

If $\omega = 1$

$$\lambda = \mu^2 \tag{53}$$

The optimum overrelaxation parameter is that which minimizes (52) and is given by

$$\omega_b = \frac{2}{1+\sqrt{1-\mu_N^2}} \tag{54}$$

where

$$\mu_N = \max_i |\mu_i| . \tag{55}$$

To the optimum overrelaxation parameter corresponds the minimum value of the maximum modulus of the roots of (50)

$$\lambda_{min} = \min \left\{ \max_i |\lambda_i(\omega)| \right\} = \omega_b - 1 . \tag{56}$$

The problem of finding the optimum overrelaxation parameter is therefore reduced to the problem of finding the maximum modulus μ_N of the eigenvalues of the matrix of the Jacobi method. If $\mu_N < 1$ the Jacobi method converges, so does the SOR method for real ω ($1 < \omega < 2$) and the best convergence rate is achieved for $\omega = \omega_b$.

The maximum modulus μ_N can be calculated as follows.

The solution Y of equation (44) satisfies exactly equation (45)

$$Y = \mathcal{L}_\omega Y + (\mathcal{J} - \omega L)^{-1} \omega c . \tag{57}$$

Subtracting (57) from (45) yields

$$Y^{n+1} - Y = \mathcal{L}_\omega (Y^n - Y) \tag{58}$$

or

$$e^{r+1} = \mathcal{L}_\omega \, e^r \tag{59}$$

with the definition of the vector error

$$e^r = Y^r - Y. \tag{60}$$

Repeated application of (59) (r, r-1 ... r= 0) yields

$$e^{r+1} = \mathcal{L}_\omega^{r+1} \cdot e^0. \tag{61}$$

Let

$$\delta^r = Y^{r+1} - Y^r = Y^{r+1} - Y - (Y^r - Y) = e^{r+1} - e^r \tag{62}$$

be the increment of the solution vector at the iteration step r.
Analogously to eq. (61) one derives

$$\delta^r = \mathcal{L}_\omega \, \delta^{r-1} = \dots = \mathcal{L}_\omega^r \, \delta^0. \tag{63}$$

Equations (61) and (63) characterize a stationary iteration scheme.

Let $b_1, b_2 \dots b_N$ be the set of the eigenvectors associated to the eigenvalues λ_j of $\mathcal{L}_\omega$.
It holds

$$\mathcal{L}_\omega \, b_j = \lambda_j \, b_j \qquad (j = 1,2 \dots N). \tag{64}$$

Let assume $\lambda_1 < \lambda_2 < \dots < \lambda_N$. The eigenvectors b_j form a basis of the N-dimensional space; hence the solution increment δ^0 can be written as a linear combination of b_j

$$\delta^0 = h_1 b_1 + h_2 b_2 + \dots + h_N b_N \tag{65}$$

where h_j (j = 1, 2,...N) are real constants.

From (63) and (64) one derives

$$\begin{aligned} \delta^r &= h_1 \lambda_1^r b_1 + h_2 \lambda_2^r b_2 + \dots + h_N \lambda_N^r b_N = \\ &= \lambda_N^r \left[h_1 \left(\frac{\lambda_1}{\lambda_N} \right)^r b_1 + h_2 \left(\frac{\lambda_2}{\lambda_N} \right)^r b_2 + \dots + h_N b_N \right] = \\ &= \lambda_N^r \left[h_N b_N + O\left(\frac{\lambda_{N-1}}{\lambda_N} \right)^r \right] \end{aligned} \tag{66}$$

The error 0 is the smaller, the larger the maximum eigenvalues λ_N is with respect to λ_{N-1} and the larger the iteration index r.

The maximum eigenvalue λ_N is then approximated by the limit of the ratio of the norms of the solution increments δ^r

$$\vartheta = \lim_{r\to\infty} \frac{\|\delta^{r+1}\|}{\|\delta^r\|} = \lim_{r\to\infty} \frac{\|\lambda_N^{r+1} h_N b_N\|}{\|\lambda_N^r h_N b_N\|} = \tag{67}$$

$$= \lim_{r\to\infty} \frac{\lambda_N^{r+1}}{\lambda_N^r} \cdot \frac{\|b_N\|}{\|b_N\|} = \lambda_N .$$

If $\omega = 1$ (Gauss-Seidel iteration)

$$\vartheta = \lambda_N = \mu_N^2 . \tag{68}$$

If $\omega \neq 1$ the relation between ϑ $(= \lambda_N)$ and μ_N is given by /12/

$$\mu_N = \frac{\vartheta + \omega - 1}{\omega \sqrt{\vartheta}} . \tag{69}$$

In the Subroutine SLØMX two iteration cycles are performed:

i) iterating with $\omega = 1$ and applying (67) yields $\vartheta = \mu_N^2$ hence a first estimation of $\tilde{\omega}_b$ by (54)

ii) iterating with $\omega = \tilde{\omega}_b$ and applying (67), (69) and (54) yields a final value for ω_b.

The iteration steps are useful not only for the estimation of the optimum relaxation parameter, but also for approaching the solution vector Y. The final solution for the time step is then obtained by entering into Subroutine SLØR with $\omega = \omega_b$.

c) Search of optimum relaxation with Subroutine SLØM

We consider the matrix equation (44) with $b \equiv o$. The solution is then $Y \equiv o$. Let try to determine this solution numerically by iterating with the Jacobi method of simultaneous displacements (49) and starting with a vector $Y^o \equiv 1$. One has

$$Y^{r+1} = B Y^r = B^2 Y^{r-1} = \dots = B^{r+1} Y^o = B^{r+1} \tag{70}$$

Let b_j (j = 1,2...N) be the set of eigenvectors of B associated to the eigenvalues μ_j ($\mu_1 < \mu_2 < \cdots < \mu_N$)

$$B\, b_j = \mu_j\, b_j . \tag{71}$$

The vector Y^o can be written as a linear combination of the b_j

$$Y^o = \sum_1^N{}_j\, h_j\, b_j \tag{72}$$

when h_j are real constants. It follows

$$Y^{n+1} = \sum_1^N{}_j\, h_j\, (\mu_j)^{n+1}\, b_j = \tag{73}$$

$$= \mu_N^{n+1} \left[h_N b_N + h_{N-1}\, b_{N-1} \left(\frac{\mu_{N-1}}{\mu_N}\right)^{n+1} + \cdots + h_1 b_1 \left(\frac{\mu_1}{\mu_N}\right)^{n+1} \right]$$

$$= \mu_N^{n+1} \left[h_N b_N + O\left(\frac{\mu_{N-1}}{\mu_N}\right)^{n+1} \right].$$

The maximum eigenvalue μ_N can then be approximated by

$$\mu_N = \lim_{n \to \infty} \left[\frac{(Y^{n+1} \cdot Y^{n+1})}{(Y^n \cdot Y^n)} \right]^{1/2} = \lim_{n \to \infty} \left[\frac{\| Y^{n+1} \|}{\| Y^n \|} \right] = \tag{74}$$

$$= \frac{\| \mu_N^{n+1} h_N b_N \|}{\| \mu_N^n h_N b_N \|} .$$

According to reference /20/ μ_N can be determined in practice by means of the bounding relations

$$\underline{\lambda}_1 \leq \cdots \leq \underline{\lambda}_m \leq \mu_N \leq \bar{\lambda}_m \leq \bar{\lambda}_{m-1} \leq \cdots \bar{\lambda}_1 \tag{75}$$

where

$$\underline{\lambda}_m = \min_i \frac{(y_i)_m}{(y_i)_{m-1}} \qquad (m = 1, 2, \ldots n) \tag{76a}$$

$$\bar{\lambda}_m = \max_i \frac{(y_i)_m}{(y_i)_{m-1}} \tag{76b}$$

where y_i are the components of the vector Y.

If successive displacements with $\omega = 1$ are used instead of simultaneous displacements the sequences (76) tend to μ_N^2.
Corresponding bounds of the optimum relaxation parameter ω_b are given by

$$\underline{\omega}_1 \leq \underline{\omega}_2 \leq \cdots \leq \underline{\omega}_m \leq \omega_b \leq \bar{\omega}_m \leq \bar{\omega}_{m-1} \leq \cdots \leq \bar{\omega}_1 \qquad (77)$$

with

$$\underline{\omega}_m = \frac{2}{1 + \sqrt{1 - \underline{\mu}_m^2}} \qquad (78a)$$

$$\bar{\omega}_m = \frac{2}{1 + \sqrt{1 - \bar{\mu}_m^2}} \; . \qquad (78b)$$

In the subroutine SLOM the upper bound ω_m is taken for the optimum relaxation parameter ω_b because a slight overestimation of ω_b is always better than an underestimation.

d) Search of optimum relaxation parameter with Subroutine SLOR2.

Assume a relaxation parameter ω presumably smaller than the optimum ω_b. We apply to equation (44) $A \cdot Y = b$ the iteration scheme (45) in three subsequent steps:

i) 1st Step. Assuming a starting vector $Y^o \equiv o$ we iterate equation (44) m times to get a first numerical solution $Y_1 = Y^{(m)}$:

$$A\,Y^o = b \quad \xrightarrow{\text{yields}} \quad Y_1 = Y^{(m)} . \qquad (79)$$

ii) 2nd Step. We set the right-hand side of equation (44) equal to zero and iterate (m-1) times starting from the previous numerical solution $Y^{(m)}$, getting a new numerical solution $Y^{(2m-1)}$:

$$A \cdot Y^{(m)} = o \quad \xrightarrow{\text{yields}} \quad Y_2 = Y^{(2\,m-1)} . \qquad (80)$$

Let

$$\ell_2 = \| Y_2 \|^2 \qquad (81)$$

be the square of the length of the vector Y_2.

iii) 3rd Step. Iterate equation (44) once more starting from the numerical solution $Y^{(2\,m-1)}$ to get $Y^{(2m)}$

$$A \cdot Y^{(2\,m-1)} = o \quad \xrightarrow{\text{yields}} \quad Y_3 = Y^{(2m)} \tag{82}$$

Let

$$\ell_3 = \| Y_3 \|^2 = \| Y^{(2m)} \|^2 \tag{83}$$

be the square of the length of the vector Y_3.

We define a new vector $Y^{(2m)*}$ as the sum of vectors Y_1 and Y_3:

$$Y^{(2m)*} = Y_1 + Y_3 = Y^{(m)} + Y^{(2m)}. \tag{84}$$

The SOR method is expressed by the iterative scheme /12/

$$Y^m = \mathcal{L}_\omega Y^{m-1} + F \tag{85}$$

with

$$F = (J-\omega L)^{-1} \omega D^{-1} b. \tag{86}$$

Equation (85) yields the iterative formula

$$Y^m = \mathcal{L}_\omega^m \cdot Y^0 + \mathcal{L}_\omega^{m-1} \cdot F + \mathcal{L}_\omega^{m-2} \cdot F + \cdots + \mathcal{L}_\omega F + F. \tag{87}$$

After the 1st step made with $Y^0 \equiv o$ one has

$$Y^m = \mathcal{L}_\omega^{m-1} \cdot F + \mathcal{L}_\omega^{m-2} \cdot F + \cdots + \mathcal{L}_\omega F + F. \tag{88}$$

The 2nd and 3rd steps have been started from this numerical solution (88) and carried out for say m' further steps. Thus they yield (with $b \equiv o$, hence $F \equiv o$ for these steps)

$$Y^{(m+m')} = \mathcal{L}_\omega^{m'} \cdot Y^m + \mathcal{L}_\omega^{m'-1} \cdot F + \cdots + F. \tag{89}$$

Using (88) one has

$$Y^{(m+m')} = \mathcal{L}_\omega^{m'} \left(\mathcal{L}_\omega^{m-1} \cdot F + \cdots + \mathcal{L}_\omega F + \bar{F} \right). \tag{90}$$

If $m = m'$

$$Y^{(2m)} = \mathcal{L}_\omega^{m} \left(\mathcal{L}_\omega^{m-1} F + \cdots + \mathcal{L}_\omega F + F \right). \tag{91}$$

Combining (88) and (91), equation (84) yields

$$Y^{(2m)*} = Y^{(m)} + Y^{(2m)} = \left(I + \mathcal{L}_\omega^{m} \right) \left(\mathcal{L}_\omega^{m-1} F + \cdots + \mathcal{L}_\omega F + F \right) \tag{92}$$

$$= \mathcal{L}_\omega^{(2m-1)} F + \cdots + \mathcal{L}_\omega^{m} F + \mathcal{L}_\omega^{m-1} F + \cdots + F. \tag{93}$$

Equation (93) is consistent with (87) because it could have been obtained by applying the first step 2m times.

When performing the 2nd and 3rd step with $b \equiv o$ the numerical solution $Y^{(2m)}$ approaches the zero vector, say $\emptyset$, which is the true solution. One has therefore

$$Y^{(2m)} - \emptyset = E^{2m} \tag{94}$$

where E is the error vector.

Let $(e_1, e_2, \ldots . e_N)$ be the set of eigenvectors associated to the eigenvalues λ_j $(j = 1,2,\ldots N)$ of $\mathcal{L}_\omega$. It holds

$$\mathcal{L}_\omega e_j = \lambda_j e_j. \tag{95}$$

The eigenvectors e_j form a basis of the N-dimensional space, therefore the error vector E^1 can be written as a linear combination of the e_j

$$E^1 = h_1 e_1 + \ldots . + h_N e_N \tag{96}$$

where h_j $(j = 1,2,\ldots .N)$ are real constants.

Recursive application of eq. (95) yields

$$E^{r} = \lambda_1^{r-1} h_1 e_1 + \lambda_2^{r-1} h_2 e_2 + \cdots + \lambda_N^{r-1} h_N e_N . \tag{97}$$

Let assume $\lambda_1 < \lambda_2 < \ldots < \lambda_N$. Dividing the right hand side of eq. (97) by the eigenvalue of maximum modulus λ_N one has

$$E^{r} = \lambda_N^{r-1} h_N e_N \left[1 + \left(\frac{\lambda_1}{\lambda_N} \right)^{r-1} h_1 e_1 + \cdots + \left(\frac{\lambda_{N-1}}{\lambda_N} \right)^{r-1} h_{N-1} e_{N-1} \right] . \tag{98}$$

The maximum eigenvalue λ_N is then approximated by the limit of the ratio of the norms of two subsequent error vectors as the iteration index r tends to infinity

$$\begin{aligned} \vartheta &= \lim_{r \to \infty} \frac{\| E^{r} \|}{\| E^{r-1} \|} = \\ &= \lim_{r \to \infty} \frac{\left\| h_N e_N \lambda_N^{r-1} \left[1 + O\left(\frac{\lambda_{N-1}}{\lambda_N} \right)^{r-1} h_{N-1} e_{N-1} \right] \right\|}{\left\| h_N e_N \lambda_N^{r-2} \left[1 + O\left(\frac{\lambda_{N-1}}{\lambda_N} \right)^{r-2} h_{N-1} e_{N-1} \right] \right\|} = \\ &= \lim_{r \to \infty} \frac{\left\| h_N e_N \lambda_N^{r-1} \right\|}{\left\| h_N e_N \lambda_N^{r-2} \right\|} = \lambda_N . \end{aligned} \tag{99}$$

In the programme λ_N is approximated by

$$\vartheta = \lambda_N \approx \sqrt{\frac{l_3}{l_2}} = \frac{\| Y^{(2m)} \|}{\| Y^{(2m-1)} \|} = \frac{\| Y^{(2m)} - \phi \|}{\| Y^{(2m-1)} - \phi \|} = \frac{\| E^{2m} \|}{\| E^{2m-1} \|} . \tag{100}$$

The corresponding eigenvalue of the iteration matrix B of the Jacobi method is then

$$\mu_N = \frac{\vartheta + \omega - 1}{\omega \sqrt{\vartheta}} . \tag{101}$$

Equation (54) yields then the optimum relaxation parameter ω_b.

3.5.2 Alternating Direction Implicit (ADI) method

Write the Poisson equation (35) in the form

$$A_{ij}\, p^{n+1}_{ij} + B_{ij}\, p^{n+1}_{i,j-1} + C_{ij}\, p^{n+1}_{i,j+1} + D_{ij}\, p^{n+1}_{i-1,j} + E_{ij}\, p^{n+1}_{i+1,j} = G^{n}_{ij} \qquad (102)$$

where G^{n}_{ij} collects all convective, diffusive and pressure terms at time level t_n.

According to the Alternating Direction Implicit (ADI) technique we integrate equation (102) in each coordinate direction separately. We reduce therefore the solution of a two dimensional problem to the simpler solution of two one-dimensional ones. After the first integration in one direction the fully updated pressure field is used for the subsequent integration. The two integration steps are as follows:

- Step 1. Integration along the axial z coordinate (j = 2,3,...MC) for every radial mesh. Equation (102) is written in the form

$$A_{ij}\, p^{(1)}_{ij} + B_{ij}\, p^{(1)}_{i,j-1} + C_{ij}\, p^{(1)}_{i,j+1} = G^{n}_{ij} - D_{ij}\, p^{n}_{i-1,j} - E_{ij}\, p^{n}_{i+1,j} \qquad (103)$$

  where pressure values at the right-hand side, provisionally considered as known, are taken from the previous time step. Equation (103) yields for every (i) a system of equations with three-diagonal matrix of coefficients. Its solution is direct and gives a new pressure field $p^{(1)}_{ij}$ which is used for the next iteration step.

- Step 2. Integration along the radial r-coordinate (i = 2,3,...NC) for every axial mesh (j). Equation (102) is written in the form

$$A_{ij}\, p^{(2)}_{ij} + D_{ij}\, p^{(2)}_{i+1,j} + E_{ij}\, p^{(2)}_{i-1,j} = G^{n}_{ij} - B_{ij}\, p^{(1)}_{i,j-1} - C_{ij}\, p^{(1)}_{i,j+1} \qquad (104)$$

The pressure field $p_{ij}^{(1)}$ from the previous step is used at the right-hand side. The solution of the system of equations (104) yields the updated pressure field $p_{ij}^{(2)}$.

Equations (103) and (104) are applied repeatedly.

The iteration is terminated when two subsequent solutions of the pressure field differ by less than a given tolerance. On an average, a few iteration sweeps (4 to 6) are necessary for reaching a tolerance of 10^{-5}.

3.5.3 Direct matrix inversion

The system of equations (35) (i = 2,3,...NC; j = 2,3,...MC) has a matrix of coefficients which can be written in the form

$$A = \begin{vmatrix} A_1 & B_1 & & & & \\ C_1 & A_2 & B_2 & & & \\ & C_2 & A_3 & B_3 & & \\ & & \cdots & \cdots & \cdots & \\ & & & C_{M-2} & A_{M-1} & B_{M-1} \\ & & & & C_{M-1} & A_M \end{vmatrix} \qquad (105)$$

with M = MC-1. Matrix A is block-tridiagonal. The blocks of the main diagonal are tridiagonal matrices with dimension (NC-1) x (NC-1) and have the form

$$A_j = \begin{vmatrix} A_{2j} & E_{2j} & & \\ D_{3j} & A_{3j} & E_{3j} & \\ & \cdots & \cdots & \\ & & D_{NC,j} & A_{NC,j} \end{vmatrix} \qquad (106)$$

The blocks B_j, C_j ($j = 1,2,\ldots M-1$) are diagonal matrices and are given by

$$B_j = \begin{vmatrix} c_{2j} & & & \\ & c_{3j} & & \\ & & \ldots & \\ & & & c_{NC,j} \end{vmatrix} \qquad (107)$$

$$C_j = \begin{vmatrix} B_{2j} & & & \\ & B_{3j} & & \\ & & \ldots & \\ & & & B_{NC,j} \end{vmatrix} \qquad (108)$$

Blocks A_j are fully stored, while blocks B_j, C_j are stored in diagonal form.

The system of equations (35) can be written as

$$A \cdot P = b \qquad (109)$$

when the unknown vector P has (NC-1) · (MC-1) components given by

$$P_k = p_{ij} \qquad \begin{aligned} i &= 2,3,\ldots NC \\ j &= 2,3,\ldots MC \\ k &= (j-2) \cdot (NC-1) + i-1 \end{aligned} \qquad (110)$$

Equation (109) is solved with respect to P by inverting matrix A with the method of reference /16/.

We apply a transformation T to matrix A and reduce it to the form

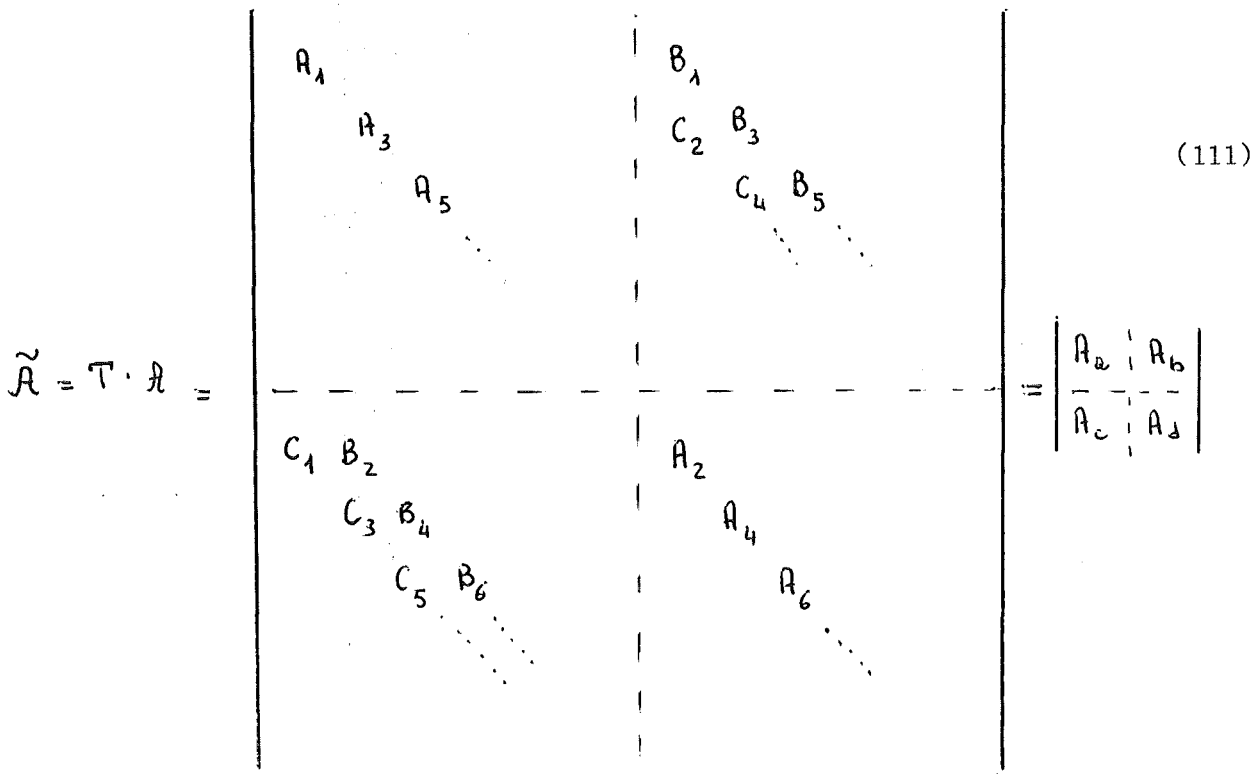

(111)

The block-dimensions of submatrices in (111) are

A_a	(n x n)	with	$k = M \div 2$
A_b	(n x k)		$n = M - k$
A_c	(k x n)		$(k \leq n)$
A_d	(k x k)		

Rearranging of blocks A_j ($j = 1,2,\ldots M$) from matrix A to matrix $\tilde{A}$ is made according to the reordering vector R_e defined by

$$R_e(\ell) = \begin{cases} 2\ell - 1 & \ell \leq m \\ 2(\ell - m) & \ell > m \end{cases} \qquad (112)$$

with the definition of the matrices

$$H = A_c \cdot A_a^{-1} \qquad (k \times n) \qquad (113)$$

$$Y = A_d - H \cdot A_b \qquad (k \times k) \qquad (114)$$

matrix $\tilde{A}$ can be written

$$\tilde{A} = \begin{vmatrix} A_a & A_b \\ A_c & A_d \end{vmatrix} = \begin{vmatrix} M & 0 \\ H & U \end{vmatrix} \cdot \begin{vmatrix} A_a & A_b \\ 0 & Y \end{vmatrix} \qquad (115)$$

where U is the identity matrix.

The inverse of matrix $\tilde{A}$ is

$$\tilde{A}^{-1} = \begin{vmatrix} A_a & A_b \\ A_c & A_d \end{vmatrix}^{-1} = \begin{vmatrix} A_a^{-1} + A_a^{-1} A_b Y^{-1} H & -A_a^{-1} A_b Y^{-1} \\ -Y^{-1} H & Y^{-1} \end{vmatrix} =$$

(116)

$$= \begin{vmatrix} I - Z Y^{-1} H & Z Y^{-1} \\ -Y^{-1} H & Y^{-1} \end{vmatrix}$$

with

$$I = A_a^{-1} \qquad (m \times m) \qquad (117)$$

$$Z = -A_a^{-1} \cdot A_b \qquad (m \times K). \qquad (118)$$

Matrices I, H, Z, Y are given in terms of the blocks of the known matrix A by

$$I = A_a^{-1} = \begin{vmatrix} I_1 & & \\ & I_2 & \\ & & I_3 \ddots \end{vmatrix} = \begin{vmatrix} A_1^{-1} & & \\ & A_3^{-1} & \\ & & A_5^{-1} \ddots \end{vmatrix} \qquad (m \times m) \qquad (119)$$

$$H = A_c \cdot A_a^{-1} = \begin{vmatrix} H_1 & E_1 & \\ & H_2 & E_2 \\ & & H_3 \ddots E_3 \ddots \end{vmatrix} \qquad (K \times m) \qquad (120)$$

with

$$H_i = C_{2i-1}\, I_i = C_{2i-1}\, A_{2i-1}^{-1} \qquad (121)$$

$$E_i = B_{2i}\, I_{i+1} = B_{2i}\, A_{2i+1}^{-1}\ ; \qquad (122)$$

$$Z = -A_a^{-1}\, A_b = \begin{vmatrix} Z_1 & & & \\ V_1 & Z_2 & & \\ & V_2 & Z_3 & \\ & & V_3 & \ddots \end{vmatrix} \qquad (m \times K) \qquad (123)$$

with

$$Z_i = -I_i\, B_{2i-1} = -A_{2i-1}^{-1} \cdot B_{2i-1} \qquad (124)$$

$$V_i = -I_{i+1}\, C_{2i} = -A_{2i+1}^{-1} \cdot C_{2i}\ ; \qquad (125)$$

$$Y = A_d - H \cdot A_b = \begin{vmatrix} A'_1 & B'_1 & & \\ C'_1 & A'_2 & B'_2 & \\ & C'_2 & A'_3 & B'_3 \\ & & \ddots & \ddots \end{vmatrix} \qquad (K \times K) \qquad (126)$$

with

$$B'_i = -E_i \cdot B_{2i+1} \qquad (i = 1,2\ldots K-1) \qquad (127)$$

$$C'_i = -H_{i+1} \cdot C_{2i} \qquad (i = 1,2\ldots K-1) \qquad (128)$$

$$A'_i = A_{2i} - H_i \cdot B_{2i-1}\ . \qquad (i = 1,2\ldots K) \qquad (129a)$$

For $i < n$ an additional term $E_i \cdot C_{2i}$ is added to A'_i in (129) which thus becomes

$$A'_i = A_{2i} - H_i \cdot B_{2i-1} - E_i \cdot C_{2i} \qquad (i = 1,2,\ldots K)\ (i < n) \qquad (129b)$$

We define further following matrices

$$X = Y^{-1} \qquad (k \times k) \qquad (130)$$

$$F = -X \cdot H \qquad (k \times u) \qquad (131)$$

$$L = Z \cdot F = -Z\ X\ H \qquad (n \times u) \qquad (132)$$

$$G = Z \cdot X \qquad (n \times k) \qquad (133)$$

Letting X_{ij} $(i,j = 1,2,\ldots k)$ be a block of matrix X, the blocks of matrices F, L, G are given by

$$F_{i1} = -X_{i1} \cdot H_1 \qquad (i = 1,2,\ldots K) \qquad (134)$$

$$F_{ij} = -\left(X_{i,j-1} \cdot E_{j-1} + X_{ij} H_j\right) \qquad (i = 1,2,\ldots K;\ j = 2,3,\ldots K) \qquad (135)$$

$$(\text{If } m>k)\quad F_{im} = -X_{iK} E_K \qquad (i = 1,2,\ldots K) \qquad (136)$$

$$G_{1j} = Z_1 \cdot X_{1j} \qquad (j = 1,2,\ldots K) \qquad (137)$$

$$G_{ij} = V_{i-1} \cdot X_{i-1,j} + Z_i \cdot X_{ij} \qquad (i = 2,3,\ldots K;\ j = 1,2,\ldots K) \qquad (138)$$

$$(\text{If } m>k)\quad G_{mj} = V_K \cdot X_{Kj} \qquad (j = 1,2,\ldots K) \qquad (139)$$

$$L_{1j} = Z_1 \cdot F_{1j} \qquad (j = 1,2,\ldots n) \qquad (140)$$

$$L_{ij} = V_{i-1} \cdot F_{i-1,j} + Z_i F_{ij} \qquad (i = 2,3,\ldots K;\ j = 1,2,\ldots K) \qquad (141)$$

$$(\text{If } m>k)\quad L_{mj} = V_K \cdot F_{Kj} \qquad (j = 1,2,\ldots n) \qquad (142)$$

With the definitions (130) to (133) matrix A^{-1} can be written

$$\tilde{A}^{-1} = \begin{vmatrix} I+L & G \\ F & X \end{vmatrix} \qquad (143)$$

If $X = Y^{-1}$ were known, matrices L, G, F could be calculated easily and therefore $\tilde{A}^{-1}$ would be known. The problem of inverting matrix A is therefore reduced to that of inverting matrix Y which is also block-tridiagonal. The same procedure followed so far for matrix A can therefore be applied in a second step to $Y = Y_{(1)}$, where index (1) refers to the application of the first step. Through application of successive steps we reduce the problems to the inversion of matrices of decreasing dimensions

$$Y_{(1)}, Y_{(2)}, \ldots \quad Y_{(\lambda)}, \ldots Y_{(S)}$$

till after S steps we get a matrix of the dimension of a single block (NC-1) x (NC-1) which can be inverted easily, thus yielding

$$X_S = (Y_{(S)})^{-1} \qquad (144)$$

This completes the forward chain of the method, consisting in reducing the problem of inverting a larger matrix to that of inverting a smaller one.

After the S-th step and after inverting Y_S we calculate

$$X_{(S-1)} = Y_{(S-1)}^{-1} \cdot T_{S-1} = \begin{vmatrix} (I+L)_S & G_S \\ F_S & X_S \end{vmatrix} \cdot T_{S-1} \qquad (145)$$

where T_{S-1} is the transformation applied at the (S-1)th step on Y_{S-1} to get $\tilde{Y}_{S-1}$, like in (111). The transformation implies in practice a rearranging of the blocks of $Y_{(S-1)}$ according to the reordering vector (112).

Repeated application of (145) for the backward chain yields X_{S-2}, X_{S-3}, ... up to $X_1 = X$. Formula (143) yields then $\tilde{A}^{-1}$.

In practice we solve equation (109) using formula (143) but without calculating the full matrix $\tilde{A}^{-1}$ which would require a large storage area in the computer. After transforming matrix A into $\tilde{A}$ as in (111) we reorder

also the vectors P and b according to the reordering vector (112) to get $\tilde{P}$, $\tilde{b}$. Equation (109) is thus transformed into the equivalent one

$$\tilde{A} \cdot \tilde{P} = \tilde{b} \quad . \tag{146}$$

Its solution is

$$\tilde{P} = \tilde{A}^{-1} \cdot \tilde{b} \tag{147}$$

or partitioning according to (143)

$$\begin{vmatrix} \tilde{P}_a \\ \tilde{P}_b \end{vmatrix} = \begin{vmatrix} I + L & G \\ F & X \end{vmatrix} \cdot \begin{vmatrix} \tilde{b}_a \\ \tilde{b}_b \end{vmatrix} \quad . \tag{148}$$

From (148) one derives

$$\tilde{P}_a = (I+L)\,\tilde{b}_a + G \cdot \tilde{b}_b \tag{149a}$$

$$\tilde{P}_b = F \cdot \tilde{b}_a + X \cdot \tilde{b}_b \quad . \tag{149b}$$

Terms in equations (149) are calculated in the following sequence, for saving storage area:

i) compute matrix G with (137) to (139) using a storage area SS

ii) compute $G \cdot \tilde{b}_b$

iii) compute matrix F (in the same storage area SS) with (134) to (136)

iv) compute $F \cdot \tilde{b}_a$

v) compute $X \cdot \tilde{b}_b$ (matrix X is known as the result of the first S-1 backward steps)

vi) compute matrix L with (140) to (142) in storage area previously used for X

vii) compute matrix I with (119) and I+L

viii) compute $(I+L)\,\tilde{b}_a$.

Thus only two storage arrays are needed for the matrices, each one as large as one forth of the matrix A.

A backward transformation of $\tilde{P}$ according to the reordering vector (112) yields the solution vector P of equation (109).

3.5.4 Comparison of the above methods

Iterative solution of large linear systems is in general compulsory when storage area requirements and computing time have to be minimized. When applying the SOR or the ADI methods only the coefficients of equation (35) and its right-hand side must be memorized. The solution method requires only negligible additional storage area. The direct inversion method explained in section 3.5.3 requires on the contrary the storage of the blocks of the tridiagonal matrix of coefficients A (105), two additional storage areas equal to one fourth of the matrix A, and additional working fields for the storage of matrices H_i, E_i, Z_i, V_i, B_i, C_i, A_i (see formulas (121), (122), (124), (125), (127) to (129). For this reason we use in the actual programme version the direct matrix inversion method for bundles with 37 pins or less and the iterative methods for larger pin bundles.

The advantages or drawbacks of each method are now outlined shortly:

i) SOR Methods.

The Gauss-Seidel iteration scheme can be applied using subroutine SLØR with $\omega = 1$. It converges unconditionally but the convergence rate is poor. Subroutine SLØR is advantageous when the optimum relaxation parameter $\omega = \omega_b$ is already known, for instance from previous calculations, or can be estimated within sufficient accuracy.

When the optimum relaxation parameter is not known it must be calculated with one of the Subroutines SLOMX, SLOM or SLOR2. These three subroutines give with a good accuracy the same results for ω_b but they require a quite different calculation effort.

Subroutine SLOMX is the fastest one. It gives a sufficient estimation of ω_b in 5 - 10 iteration steps and presents the advantage that, when searching for ω_b, the iterations contribute already to the solution of equation (44) (see 5.3.1 b). However a very accurate estimation of ω_b requires about 30 - 40 iteration steps.

The method used in subroutine SLOM solves the matrix equation $AY = b$ with $b = o$. Its solution $Y = o$ is approached by the error vector $E^r = Y^r$. According to reference /11/ greater accuracy in the estimation of ω_b is attained in fewer iterations when the solution coincides with the error vector. The disadvantage consists in the fact that, when iterating with

b = o for determining ω_b, the iterations are wasted because they do not contribute to the solution of equation (44).

The disadvantage of subroutine SLOM is removed in subroutine SLOR2 which iterates eq. (44) without modifying the right-hand side. Subroutine SLOR2 yields a very accurate estimation of ω_b but requires a large number of iterations (more than one hundred). It cannot therefore be used for every time step in a larger calculation. It can be applied in a separate run to estimate ω_b for subsequent use in subroutine SLOR.

In practice we suggest the application of Subroutine SLOR when ω_b has been already estimated, otherwise the application of Subroutine SLOMX.

ii) The ADI Method

In case of large bundles the Alternating Directions Implicit method is slightly more efficient than the SOR methods. For blockage calculations the mass unbalance, calculated for every cell by verifying the coolant continuity equation, is smaller than with other iterative methods. However, a small time step (about 0.5 ms) is required. So far it has not been attempted to accelerate the convergence of the ADI method.

iii) The direct inversion method

As explained above it is used at present only for small bundles (37 pins or less) for the purpose of saving storage memory. The calculation time per time step is considerably larger than with the iteration methods but it allows, even in case of blockages, a larger time step. The mass unbalance is several orders of magnitude smaller than with iterative methods. The matrix inversion allows therefore a steady-state to be approached in blockage calculations more rapidly than with the other methods. When calculating transients with fast mass flow run downs the numerical solution does not present oscillations typical of the iterative methods.

The following Table I gives the computer time required on the IBM-3033 for one numerical solution of the Poisson equation for the pressure field in case of 7, 19 and 37 pin bundles with 40 axial meshes. The CPU time given in the table includes the time necessary for filling the matrix of coefficients, for calculating the residuals and the time for printing the solution vector (pressure field), and the vector of residuals.

Bundle	Number of axial meshes	Number of radial meshes	Dimension of matrix of coefficients	CPU-time (s)
7-Pin	40	2	80 x 80	0·37
19-Pin	40	3	120 x 120	0·69
37-Pin	40	4	160 x 160	1·18

Table I. CPU time required on the computer IBM-3033 for one solution of the Poisson equation for the pressure field with the matrix inversion method (including calculation of residuals and printing of results).

3.6 Numerical solution of the momentum equations

Once the numerical solution of the Poisson-equation (35) has given the coolant pressure field at time level t_{n+1}, the discretized momentum equations (24), (29) yield directly the mass flows in the two coordinate directions at the same time level. The stability of the numerical solution of the coupled continuity and momentum equations is favoured by the half-implicit treatment of the terms representing friction pressure drops in equations (19), (25).

3.7 Numerical solution of the energy equation

The discretized energy equation is solved explicitly with respect to $(h)_{ij}^{n+1}$ using the mass flows at time level t_{n+1} and enthalpies at time level t_n. From (30) one derives:

$$(\rho h)_{ij}^{n+1} = (\rho h)_{ij}^{n} + \frac{\Delta t_n}{\varepsilon_{ij}} \left[-CVEZ - CVER + QZ + QR + Q \right]_{ij}^{n} \qquad (150)$$

where the convective and diffusive terms are given by

$$CVEZ^{m}_{i,j} = \frac{\varepsilon_{i,j}}{\Delta z_j}\left[(\rho h w)^{m}_{i,j+1/2} - (\rho h w)^{m}_{i,j-1/2}\right] \tag{151}$$

$$CVER^{m}_{i,j} = \frac{1}{\Delta r_i}\left[(\psi F \rho h u)^{m}_{i+1/2,j} - (\psi F \rho h u)^{n}_{i-1/2,j}\right] \tag{152}$$

$$QZ^{m}_{i,j} = \frac{\varepsilon_{i,j}}{\Delta z_j}\left[\left(\rho\tilde{\alpha}\frac{\partial h}{\partial z}\right)^{m}_{i,j+1/2} - \left(\rho\tilde{\alpha}\frac{\partial h}{\partial z}\right)^{m}_{i,j-1/2}\right] \tag{153}$$

$$QR^{m}_{i,j} = \frac{1}{\Delta r_i}\left[\left(\rho\psi F\tilde{\alpha}\frac{\partial h}{\partial r}\right)^{m}_{i+1/2,j} - \left(\rho\psi F\tilde{\alpha}\frac{\partial h}{\partial r}\right)^{n}_{i-1/2,j}\right]. \tag{154}$$

Further programme details regarding the finite differences schemes used for calculating convective and diffusive terms in the above equations are given in section 6.2.

4. Numerical treatment of time dependent heat diffusion equations for fuel pin and hexagonal can

The coolant temperature in every control volume is assumed as boundary condition for calculating the temperature distributions in fuel and cladding. For the outermost control volumes the temperature of the hexagonal can is also calculated, taking into account the heat flux beyond the outer surface.

Referring to a given axial mesh zone with index M (M = 1,...NM2) space and time discretisation of the equations of section B.2 is done as follows. With reference to the sketch shown in Fig. 7, the fuel radius R_B is divided into NN segments of length $\Delta r_B = R_B/NN$ defining the position of NN+1 radial nodes: $r_o = 0$, r_n (n=1,..NN) with $r_{NN} = R_B$. To every internal node is associated the mass of fuel material comprised in the annulus of radii $r_{n-1/2}$, $r_{n+1/2}$, represented in the figure by the shaded area around the node of coordinates $(Z_{M+1/2}, r_n)$. To the axial node is associated the mass within the cylinder of radius $r_{1/2}$; to the outermost node the mass in the annulus with radii $r_{n-1/2}$, R_B. The clad material is associated to three nodes of radial coordinates r_i, r_m, r_a (inner, middle, outer node) (with $r_m = (r_i + r_a)/2$). Let $\Delta r_H = (r_a - r_i)/2$. The mass of clad material associated to the middle node is therefore roughly twice the masses associated to the lateral nodes. The problem time is discretized in a sequence of time steps $\Delta t_n = t_n - t_{n-1}$. We use indexes h, h-1 for the symbols of physical magnitudes calculated at the time points t_n, t_{n-1}, respectively.

a) Fuel

i) Inner node

With reference to the annulus $(r_{n-1/2}, r_{n+1/2})$ of unit axial length as control volume, equation (B.2.1) may be written:

$$-\int_{S_n} \lambda \frac{\partial T_B(r,t)}{\partial r} \, dS + q_n V_n = \rho_n c_{p_n} V_n \frac{\partial T_B}{\partial t} \qquad (1)$$

where V_n denotes the volume of the annulus and the integral is calculated for both lateral surfaces ($S_n = S_{n-1/2} \cup S_{n+1/2}$).
Hence:

$$-\lambda_{r_{n-1/2}}\left(\frac{\partial T_B}{\partial r}\right)_{r_{n-1/2}} 2\pi r_{n-1/2} + \lambda_{r_{n+1/2}}\left(\frac{\partial T_B}{\partial r}\right)_{r_{n+1/2}} 2\pi r_{n+1/2} + q_n 2\pi r_n \Delta r = \rho_n c_{p_n} 2\pi r_n \Delta r \frac{\partial T_B}{\partial t} . \tag{2}$$

Terms of this equation are approximated by

$$\lambda_{r_{n-1/2}}\left(\frac{\partial T_B}{\partial r}\right)_{r_{n-1/2}} = \theta\left[\lambda_{r_{n-1/2}}\left(\frac{\partial T_B}{\partial r}\right)_{r_{n-1/2}}\right]^h + (1-\theta)\left[\lambda_{r_{n-1/2}}\left(\frac{\partial T_B}{\partial r}\right)_{r_{n-1/2}}\right]^{h-1}$$
$$= \theta\left[\lambda^h_{r_{n-1/2}}\frac{T^h_{B,n} - T^h_{B,n-1}}{\Delta r}\right] + (1-\theta)\left[\lambda^{h-1}_{r_{n-1/2}}\frac{T^{h-1}_{B,n} - T^{h-1}_{B,n-1}}{\Delta r}\right] \tag{3}$$

$$\lambda_{r_{n+1/2}}\left(\frac{\partial T_B}{\partial r}\right)_{r_{n+1/2}} = \theta\left[\lambda_{r_{n+1/2}}\left(\frac{\partial T_B}{\partial r}\right)_{r_{n+1/2}}\right]^h + (1-\theta)\left[\lambda_{r_{n+1/2}}\left(\frac{\partial T_B}{\partial r}\right)_{r_{n+1/2}}\right]^{h-1}$$
$$= \theta\left[\lambda^h_{r_{n+1/2}}\frac{T^h_{B,n+1} - T^h_{B,n}}{\Delta r}\right] + (1-\theta)\left[\lambda^{h-1}_{r_{n+1/2}}\frac{T^{h-1}_{B,n+1} - T^{h-1}_{B,n}}{\Delta r}\right] \tag{4}$$

$$q_n = \theta\, q^h_n + (1-\theta) q^{h-1}_n \tag{5}$$

$$\frac{\partial T_B}{\partial t} = \frac{T^h_{B,n} - T^{h-1}_{B,n}}{\Delta t_n} \tag{6a}$$

$$\rho_n\, c_{p_n} = \theta\, \rho^h_n\, c^h_{p_n} + (1-\theta)\, \rho^{h-1}_n\, c^{h-1}_{p_n} \tag{6b}$$

where θ is the time discretization parameter.

Introducing equations (3) to (6) in (2) one has:

$$A_n^h \, T_{B_n}^h + B_n^h \, T_{B_{n-1}}^h + C_n^h \, T_{B_{n+1}}^h = \tag{7}$$

$$= A_n^{h-1} \, T_{B_n}^{h-1} + B_n^{h-1} \, T_{B_{n-1}}^{h-1} + C_n^{h-1} \, T_{B_{n+1}}^{h-1} + Q_n$$

with

$$A_n^h = \theta \left(\lambda_{B,r_{n-1/2}}^h \frac{r_{n-1/2}}{r_n} + \lambda_{B,r_{n+1/2}}^h \frac{r_{n+1/2}}{r_n} \right) +$$

$$+ \frac{\Delta r_B^{\,2}}{\Delta t} \left(\theta \rho_{B,n}^h \, c_{p_{B,n}}^h + (1-\theta) \rho_{B,n}^{h-1} \, c_{p_{B,n}}^{h-1} \right) \tag{8a}$$

$$B_n^h = -\theta \, \lambda_{B,r_{n-1/2}}^h \frac{r_{n-1/2}}{r_n} \tag{8b}$$

$$C_n^h = -\theta \, \lambda_{B,r_{n+1/2}}^h \frac{r_{n+1/2}}{r_n} \tag{8c}$$

$$A_n^{h-1} = -(1-\theta) \left(\lambda_{B,r_{n-1/2}}^{h-1} \frac{r_{n-1/2}}{r_n} + \lambda_{B,r_{n+1/2}}^{h-1} \frac{r_{n+1/2}}{r_n} \right)$$

$$+ \frac{\Delta r_B^{\,2}}{\Delta t_n} \left(\theta \rho_{B,n}^h \, c_{p_{B,n}}^h + (1-\theta) \, \rho_{B,n}^{h-1} \, c_{p_{B,n}}^{h-1} \right) \tag{8d}$$

$$B_n^{h-1} = (1-\theta) \, \lambda_{B,r_{n-1/2}}^{h-1} \frac{r_{n-1/2}}{r_n} \tag{8e}$$

$$C_n^{h-1} = (1-\theta) \, \lambda_{B,r_{n+1/2}}^{h-1} \frac{r_{n+1/2}}{r_n} \tag{8f}$$

$$Q_n = \Delta r_B^{\,2} \, (\theta q_n^h + (1-\theta) q_n^{h-1}) \, . \tag{8g}$$

ii) Outermost node

Making a thermal balance for the annulus ($r_{NN-1/2}$, $r_{NN} = R_B$), taking into account the boundary condition for the heat transfer to the clad, equation (B.2.1) yields

$$-\int_{S_{NN-1/2}} \lambda_B \frac{\partial T_B}{\partial r}\, dS - \alpha_{BH}\, S_{NN}(T_{B,NN} - T_{Hi}) + q_{NN} V_{NN} = \rho_{NN} c_{p_{NN}} V_{NN} \frac{\partial T_B}{\partial t} \tag{9}$$

With space and time discretization as above, the following algebraic equation is obtained

$$A^h_{NN} T^h_{B,NN} + B^h_{NN} T^h_{B,NN-1} + C^h_{NN} T^h_{Hi} = A^{h-1}_{NN} T^{h-1}_{B,NN} + B^{h-1}_{NN} T^{h-1}_{B,NN-1} + C^{h-1}_{NN} T^{h-1}_{Hi} + Q_{NN} \tag{10}$$

with

$$A^h_{NN} = + \theta \lambda^h_{r_{NN-1/2}} \frac{r_{NN-1/2}}{r_{NN}} + \theta \alpha^h_{BH} \Delta r_B + \frac{\Delta r_B^2}{2\Delta t_n} \frac{r_{NN-1/4}}{r_{NN}} \left(\theta \rho^h_{NN} c^h_{p_{NN}} + (1-\theta) \rho^{h-1}_{NN} c^{h-1}_{p_{NN}} \right) \tag{11a}$$

$$B^h_{NN} = - \theta \lambda^h_{r_{NN-1/2}} \frac{r_{NN-1/2}}{r_{NN}} \tag{11b}$$

$$C^h_{NN} = - \theta \alpha^h_{BH} \Delta r_B \tag{11c}$$

$$A^{h-1}_{NN} = - (1-\theta) \lambda^h_{r_{NN-1/2}} \frac{r_{NN-1/2}}{r_{NN}} - (1-\theta) \alpha^{h-1}_{BH} \Delta r_B + \frac{\Delta r_B^2}{2\Delta t_n} \frac{r_{NN-1/4}}{r_{NN}} \left(\theta \rho^h_{NN} c^h_{p_{NN}} + (1-\theta) \rho^{h-1}_{NN} c^{h-1}_{p_{NN}} \right) \tag{11d}$$

$$B_{NN}^{h-1} = (1-\theta)\ \lambda_{r_{NN-1/2}}^{h-1}\ \frac{r_{NN-1/2}}{r_{NN}} \tag{11e}$$

$$C_{NN}^{h-1} = (1-\theta)\ \alpha_{BH}^{h-1}\ \Delta r_B \tag{11f}$$

$$Q_{NN} = \frac{\Delta r_B^{\,2}}{2}\ \frac{r_{NN-1/4}}{r_{NN}}\ \left(\theta q_{NN}^{h} + (1-\theta)\ q_{NN}^{h-1}\right) \tag{11g}$$

iii) Central node

Similarly, for the fuel central node one derives the algebraic equation

$$A_o^h\ T_{Bo}^h + {}_o^h\ T_{B1}^h = A_o^{h-1}\ T_{Bo}^{h-1} + {}_o^{h-1}\ T_{B1}^{h-1} + Q_o \tag{12}$$

with

$$A_o^h = 4\theta\ \lambda_{r_{1/2}}^h + \frac{1}{\Delta t_n}\left(\theta\rho_o^h\ c_{p_o}^h + (1-\theta)\ \rho_o^{h-1}\ c_{p_o}^{h-1}\right)\ \Delta r_B^2 \tag{13a}$$

$$C_o^h = -4\theta\ \lambda_{r_{1/2}}^h \tag{13b}$$

$$A_o^{h-1} = -4(1-\theta)\ \lambda_{r_{1/2}}^{h-1} + \frac{1}{\Delta t_n}\left(\theta\rho_o^h\ c_{p_o} + (1-\theta)\ \rho_o^{h-1}\ c_{p_o}^{h-1}\right)\ \Delta r_B^2 \tag{13c}$$

$$C_o^{h-1} = 4(1-\theta)\ \lambda_{r_{1/2}}^{h-1} \tag{13d}$$

$$Q_o = (\theta\ q_o^h + (1-\theta)\ q_o^{h-1})\Delta r_B^{\,2}\ . \tag{13e}$$

b) Cladding

i) Inner node

Equation (B.2.6) yields, with the same space and time discretization as above, the algebraic equation

$$A^h_{Hi}\ T^h_{Hi} + B^h_{Hi}\ T^h_{B,NN} + C^h_{Hi}\ T^h_{Hm} = \tag{14}$$

$$= A^{h-1}_{Hi}\ T^{h-1}_{Hi} + B^{h-1}_{Hi}\ T^{h-1}_{B,NN} + C^{h-1}_{Hi}\ T^{h-1}_{Hm} + Q_{Hi}$$

with

$$A^h_{Hi} = \theta\alpha^h_{BH}\ \Delta r_H + \theta\ \lambda^h_{H_{ri+1/2}}\ \frac{r_{i+1/2}}{r_i} \tag{15a}$$

$$+ \frac{1}{\Delta t_n}\ \frac{r_{i+1/4}}{r_i}\ \frac{\Delta r_H^2}{2}\ \left(\theta\rho^h_{Hi}\ c^h_{p_{Hi}} + (1-\theta)\ \rho^{h-1}_{Hi}\ c^{h-1}_{p_{Hi}}\right)$$

$$B^h_{Hi} = -\theta\ \alpha^h_{BH}\ \Delta r_H \tag{15b}$$

$$C^h_{Hi} = -\theta\ \lambda^h_{H_{r_{i+1/2}}}\ \frac{r_{i+1/2}}{r_i} \tag{15c}$$

$$A^{h-1}_{Hi} = -(1-\theta)\ \alpha^{h-1}_{BH}\ \Delta r_H - (1-\theta)\ \lambda^{h-1}_{H_{ri+1/2}}\ \frac{r_{i+1/2}}{r_i}$$

$$+ \frac{1}{\Delta t_n}\ \frac{r_{i+1/4}}{r_i}\ \frac{\Delta r_H^2}{2}\ \left(\theta\rho^h_{Hi}\ c^h_{p_{Hi}} + (1-\theta)\ \rho^{h-1}_{Hi}\ c^{h-1}_{p_{Hi}}\right) \tag{15d}$$

$$B^{h-1}_{Hi} = (1-\theta)\alpha^{h-1}_{BH}\ \Delta r_H \tag{15e}$$

$$C^{h-1}_{Hi} = (1-\theta)\ \lambda^{h-1}_{H_{r_{i+1/2}}}\ \frac{r_{i+1/2}}{r_i} \tag{15f}$$

$$Q_{Hi} = \frac{r_{i+1/4}}{r_i}\ \frac{\Delta r_H^2}{2}\ \left(\theta\ q^h_{Hi} + (1-\theta)\ q^{h-1}_{Hi}\right) \tag{15g}$$

ii) Middle node

For the middle clad node one derives

$$A^h_{Hm}\ T^h_{Hm} + B^h_{Hm}\ T^h_{Hi} + C^h_{Hm}\ T^h_{Ha} = \tag{16}$$

$$= A^{h-1}_{Hm}\ T^{h-1}_{Hm} + B^{h-1}_{Hm}\ T^{h-1}_{Hi} + C^{h-1}_{Hm}\ T^{h-1}_{Ha} + Q_{Hm}$$

with

$$A^h_{Hm} = \theta \left(\lambda^h_{Hr_{m-1/2}} \frac{r_{m-1/2}}{r_m} + \lambda^h_{Hr_{m+1/2}} \frac{r_{m+1/2}}{r_m} \right) + \frac{1}{\Delta t_n} \left(\theta \rho^h_{H_m}\ c^h_{p_m} + (1-\theta)\ \rho^{h-1}_{Hm}\ c^{h-1}_{p_{Hm}} \right) \Delta r_H^{\,2} \tag{17a}$$

$$B^h_{Hm} = -\theta\ \lambda^h_{Hr_{m-1/2}} \frac{r_{m-1/2}}{r_m} \tag{17b}$$

$$C^h_{Hm} = -\theta\ \lambda^h_{Hr_{m+1/2}} \frac{r_{m+1/2}}{r_m} \tag{17c}$$

$$A^{h-1}_{Hm} = -(1-\theta) \left(\lambda^{h-1}_{Hr_{m-1/2}} \frac{r_{m-1/2}}{r_m} + \lambda^{h-1}_{Hr_{m+1/2}} \frac{r_{m+1/2}}{r_m} \right) + \frac{1}{\Delta t_n} \left(\theta\ \rho^h_{Hm}\ c^h_{p_{Hm}} + (1-\theta)\ \rho^{h-1}_{Hm}\ c^{h-1}_{p_{Hm}} \right) \Delta r_H^{\,2} \tag{17d}$$

$$B^{h-1}_{Hm} = (1-\theta)\ \lambda^{h-1}_{Hr_{m-1/2}} \frac{r_{m-1/2}}{r_m} \tag{17e}$$

$$C^{h-1}_{Hm} = (1-\theta)\ \lambda^{h-1}_{Hr_{m+1/2}} \frac{r_{m+1/2}}{r_m} \tag{17f}$$

$$Q_{Hm} = (\theta\ q^h_{Hm} + (1-\theta) q^{h-1}_{Hm})\ \Delta r_H^{\,2} \tag{17g}$$

iii) Outer node

For the outer clad node one derives

$$A^h_{Ha}\ T^h_{Ha} + B^h_{Ha}\ T^h_{Hm} + C^h_{Ha}\ T^h_K = \tag{18}$$

$$= A^{h-1}_{Ha}\ T^{h-1}_{Ha} + B^{h-1}_{Ha}\ T^{h-1}_{Hm} + C^{h-1}_{Ha}\ T^{h-1}_K + Q_{Ha}$$

with

$$A^h_{Ha} = \theta\ \lambda^h_{Hr_{a-1/2}}\ \frac{r_{a-1/2}}{r_a} + \theta\alpha^h_{HK}\ \Delta r_H + \tag{19a}$$

$$+ \frac{1}{\Delta t_h}\ \frac{\Delta r_H^2}{2}\ \frac{r_{a-1/4}}{r_a}\ \left(\theta\rho^h_{Ha}\ c^h_{p_{Ha}} + (1-\theta)\ \rho^{h-1}_{Ha}\ c^{h-1}_{p_{Ha}}\right)$$

$$B^h_{Ha} = -\theta\ \lambda^h_{Hr_{a-1/2}}\ \frac{r_{a-1/2}}{r_a} \tag{19b}$$

$$C_{Ha} = -\theta\ \alpha^h_{HK}\ \Delta r_H \tag{19c}$$

$$A^{h-1}_{Ha} = -(1-\theta)\ \alpha^{h-1}_{HK}\ \Delta r_H - (1-\theta)\ \lambda^{h-1}_{Hr_{a-1/2}}\ \frac{r_{a-1/2}}{r_a} \tag{19d}$$

$$+ \frac{1}{\Delta t_h}\ \frac{\Delta r_H^2}{2}\ \frac{r_{a-1/4}}{r_a}\ \left(\theta\rho^h_{Ha}\ c^h_{p_{Ha}} + (1-\theta)\ \rho^{h-1}_{Ha}\ c^{h-1}_{p_{Ha}}\right)$$

$$B^{h-1}_{Ha} = (1-\theta)\ \lambda^{h-1}_{Hr_{a-1/2}}\ \frac{r_{a-1/2}}{r_a} \tag{19e}$$

$$C^{h-1}_{Ha} = (1-\theta)\ \alpha^{h-1}_{HK}\ \Delta r_H \tag{19f}$$

$$Q_{Ha} = \frac{\Delta r_H}{2}\ \frac{r_{a-1/4}}{r_a}\ \left(\theta\ q^h_{Ha} + (1-\theta)\ q^{h-1}_{Ha}\right) \tag{19g}$$

c) Hexagonal can

Similarly, discretization of equation (B.2.10) for the hexagonal can yields

$$\frac{F_S}{V_S}\left[\theta\alpha_{KS}^{h}(T_K^h - T_S^h) + (1-\theta)\alpha_{KS}^{h-1}\ (T_K^{h-1} - T_S^{h-1})\right] +$$

$$- \frac{F_w}{V_S}\left[\theta\ \alpha_w^h\ (T_S^h - T_w^h) + (1-\theta)\ \alpha_w^{h-1}\ (T_S^{h-1} - T_w^{h-1})\right] +$$

$$+ \theta\ q_S^h + (1-\theta)\ q_S^{h-1} = (\theta\rho_S^h\ C_{p_S}^h + (1-\theta)\rho_S^{h-1}\ C_{p_S}^{h-1})\ \frac{T_S^h - T_S^{h-1}}{\Delta t_h}$$

which can be written:

$$A_S^h\ T_S^h + B_S^h\ T_K^h + C_S^h\ T_w^h = \tag{21}$$

$$= A_S^{h-1}\ T_S^{h-1} + B_S^{h-1}\ T_K^{h-1} + C_S^{h-1}\ T_w^{h-1} + Q_S$$

with:

$$A_S^h = \theta\left(\alpha_{KS}^h + \frac{F_w}{F_S}\ \alpha_w^h\right) + \frac{1}{\Delta t_h}\ \frac{V_S}{F_S}\left(\theta\rho_S^h\ c_{p_S}^h + (1-\theta)\ \rho_S^{h-1}\ c_{p_S}^{h-1}\right) \tag{22a}$$

$$B_S^h = -\theta\ \alpha_{KS}^h \tag{22b}$$

$$C_S^h = -\theta\ \frac{F_w}{F_S}\ \alpha_w^h \tag{22c}$$

$$A_S^{h-1} = -(1-\theta)\left(\alpha_{KS}^{h-1} + \frac{F_w}{F_S}\ \alpha_w^{h-1}\right) + \frac{1}{\Delta t_h}\ \frac{V_S}{F_S}\ (\theta\rho_S^h\ c_{p_S}^h + (1-\theta)\ \rho_s^{h-1}\ c_{p_S}^{h-1})$$

(22d)

$$B_S^{h-1} = (1-\theta)\alpha_{KS}^{h-1} \tag{22e}$$

$$C_S^{h-1} = (1-\theta)\frac{F_w}{F_S}\ \alpha_w^{h-1} \tag{22f}$$

$$Q_S = \frac{V_S}{F_S}\ (\theta\ q_S^h + (1-\theta)\ q_S^{h-1}) \tag{22g}$$

In the above equations, the coefficient A always refers to the node under consideration, the coefficient B refers to the adjacent node at the fuel axis side, C refers to the adjacent node in the outward direction.

d) Numerical solution

The above difference equations may be written in matricial form as

$$M \cdot T = B \tag{23}$$

where M is a tridiagonal matrix containing the left-hand side coefficients. Taking NN+1 nodes in the fuel and 3 in the clad M becomes a square matrix with NN+4 rows and columns. T is a column vector containing the unknown temperatures at time t_n. B is a column vector formed by the right hand side of the above discretized equations. It is not completely known because, besides all temperatures and physical quantities at time t_{n-1} (with index h-1) it also contains the unknown terms $\rho^h c_p^h$. These are calculated with reference to a temperature obtained extrapolating the gradient from the previous time step

$$T^{n+1} = T^n + \left(\frac{\partial T}{\partial t}\right)^n \cdot \Delta t_n \ . \tag{24}$$

Equation (23) is solved by means of a direct numerical method using the Thomas algorithm /7/.

e) Programming details

FORTRAN symbols are given hereafter with reference to

i) equation (7) for fuel inner nodes

ii) equation (16) for the clad middle node

iii) equation (21) for the hexagonal can.

i) Fuel inner node

DRBR = RBR/NN

DRBR2 = DRBR**2

QRMIN(N) = $r_{n-1/2}/r_n$

QRPL(N) = $r_{n+1/2}/r_n$

RØB = fuel density at node n

CPB = fuel specific heat at node n

XLBN1(N) = fuel thermal conductivity at node n

ii) Clad middle node

DCAN = $r_a - r_i$

DRCC = $r_m - r_i$ = DCAN/2

DRCC2 = DRCC**2

QRPLV = $\dfrac{r_i + (r_m - r_i)/4}{r_i}$

QRPLH = $\dfrac{r_i + (r_m - r_i)/2}{r_i}$

QRCMI = $r_{m-1/2}/r_m$

QRCPL = $r_{m+1/2}/r_m$

RØH = middle node clad density

CPH = middle node clad specific heat

XLCIN1 = inner node clad thermal conductivity

XLCAN1 = outer node clad thermal conductivity

iii) Hexagonal can

FWFS = F_W/F_S

VDUF = F_S/F_S

RØS = density of structure material

CPS = specific heat of structure

WWST = α_W = heat transfer coefficient from the structure outer surface to the surrounding medium.

HKEX = α_{KS} = heat transfer coefficient coolant-structure.

5. Constitutive equations

The basic equations describing the thermal-hydraulic behaviour of the coolant must be complemented by additional equations for calculating friction pressure drops, heat transfer coefficients and turbulent momentum exchanges of mass and enthalpy.

5.1 Friction pressure drops and pressure drops due to grid spacers

The frictional pressure drops are calculated by means of the relationship by Novendstern /21/ which also takes into account the contribution due to the wire wraps. The friction coefficient is given by

$$f = f_o \cdot f_m \qquad (1)$$

with

$$f_o = a \cdot R_e^{-b} \qquad (2a)$$

$$f_m = CFM = (CFM1 + CFM2 \cdot R_e^{CFME1})^{CFME2} \qquad (2b)$$

$$CFM1 = 1.034 \,/\, ((P/D)^{**}0.124) \qquad (2c)$$

$$CFM2 = (29.7 \cdot (P/D)^{**}6.94)/((\lambda/D)^{**}2.239). \qquad (2d)$$

R_e is the Reynolds number of the undisturbed flow, P is the pitch, D the diameter of the pins, λ the pitch length of the wire wraps. For turbulent flow the following values of the coefficients are suggested:

$$a = 0.316$$
$$b = 0.25$$
$$CFME1 = 0.086$$
$$CFME2 = 0.855$$

In case wire wraps have not to be simulated the input parameter λ (=HELIC) is set to a large value, thus giving CFM2 $\approx$ 0.

If grid spacers must be simulated, the pressure drops in the grids are calculated as the sum of two contributions: an irreversible pressure drop at the grid entry and frictional pressure drop along the grid. The pressure recovery at the downstream edge of the grid is considered as negligible. Within the grids mass flows in transverse directions are suppressed, therefore only pressure drops in axial directions are taken into account. These are given by

$$\Delta p_g = (\Delta p)_{entry} + (\Delta p)_{friction} =$$

$$= \frac{\rho}{2} w_o^2 \left(1 - \frac{1}{A}\right)^2 + \frac{f_r \rho L_g w_o^2}{2 D_{h_g} A^2} = \tag{3}$$

$$= \frac{\rho}{2} \bar{K}_e w_o^2 + \frac{f_r \rho L_g w_o^2}{2 D_{h_g} A^2}$$

where:

$A = \frac{S_g}{S_o} = \frac{w_o}{w_g}$ ratio of reduced to undisturbed flow area

D_{h_g} = hydraulic diameter of the grid [m]

f_r = friction coefficient for the grid

$K_e = \left(1 - S_o/S_g\right)^2 = \left(1 - \frac{1}{A}\right)^2$ resistance coefficient at grid inlet

L_g = grid axial length (m) ($L_g \leq \Delta z$)

S_o = flow area upstream of the grid (m^2)

S_g = flow area through the grid (m^2)

w_o = flow velocity upstream of the grid (undisturbed bundle) (m/s)

w_g = flow velocity through the grid (m/s)

ρ = coolant density (kg/m^3).

An equivalent resistance coefficient for the grid is defined by

$$\bar{K}_g = K_e + \frac{f_r L_g}{D_{h_g} A^2} = \left(1 - \frac{1}{A}\right)^2 + \frac{f_r L_g}{D_{h_g} A^2} = \left[\Delta p_g \Big/ \left(\frac{\rho w_o^2}{2} \right) \right] \tag{4}$$

and an equivalent friction coefficient by

$$f_g = \bar{K}_g \cdot D_h / \Delta z \,. \tag{5}$$

D_h is the hydraulic diameter of the channel flow without grid and Δz is the mesh length. The programme user can choose between modelling the grid spacers in their actual position, as explained above, or simulating the pressure drop by smearing the local contribution uniformly over all axial meshes. In the latter case, the friction coefficient due to the grid is

$$f_g = K_g \cdot D_h \,/\, \text{DABST} \tag{6}$$

where DABST is the distance between two consecutive grids.
The roughness of the upstream edge of the grid is taken into account by replacing the flow areas ratio in $K_e = (1 - 1/A)^2$ by

$$A' = (c(A^2 - 1) + 1)\, A \tag{7}$$

where c is an input coefficient ranging from 0 to 0.4.

Taking into account the contribution to the pressure drop due to the grid spacers the total friction coefficient is calculated as

$$f_t = f + f_g \tag{8}$$

which is introduced into equation C.2.5 to give

$$FC\emptyset Z = \frac{(f+f_g)\,|W_o|}{2D_h}\,. \tag{9}$$

5.2 Laminar and turbulent shear stresses

The momentum exchange between adjacent control volumes is calculated by adding a turbulent contribution to the molecular shear stresses. This is justified by a time-smoothing procedure which is applied to the momentum conservation equations as explained in the following section.

5.2.1 Time-smoothed momentum equations

The volume-averaging technique applied to the conservation equations, as explained in section B 1.2, yields a balance of bulk values for physical quantities defined at a given time. In reality the flow is characterized by turbulent fluctuations of all dependent variables (pressure, velocity components, enthalpy) around mean values. These fluctuations are taken into account by the introduction of an effective viscosity which is derived as follows.

Let us consider for instance the axial component of the momentum equation for the coolant, written in the local form

$$\frac{\partial(\rho w)}{\partial t} + \nabla\cdot(\rho w V) = \nabla\cdot(\mu^{\ell}\nabla w) - \frac{\partial p}{\partial z} \tag{10}$$

where we neglect for simplicity the gravity and the frictional resistance terms. μ^{ℓ} is the molecular dynamic viscosity. In eq. (10) the pressure and velocity components are instantaneous values, including turbulent fluctuations.

We write the dependent variables of eq. (10) as the sum of a mean value and of an instantaneous fluctuation

$$u = \bar{u} + u' \tag{11a}$$

$$w = \bar{w} + w' \tag{11b}$$

$$v = \bar{v} + v' \tag{11c}$$

$$p = \bar{p} + p' \tag{11d}$$

where the mean values are defined by

$$\bar{u} = \frac{1}{\Delta t} \int_{t}^{t+\Delta t} u \, dt \tag{12}$$

and similar expressions for the other variables. The time interval Δt should be large enough with respect to the period of the turbulent oscillations to insure that the time-average of the fluctuations of the dependent variables vanishes ($\bar{u}' = o$ and similar).

Introducing eqs. (11) into eq. (10) yields

$$\frac{\partial}{\partial t}\left[\rho(\bar{w}+w')\right] + \frac{\partial}{\partial x}\left[\rho(\bar{w}+w')(\bar{u}+u')\right] + \frac{\partial}{\partial z}\left[\rho(\bar{w}+w')(\bar{w}+w')\right] + \tag{13}$$

$$+ \frac{\partial}{\partial y}\left[\rho(\bar{w}+w')(\bar{v}+v')\right] = \nabla\cdot\left[\mu^{\ell}\nabla(\bar{w}+w')\right] - \frac{\partial}{\partial z}(\bar{p}+p') \, .$$

Whilst the time-average of the turbulent fluctuations are equal to zero, the cross correlation terms $\overline{w'w'}$, $\overline{w'u'}$, $\overline{w'v'}$ give a non-vanishing contribution in the time-smoothing of eq. (13), which therefore yields

$$\frac{\partial}{\partial t}\rho\bar{w} + \frac{\partial}{\partial r}\left(\rho\bar{w}\bar{u}\right) + \frac{\partial}{\partial z}\left(\rho\bar{w}\bar{w}\right) + \frac{\partial}{\partial \varphi}\left(\rho\bar{w}\bar{v}\right) + \tag{14}$$

$$+\frac{\partial}{\partial r}\left(\rho\overline{w'u'}\right) + \frac{\partial}{\partial z}\left(\rho\overline{w'w'}\right) + \frac{\partial}{\partial \varphi}\left(\rho\overline{w'v'}\right) = \nabla\cdot\mu^{\ell}\nabla\bar{w} - \frac{\partial\bar{p}}{\partial z}\,.$$

The last three terms at the left side are the contributions of the turbulent fluctuations and usually referred to as "Reynolds stresses". They are considered as components of a second-order tensor

$$\tau^{t}_{zr} = \rho\overline{w'u'} \tag{15a}$$

$$\tau^{t}_{zz} = \rho\overline{w'w'} \tag{15b}$$

$$\tau^{t}_{z\varphi} = \rho\overline{w'v'} \tag{15c}$$

where the superscript t means turbulent.

A similar treatment is made for the radial and azimuthal scalar momentum equations which yield the following time-smoothed equations:

$$\frac{\partial}{\partial t}\left(\rho\bar{u}\right) + \frac{\partial}{\partial r}\left(\rho\bar{u}\bar{u}\right) + \frac{\partial}{\partial z}\left(\rho\bar{u}\bar{w}\right) + \frac{\partial}{\partial \varphi}\left(\rho\bar{u}\bar{v}\right) + \tag{16}$$

$$+\frac{\partial}{\partial r}\left(\rho\overline{u'u'}\right) + \frac{\partial}{\partial z}\left(\rho\overline{u'w'}\right) + \frac{\partial}{\partial \varphi}\left(\rho\overline{u'v'}\right) = \nabla\cdot\mu^{\ell}\nabla\bar{u} + \frac{\partial\bar{p}}{\partial r}$$

$$\frac{\partial}{\partial t}\left(\rho\bar{v}\right) + \frac{\partial}{\partial r}\left(\rho\bar{v}\bar{u}\right) + \frac{\partial}{\partial z}\left(\rho\bar{v}\bar{w}\right) + \frac{\partial}{\partial \varphi}\left(\rho\bar{v}\bar{v}\right) + \tag{17}$$

$$+\frac{\partial}{\partial r}\left(\rho\overline{v'u'}\right) + \frac{\partial}{\partial z}\left(\rho\overline{v'w'}\right) + \frac{\partial}{\partial \varphi}\left(\rho\overline{v'v'}\right) = \nabla\cdot\mu^{\ell}\nabla\bar{v} + \frac{\partial\bar{p}}{\partial \varphi}\,.$$

Eqs. (14), (16), (17) are the so-called Reynolds equations. They can be written in vector notation as

$$\frac{\partial}{\partial t}\left(\rho \bar{V}\right) + \nabla \cdot \rho \bar{V}\bar{V} = -\nabla \cdot \tau^{l} - \nabla \cdot \tau^{t} - \nabla \bar{p} \tag{18}$$

where τ^{l} is the laminar shear stress tensor which depends on the time-smoothed components of the velocity vector V (the bar denotes here time-average) and

$$\tau^{t} = \rho \begin{vmatrix} \overline{u'u'} & \overline{u'w'} & \overline{u'v'} \\ \overline{w'u'} & \overline{w'w'} & \overline{w'v'} \\ \overline{v'u'} & \overline{v'w'} & \overline{v'v'} \end{vmatrix} \tag{19}$$

is the turbulent stress tensor. The laminar and turbulent shear stresses are calculated as follows.

5.2.2 Laminar shear stress tensor

The components of the laminar stress tensor are given by

$$\tau^{l}_{ik} = -\mu^{l}\left[\frac{\partial \bar{V}_i}{\partial \ell_k} + \frac{\partial \bar{V}_k}{\partial \ell_i}\right] + \delta_{ik}\left(\frac{2}{3}\mu^{l} - \kappa\right)\left(\nabla \cdot \bar{V}\right) \quad (i,k=1,2,3) \tag{20}$$

where $\bar{V}_i$ are the components of the time-smoothed velocity vector $\bar{V}$ in the ℓ_i coordinate directions, δ_{ik} is the Kronecker delta, k is the bulk viscosity. In the following we assume k=o.
This equation shows the symmetry of the laminar shear stress tensor.

The vector term $-\left[\nabla \cdot \tau^{l}\right]$ in eq. (18) is given by

$$-\left[\nabla \cdot \tau^{l}\right] = \sum_k \bar{m}_k \left(\sum_i \frac{\partial}{\partial \ell_i} \tau_{ik}\right) \qquad (i,k=r,z,s) \tag{21}$$

The component in the axial direction is for instance

$$
\begin{aligned}
-\left[\nabla\cdot\tau^{l}\right]_{z} &= -\bar{n}_{z}\left(\frac{\partial}{\partial r}\tau_{rz}+\frac{\partial}{\partial z}\tau_{zz}+\frac{\partial}{\partial s}\tau_{sz}\right)= \\
&= \bar{n}_{z}\left\{\frac{\partial}{\partial r}\left[\mu^{l}\left(\frac{\partial u}{\partial z}+\frac{\partial w}{\partial r}\right)\right]+\frac{\partial}{\partial z}\left[\mu^{l}\left(2\frac{\partial w}{\partial z}-\frac{2}{3}\nabla\cdot\bar{V}\right)\right]+\frac{\partial}{\partial s}\left[\mu^{l}\left(\frac{\partial v}{\partial z}+\frac{\partial w}{\partial s}\right)\right]\right\}= \\
&= \bar{n}_{z}\left\{\frac{\partial}{\partial r}\left(\mu^{l}\frac{\partial w}{\partial r}\right)+\frac{\partial}{\partial z}\left(\mu^{l}\frac{\partial w}{\partial z}\right)+\frac{\partial}{\partial s}\left(\mu^{l}\frac{\partial w}{\partial s}\right)+\frac{1}{3}\frac{\partial}{\partial z}\left(\mu^{l}\nabla\cdot\bar{V}\right)\right\}.
\end{aligned}
\tag{22}
$$

For the derivation of eq. (22) we made the assumption that the dynamic viscosity is constant. Furthermore, we use eq. (22), and the equivalent ones for the other two coordinate directions, for an incompressible flow so that the divergence of the velocity vector is zero, hence

$$
-\nabla\cdot\tau^{l} = \nabla\cdot\left(\mu^{l}\nabla\bar{V}\right) \tag{23}
$$

which has the form of the viscosity term in equation B 1.1 (2).

5.2.3 Turbulent momentum transfer

The definition of the turbulent stress tensor (19) shows its symmetry. Its components are calculated by means of half-empirical expressions which take into account: i) an analogy with the analytical form (20) of the laminar components; ii) geometry coefficients represented by the volume porosity and surface permeabilities; iii) a typical length which is intended as a generalization of the "Prandtl's mixing length" representing the penetration depth of the momentum transfer; iv) the constraint imposed by the symmetry. Thus the following expressions are used for the components of the turbulent stress tensor:

$$\tau^t_{xz} = \rho\overline{u'w'} = -\rho c_o\left[\left(\varepsilon\Delta z\,\bar{u}\right)^2 + \left(\psi\Delta x\,\bar{w}\right)^2\right]^{1/2}\left(\frac{\partial\bar{w}}{\partial x} + \frac{\partial\bar{u}}{\partial z}\right) \tag{24a}$$

$$\tau^t_{xx} = \rho\overline{u'u'} = -\rho c_o\,\psi\Delta x\,|\bar{u}|\,2\frac{\partial\bar{u}}{\partial x} \tag{24b}$$

$$\tau^t_{xy} = \rho\overline{u'v'} = -\rho c_o\left[\left(\xi\Delta y\,\bar{u}\right)^2 + \left(\psi\Delta x\,\bar{v}\right)^2\right]^{1/2}\left(\frac{\partial\bar{v}}{\partial x} + \frac{\partial\bar{u}}{\partial y}\right) \tag{24c}$$

$$\tau^t_{zx} = \rho\overline{w'u'} = -\rho c_o\left[\left(\psi\Delta x\,\bar{w}\right)^2 + \left(\varepsilon\Delta z\,\bar{u}\right)^2\right]^{1/2}\left(\frac{\partial\bar{u}}{\partial x} + \frac{\partial\bar{w}}{\partial z}\right) \tag{24d}$$

$$\tau^t_{zz} = \rho\overline{w'w'} = -\rho c_o\,\varepsilon\Delta z\,|\bar{w}|\,2\frac{\partial\bar{w}}{\partial z} \tag{24e}$$

$$\tau^t_{zy} = \rho\overline{w'v'} = -\rho c_o\left[\left(\xi\Delta y\,\bar{w}\right)^2 + \left(\varepsilon\Delta z\,\bar{v}\right)^2\right]^{1/2}\left(\frac{\partial\bar{v}}{\partial z} + \frac{\partial\bar{w}}{\partial y}\right) \tag{24f}$$

$$\tau^t_{yx} = \rho\overline{v'u'} = -\rho c_o\left[\left(\psi\Delta x\,\bar{v}\right)^2 + \left(\xi\Delta y\,\bar{u}\right)^2\right]^{1/2}\left(\frac{\partial\bar{u}}{\partial y} + \frac{\partial\bar{v}}{\partial x}\right) \tag{24g}$$

$$\tau^t_{yz} = \rho\overline{v'w'} = -\rho c_o\left[\left(\varepsilon\Delta z\,\bar{v}\right)^2 + \left(\xi\Delta y\,\bar{w}\right)^2\right]^{1/2}\left(\frac{\partial\bar{w}}{\partial y} + \frac{\partial\bar{v}}{\partial z}\right) \tag{24h}$$

$$\tau^t_{yy} = \rho\overline{v'v'} = -\rho c_o\,\xi\Delta y\,|\bar{v}|\,2\frac{\partial\bar{v}}{\partial y} \tag{24i}$$

where c_o is a dimensionless coefficient to be determined by comparison of computed with experimental results.

The expressions (24) can be written

$$\tau^t_{ik} = \rho \overline{V'_i V'_k} = -\rho c_0 \left[\left(L_i \bar{V}_k \right)^2 + \left(L_k \bar{V}_i \right)^2 \right]^{1/2} \left(\frac{\partial \bar{V}_i}{\partial \ell_k} + \frac{\partial \bar{V}_k}{\partial \ell_i} \right) \quad (i \neq k) \tag{25}$$

$$= -\rho c_0 L_i |\bar{V}_k| \, 2 \frac{\partial \bar{V}_i}{\partial \ell_i} \quad (i=k)$$

where the mixing lengths L_i are given by

$$L_r = \psi \, \Delta r \tag{26a}$$

$$L_z = \varepsilon \, \Delta z \tag{26b}$$

$$L_s = \xi \, \Delta s, \tag{26c}$$

or in the compact form

$$\tau^t_{ik} = -\mu^t_{ik} \left(\frac{\partial \bar{V}_i}{\partial \ell_k} + \frac{\partial \bar{V}_k}{\partial \ell_i} \right) \qquad (i,k=r,z,s) \tag{27}$$

with the definition of the turbulent dynamic viscosity

$$\mu^t_{ik} = \rho c_0 \left[\left(L_i \bar{V}_k \right)^2 + \left(L_k \bar{V}_i \right)^2 \right]^{1/2} \quad (i \neq k) \tag{28}$$

$$= \rho c_0 L_i |\bar{V}_k| \quad (i=k)$$

which takes into account the anysotropy of the porous medium.
We therefore write formally the turbulent momentum transfer for the j-th component of the momentum equation as

$$\frac{\partial}{\partial r} \left(\mu^t_{rj} \frac{\partial \bar{V}_j}{\partial r} \right) + \frac{\partial}{\partial z} \left(\mu^t_{zj} \frac{\partial \bar{V}_j}{\partial z} \right) + \frac{\partial}{\partial s} \left(\mu^t_{sj} \frac{\partial \bar{V}_j}{\partial s} \right) \qquad (j=r,z,s) \tag{29}$$

and the divergence of the turbulent stress tensor, similarly to eq. (23), as

$$-\nabla \cdot \tau^t = \nabla \circ \left(\mu^t \nabla \bar{V} \right) . \tag{30}$$

5.2.4 Effective shear stress tensor

From a formal viewpoint an effective shear stress term can be defined by

$$\tau = \tau^{\ell} + \tau^{t} \tag{31}$$

as the sum of the molecular and the turbulent contributions.

The time-smoothed momentum equation (18) can thus be written

$$\frac{\partial}{\partial t}\left(\rho \bar{v}\right) + \nabla \cdot \rho \bar{v}\bar{v} = -\nabla \cdot \tau - \nabla \bar{p} \; . \tag{32}$$

The divergence of the stress tensor is given, according to eqs. (23) and (30) by

$$\begin{aligned} -\nabla \cdot \tau = -\nabla \cdot \left(\tau^{\ell} + \tau^{t}\right) &= \nabla \cdot \left(\mu^{\ell} + \mu^{t}\right) \nabla \bar{v} \\ &= \nabla \cdot \left(\mu \nabla \bar{v}\right) \end{aligned} \tag{33}$$

with the definition of the effective dynamic viscosity

$$\mu = \mu^{\ell} + \mu^{t} \; . \tag{34}$$

Eq. (32), with the divergence of the stress tensor given by (33), is the governing momentum equation of section B 1.1 (eq. (2)), upon which the volume-averaging procedure is then applied, as explained in section B 1.2.

The calculation of water experiments in unheated 19-pin bundle /22/ and comparison with the experimental results have allowed an estimation of the optimum value of the coefficient c_o in (24) ($c_o = 0.12$). Previous results of the theoretical interpretation of these experiments are given in reference /23/.

5.3 Turbulent exchange of enthalpy

The enthalpy exchange between adjacent control volumes is calculated, like the momentum transfer, by taking into account a molecular and a turbulent contribution. The theoretical justification for the latter arises from time-smoothing of the energy equation for the coolant, which takes into account the mixing effects due to the turbulent fluctuations of the depending variables.

Omitting the unessential source term, we recall the energy eq. B 1 (3), which refers to the instantaneous values of the variables

$$\frac{\partial}{\partial t}(\rho h) + \nabla \cdot \rho h V = \nabla \cdot \rho a^{\ell} \nabla h \tag{35}$$

where a^{ℓ} is the molecular thermal diffusivity.

Using eqs. (11a) to (11c), also writing the instantaneous coolant enthalpy as sum of a mean value and of a turbulent fluctuation

$$h = \bar{h} + h' \tag{36}$$

and applying to eq. (35) the time-smoothing procedure, as in the previous section, one derives

$$\begin{aligned} &\frac{\partial}{\partial t}(\rho \bar{h}) + \frac{\partial}{\partial r}(\rho \bar{h} \bar{u}) + \frac{\partial}{\partial z}(\rho \bar{h} \bar{w}) + \frac{\partial}{\partial s}(\rho \bar{h} \bar{v}) + \\ &+ \frac{\partial}{\partial r}(\rho \overline{h'u'}) + \frac{\partial}{\partial t}(\rho \overline{h'w'}) + \frac{\partial}{\partial s}(\rho \overline{h'v'}) = \nabla \cdot \rho a^{\ell} \nabla \bar{h} . \end{aligned} \tag{37}$$

The last three terms at the left side arise from the cross-correlations between the turbulent fluctuations of the coolant enthalpy and of the velocity components and represent an additional energy flux in the coolant. The terms in brackets can be considered as the components of a "turbulent energy flux" vector defined by

$$q_r^t = \rho \overline{h'u'} \tag{38a}$$

$$q_z^t = \rho \overline{h'w'} \tag{38b}$$

$$q_s^t = \rho \overline{h'v'} \tag{38c}$$

which add to the molecular contributions

$$q_r^{\ell} = -\rho a^{\ell} \frac{\partial \bar{h}}{\partial r} \tag{39a}$$

$$q_z^{\ell} = -\rho a^{\ell} \frac{\partial \bar{h}}{\partial t} \tag{39b}$$

$$q_s^{\ell} = -\rho a^{\ell} \frac{\partial \bar{h}}{\partial s} . \tag{39c}$$

The components of the turbulent energy flux vector are calculated in the programme BACCHUS by means of the following half-empirical expressions

$$q_r^t = \rho \overline{h'u'} = -\rho c_{oT} \psi \Delta r \left(\bar{w}^2 + \bar{v}^2\right)^{1/2} \frac{\partial \bar{h}}{\partial r} \tag{40a}$$

$$q_z^t = \rho \overline{h'w'} = -\rho c_{oT} \varepsilon \Delta z \left(\bar{u}^2 + \bar{v}^2\right)^{1/2} \frac{\partial \bar{h}}{\partial z} \tag{40b}$$

$$q_s^t = \rho \overline{h'v'} = -\rho c_{oT} \xi \Delta s \left(\bar{u}^2 + \bar{w}^2\right)^{1/2} \frac{\partial \bar{h}}{\partial s} \tag{40c}$$

where c_{oT} is a dimensionless coefficient to be determined by comparison with experimental results. The use of the surface permeabilities in these equations accounts for the anisotropy of the porous medium.

The expressions (40) can be written

$$q_i^t = \rho \overline{h'V_i} = -\rho a^t \frac{\partial \bar{h}}{\partial \rho_i} \qquad (i=r,z,s) \tag{41}$$

with the definition of the eddy diffusivities for heat transfer

$$a_i^t = c_{oT} L_i \left(\bar{V}_j^2 + \bar{V}_k^2\right)^{1/2} \qquad \begin{matrix}(i=r,z,s)\\(j,k\neq i)\end{matrix} \tag{42a}$$

or

$$a_r^t = c_{oT} \psi \Delta r \left(\bar{w}^2 + \bar{v}^2\right)^{1/2} \tag{42b}$$

$$a_z^t = c_{oT} \varepsilon \Delta z \left(\bar{u}^2 + \bar{v}^2\right)^{1/2} \tag{42c}$$

$$a_s^t = c_{oT} \xi \Delta s \left(\bar{u}^2 + \bar{w}^2\right)^{1/2}. \tag{42d}$$

An effective energy flux vector can then be defined as the sum of the molecular and eddy contributions by

$$\vec{q} = \vec{q}^{\,\ell} + \vec{q}^{\,t} = -\varrho\alpha^{\ell}\frac{\partial\bar{h}}{\partial\ell_i}\vec{n}_i - \varrho\alpha^{t}\frac{\partial\bar{h}}{\partial\ell_i}\vec{n}_i \qquad (43)$$

$$= -\varrho(\alpha^{\ell}+\alpha^{t})\frac{\partial\bar{h}}{\partial\ell_i}\vec{n}_i = -\varrho\left(\alpha^{\ell}+c_{oT}L_i\left(\bar{V}_j^{\,2}+\bar{V}_k^{\,2}\right)^{1/2}\right)\frac{\partial\bar{h}}{\partial\ell_i}\vec{n}_i$$

$$= -\varrho\,\tilde{\alpha}\,\nabla\bar{h} \qquad \begin{matrix}(i=r,z,s)\\(j,k\neq i)\end{matrix}$$

with the definition of the effective diffusivity for heat transfer

$$\tilde{\alpha} = \alpha^{\ell} + \alpha^{t}\,. \qquad (44)$$

The divergence of the energy flux vector is

$$\nabla\cdot\vec{q} = \nabla\cdot\left(\vec{q}^{\,\ell}+\vec{q}^{\,t}\right) = -\nabla\cdot\left[\varrho(\alpha^{\ell}+\alpha^{t})\nabla\bar{h}\right] = -\nabla\cdot\varrho\,\tilde{\alpha}\nabla\bar{h}\,. \qquad (45)$$

Using eq. (45) the time-smoothed energy eq. (37) can be written

$$\frac{\partial}{\partial t}(\varrho\bar{h}) + \nabla\cdot\varrho\bar{h}\bar{V} = \nabla\cdot\varrho\tilde{\alpha}\nabla\bar{h} \qquad (46)$$

which has the form of eq. B 1.1 (3). This is the time-smoothed equation upon which the volume-averaging procedure is applied, as explained in section B 1.2.

The dimensionless coefficient c_{oT} has been estimated with the interpretation of sodium experiments in electrically heated 19-pin bundle /24/. The suggested value is $c_{oT} = 0.01$.

5.4 Wall-coolant heat transfer coefficient

The cladding to coolant heat transfer coefficient h_{CK} is calculated for single phase flow by means of the Nusselt number

$$N_u = \frac{h_{CK} D_h}{\lambda} = CNN1 + CNN2 \cdot R_e^{CN1} \cdot P_r^{CN2} \left(\frac{T_{bulk}}{T_{wall}} \right)^{CN3} \qquad (47)$$

where

λ = coolant thermal conductivity (W/m ^{o}C)

D_h = hydraulic diameter (m)

R_e = flow Reynolds number

P_r = Prandt number

T_{bulk} = coolant bulk temperature (^{o}C)

T_{wall} = wall temperature (^{o}C).

Default values of the coefficients are /25/

a) for sodium:

CNN1	=	7
CNN2	=	0.025
CN1	=	0.8
CN2	=	0.8
CN3	=	0

(48)

b) for water:

CNN1	=	0.
CNN2	=	0.023
CN1	=	0.8
CN2	=	0.4
CN3	=	0.

(49)

The heat transfer coefficient h between the coolant in the outermost radial control volume and the hexagonal can is calculated by means of the formula

$$\frac{1}{h} = \frac{1}{h_{SK}} + \frac{1}{h_c} \; . \qquad (50)$$

h_{SK} is the heat transfer coefficient structure to coolant due to convection given by (47) and h_c is the heat transfer coefficient due to conduction in the hexagonal can under the assumption of a linear temperature distribution through its thickness.

The conductive term is calculated as follows. Let

T_K be the bulk sodium temperature

T_S be the structure temperature (calculated in only one node at the centre of the hexagonal can)

S be the thickness of the hexagonal can

VSTRUK the structure volume per unit axial length

F the structure inner surface per unit axial length

VDUF (=VSTRUK/F) ratio volume to inner surface of the hexagonal can

q heat flux through the structure

λ_S structure thermal conductivity

x a coordinate with respect to an axis with origin at the structure inner surface and oriented outwards.

In case a linear temperature distribution through the hexagonal can is assumed

$$T(x) = T_K - 2 \frac{(T_K-T_S)}{S} x \tag{51}$$

the heat flux q is given by

$$q = -\lambda_S \text{ grad } T \simeq \lambda_S \frac{(T_K-T_S)}{S/2} . \tag{52}$$

Equation (52) can be written

$$q = h_c (T_K-T_S) \tag{53}$$

with

$$h_c = \frac{\lambda_S}{S/2} \simeq \frac{\lambda_S}{VDUF/2} . \tag{54}$$

The overall heat transfer coefficient will therefore be given by

$$\frac{1}{h} = \frac{1}{h_{SK}} + \frac{1}{\lambda_S/(VDUF/2)} . \tag{55}$$

6. Further programme details

6.1 Boundary conditions

According to the original MAC method /26/, from which the ICE technique has been derived, the boundary conditions are imposed both at free surfaces and at solid boundaries by using virtual cells.

In general, the application of boundary conditions for the scalar quantities (pressure, enthalpy and density of the coolant) is straightforward: the values in virtual cells are set equal to those in the adjacent physical cells. This applies for free surfaces and for solid boundaries. The only exception is made when the value corresponds to a given input function.

The boundary conditions for the velocity components depend on the physical conditions at the boundary cells. We therefore distinguish

a) free surfaces: the velocity component normal to the free surface is conserved; the velocity components parallel to the free surface are assumed to vanish at the surface (the value in the virtual cell is set equal in absolute value to the value in the physical cell, but with opposite sign).

b) solid boundaries: the velocity component normal to the solid surface is set to zero in the virtual cells; the velocity components parallel to the surface are assumed to vanish at the surface.

According to these rules, the most usual boundary conditions are as follows:

i) Bundle inlet ("South" boundary)

In case pressure boundary conditions are imposed:

$$P_{i,1,k} = f_p^s(t) \qquad (1a)$$

$$w_{i,1,k} = w_{i,2,k} \qquad (i = 2,\ldots NC) \qquad (1b)$$

$$u_{i,1,k} = -u_{i,2,k} \qquad (k = 2,\ldots NTH) \qquad (1c)$$

$$v_{i,1,k} = -v_{i,2,k}. \qquad (1d)$$

In case velocity boundary conditions are imposed:

$$p_{i,1,k} = p_{i,2,k} \tag{2a}$$

$$w_{i,1,k} = f_w^s(t) \tag{2b}$$

$$u_{i,1,k} = -u_{i,2,k} \tag{2c}$$

$$v_{i,1,k} = -v_{i,2,k}. \tag{2d}$$

f_p^s, f_w^s are given time functions for pressure and axial velocity components. For the other scalar quantities yield the same boundary conditions as for pressure.

ii) Bundel outlet ("North" boundary)

For pressure boundary conditions:

$$p_{i,MC+1,k} = f_p^N(t) \tag{3a}$$

$$w_{i,MZ+1,k} = w_{i,MZ,k} \tag{3b}$$

$$u_{i,MC+1,k} = u_{i,MC,k} \tag{3c}$$

$$v_{i,MC+1,k} = v_{i,MC,k} \tag{3d}$$

where f_p^N is a given time function. In this case it is meaningful not to suppress the radial and azimuthal components of the velocity at bundle outlet.

For velocity boundary conditions

$$p_{i,MC+1,k} = p_{i,MC,k} \tag{4a}$$

$$w_{i,MZ+1,k} = f_w^N(t) \tag{4b}$$

$$u_{i,MC+1,k} = -u_{i,MC,k} \tag{4c}$$

$$v_{i,MC+1,k} = -v_{i,MC,k} \tag{4d}$$

where f_w^N is a given time function.

iii) Inner pin boundary ("West" boundary)

This is usually a solid boundary, therefore

$$p_{1,j,k} = p_{2,j,k} \tag{5a}$$

$$w_{1,j,k} = -w_{2,j,k} \tag{5b}$$

$$u_{1,j,k} = 0 \tag{5c}$$

$$v_{1,j,k} = -v_{2,j,k} \tag{5d}$$

iv) Inner surface of hexagonal can ("East"boundary)

$$p_{NC+1,j,k} = p_{NC,j,k} \tag{6a}$$

$$w_{NR+1,j,k} = w_{NR,j,k} = 0 \tag{6b}$$

$$u_{NC+1,j,k} = 0 \tag{6c}$$

$$v_{NC+1,j,k} = -v_{NC,j,k} \tag{6d}$$

The axial velocity component is defined at the physical boundary IR = NR which coincides with the inner surface of the hexagonal can, and therefore set to zero.

Boundary conditions (5) and (6) could be replaced by other ones if the "east" or "west" boundaries were not solid.

In the azimuthal direction there are not physical boundaries for the full bundle, we therefore set, for the virtual cells K = 1 and K =NTH+1

$$p_{i,j,1} = p_{i,j,2} \tag{7}$$

$$p_{i,j,NTH+1} = p_{i,j,NTH} \tag{8}$$

and similarly for the velocity components.

The mostly used boundary conditions are (5) and (6) at the solid boundaries, pressure boundary conditions (3) at outlet and either (1) or (2) (pressure or velocity imposed) at bundle inlet.

6.2 Finite difference schemes

The programme user can choose between central and upwind differences for calculating the convective and diffusive terms in the momentum and energy equations. We show some examples of the application of these differencing methods.

i) Calculation of $\left[(\rho w)\, w\right]_{i,j,k}$

a) Central difference

$$\left[(\rho w)\, w\right]_{i,j,k} = \frac{1}{4}\,\rho_{i,j,k}\left(w_{i,j+1/2,k} + w_{i,j-1/2,k}\right)^2 = \rho_{i,j,k}\, w_m^2 \qquad (9)$$

b) Upwind (donor-cell) difference

$$\left[(\rho w)\, w\right]_{i,j,k} = \frac{1}{2}\,\rho_{i,j,k}\, w^2_{i,j-1/2,k}\left(1 + \mathrm{Sign}\, w_m\right) + \frac{1}{2}\,\rho_{i,j,k}\, w^2_{i,j+1/2,k}\left(1 - \mathrm{Sign}\, w_m\right) \qquad (10)$$

with

$$w_m = \frac{1}{2}\left(w_{i,j+1/2,k} + w_{i,j-1/2,k}\right). \qquad (11)$$

ii) Calculation of $\left[(\rho w)\, u\right]_{i+1/2,\, j+1/2,\, k}$

((ρw) is the convective term; u is the transported quantity)

a) Central difference

$$\left[(\rho w)\, u\right]_{\substack{i+1/2,\\ j+1/2,k}} = \frac{1}{2}\,\rho_m\, u_m\left(w_{i,j+1/2,k} + w_{i+1,j+1/2,k}\right) \qquad (12)$$

b) Donor-cell difference

$$\left[(\rho w)u\right]_{i+1/2,\,j+1/2,\,k} = \frac{1}{2}\rho_m w_{i,\,j+1/2,\,k}\left(u_m + |u_m|\right) + \frac{1}{2}\rho_m w_{i+1,\,j+1/2,\,k}\left(u_m - |u_m|\right) \tag{13}$$

with:

$$\rho_m = \frac{1}{2}\left[\left(\rho_{ijk}\Delta z_{j+1} + \rho_{i,j+1,k}\Delta z_j\right)/\left(\Delta z_j + \Delta z_{j+1}\right) + \left(\rho_{i+1,jk}\Delta z_{j+1} + \rho_{i+1,j+1,k}\Delta z_j\right)/\left(\Delta z_j + \Delta z_{j+1}\right)\right] \tag{14}$$

$$u_m = \frac{1}{2}\left(u_{i+1/2,j,k}\Delta z_{j+1} + u_{i+1/2,j+1,k}\Delta z_j\right)/\left(\Delta z_j + \Delta z_{j+1}\right) \tag{15}$$

iii) Calculation of $(\rho h w)_{i,j+1/2,k}$ in the energy equation

a) Central difference

$$(\rho h w)_{i,j+1/2,k} = \rho_m h_m w_{i,j+1/2,k} \tag{16}$$

with

$$\rho_m = \left(\rho_{ijk}\Delta z_{j+1} + \rho_{i,j+1,k}\Delta z_j\right)/\left(\Delta z_j + \Delta z_{j+1}\right) \tag{17}$$

$$h_m = \left(h_{ijk}\Delta z_{j+1} + h_{i,j+1,k}\Delta z_j\right)/\left(\Delta z_j + \Delta z_{j+1}\right) \tag{18}$$

b) Donor-cell difference

$$(\rho h w)_{i,j+1/2,k} = \frac{1}{2}h_{ijk}\left((\rho w)_{i,j+1/2,k} + |\rho w|_{i,j+1/2,k}\right) + \frac{1}{2}h_{i,j+1,k}\left((\rho w)_{i,j+1/2,k} - |\rho w|_{i,j+1/2,k}\right) \tag{19}$$

iv) $$\left(\lambda \frac{\partial T}{\partial z}\right)_{i,j+1/2,k} = \lambda_m \frac{1}{\Delta z_{j+1/2}} \left(T_{i,j+1,k} - T_{i,j,k}\right) \qquad (20)$$

with

$$\lambda_m = \left(\lambda_{i,j,k} \cdot \Delta z_{j+1} + \lambda_{i,j+1,k} \cdot \Delta z_j\right) / \left(\Delta z_j + \Delta z_{j+1}\right) \qquad (21)$$

v) $$\left(\mu \frac{\partial w}{\partial z}\right)_{i,j,k} = \mu_{i,j,k} \frac{1}{\Delta z_j} \left(w_{i,j+1/2,k} - w_{i,j-1/2,k}\right). \qquad (22)$$

Table II shows the three-dimensional arrays used for calculating the convective and diffusive terms in the momentum and energy equations. The meaning of the symbols, for instance for the axial z direction, is as follows:

GZ = ρw
RØW2 = $(\rho w) w$
RØWU = $(\rho w) u$
RØWUT = $(\rho w) v$
DWDZ = $(\partial w/\partial z)\mu$
DWDR = $(\partial w/\partial r)\mu$
DWDT = $(\partial w/\partial s)\mu$

CVZZ, CVZR, CVZT *
FZZ, FZR, FZT *
FWZ,GVZ *
RØEW = $\rho h w$
DTDZ = $(\partial T/\partial z)\lambda$

* See list of symbols at section C.2.3, Page 79 ff.

and similarly for the other coordinate directions. (UT is the FORTRAN symbol for the azimuthal velocity component v).

U(IR,JC,IT)	W(IC,JZ,IT)	UT(IC,JC,ITR)
GR(IR,JC,IT)	GZ(IC,JZ,IT)	GT(IC,JC,ITR)
[RØU2(IC,JC,IT)]	[RØW2(IC,JC,IT)]	[RØUT2(IC,JC,IT)]
[RØUW(IR,JZ,IT)]	[RØWU(IR,JZ,IT)]	[RØUTW(IC,JZ,ITR)]
[RØUUT(IR,JC,ITR)]	[RØWUT(IC,JZ,ITR)]	[RØUTU(IR,JC,ITR)]
[DUDR(IC,JC,IT)]	[DWDZ(IC,JC,IT)]	[DUTDT(IC,JC,IT)]
[DUDZ(IR,JZ,IT)]	[DWDR(IR,JZ,IT)]	[DUTDR(IR,JC,ITR)]
[DUDT(IR,JC,ITR)]	[DWDT(IC,JZ,ITR)]	[DUTDZ(IC,JZ,ITR)]
CVRZ(IR,JC,IT)	CVZZ(IC,JZ,IT)	CVTZ(IC,JC,ITR)
CVRR(IR,JC,IT)	CVZR(IC,JZ,IT	CVTR(IC,JC,ITR)
CVRT(IR,JC,IT)	CVZT(IC,JZ,IT)	CVTT(IC,JC,ITR)
[FRZ(IR,JC,IT)]	[FZZ(IC,JZ,IT)]	[FTZ(IC,JC,ITR)]
[FRR(IR,JC,IT)]	[FZR(IC,JZ,IT)]	[FTR(IC,JC,ITR)]
[FRT(IR,JC,IT)]	[FZT(IC,JZ,IT)]	[FTT(IC,JC,ITR)]
FWR(IR,JC,IT)	FWZ(IC,JZ,IT)	FWT (IC,JC,ITR)
	GVZ(IC,JZ,IT)	
[RØEU(IR,JC,IT)]	[RØEW(IC,JZ,IT)]	[RØEUT(IC,JC,ITR)]
[DTDR(IR,JC,IT)]	[DTDZ(IC,JZ,IT)]	[DTDT(IC,JC,ITR)]

Table II

List of arrays for calculating convective and diffusive terms of the momentum and energy equations. Indexes IC,JC,IT (= i,j,k) refer to the centre of a cell; indexes IR,JZ,ITR (= i $\pm$ 1/2, j $\pm$ 1/2, K $\pm$ 1/2) (underlined) refer to the cell boundaries. Arrays in parenthesis /‾ _‾/ have been spared in the most recent programme version (for instance RØW2 is stored temporarily in CVZZ) but they are listed for the sake of clarity.

6.3 Power Normalization

We define the power of the fuel bundle P and the power distribution by means of three sets of coefficients which give relative values of the specific power:

a) $f_1, f_2, \ldots f_{NN}$ — for the radial power distribution in the fuel or electrically heated pins

b) $\eta_2, \eta_3, \ldots \eta_j, \ldots \eta_{MC}$ — for the axial power distribution

c) $\alpha_{22}, \ldots \alpha_{ik}, \ldots \alpha_{NC,NTH}$ — for the power distribution at an axial level in radial and azimuthal directions.

The bundle power can be written

$$P = \sum_{2}^{NTH}{}_{k} \sum_{2}^{MC}{}_{j} \sum_{2}^{NC}{}_{i} P_{ijk} \tag{23}$$

where P_{ijk} is the power in a control volume given by:

$$\begin{aligned} P_{ijk} &= Q_{ijk} \sum_{1}^{4}{}_{\ell} T_\ell V_\ell = \\ &= Q_{ijk} \left(T_B \cdot V_B + T_C \cdot V_C + T_K \cdot V_K + T_S \cdot V_S \right). \end{aligned} \tag{24}$$

Q_{ijk} is the mean specific power in the cell and the T's are the fractions of the power generated in fuel, cladding, coolant and structural material respectively. These fractions are given by:

$$T_B = q_B / Q \tag{25a}$$

$$T_C = q_C / Q \tag{25b}$$

$$T_K = q_K / Q \tag{25c}$$

$$T_S = q_S / Q \tag{25d}$$

where q_B, q_C, q_K, q_S are the specific powers in the four media. These are normally known by experimental information or theoretical calculations.

Equation (24) can be written

$$P_{ijk} = q_B V_B + q_C V_C + q_K V_K + q_S V_S \tag{26}$$

using (25), or

$$P_{i'j'k} = Q_{i'j'k} \cdot V^{*}_{i'j'k} \tag{27}$$

with the definition

$$V^{*}_{i'j'k} = \sum_{1}^{4} e \; T_e V_e \quad . \tag{28}$$

The power in the cells, P_{ijk}, is obtained by normalizing the total power P by means of the sets of coefficients b) and c) in two subsequent steps:

i) Normalization with respect to the axial direction

From the relation:

$$\frac{\text{(power generated at axial level j)}}{\text{bundle power}} = \frac{Q^{(A)}_{j} \cdot \bar{V}_j}{P} = \frac{\eta_j \bar{V}_j}{\sum_{2}^{ML}{}_j \eta_j \bar{V}_j} \tag{29}$$

we derive the mean specific power at axial level j

$$Q^{(A)}_{j} = \frac{\eta_j \cdot P}{\sum_{1}^{ML}{}_j \eta_j \bar{V}_j} \left[\equiv \bar{Q}_j = \frac{\sum_{i'k} Q_{i'jk} V^{*}_{i'jk}}{\sum_{i'k} V^{*}_{i'jk}} \right] \tag{30}$$

where

$$\bar{V}_j = \sum_{2}^{NTH}{}_k \sum_{2}^{NC}{}_i V^{*}_{ijk} \tag{31}$$

takes into account the volume of the j-th axial mesh of the bundle.

ii) Normalization with respect to the radial and azimuthal distributions.

From the relation

$$\frac{\text{cell power}}{\text{(power generated at axial level j)}} = \frac{Q_{i'j'k} \cdot V^{*}_{i'j'k}}{\bar{Q}_j \sum_{i'k} V^{*}_{i'j'k}} = \frac{\alpha_{i'k} \cdot \bar{V}^{*}_{i'j'k}}{\sum_{i'k} \alpha_{i'k} V^{*}_{ijk}} \tag{32}$$

we derive

$$Q_{i'j'k} = \frac{\left(\bar{Q}_j \sum_{i'k} \bar{V}^{*}_{i'j'k} \right) \alpha_{i'k}}{\sum_{i'k} \alpha_{i'k} V^{*}_{i'j'k}} \cdot \quad \left[W/m^3 \right] \tag{33}$$

The linear pin power is given by

$$\chi_{ijk} = Q_{ijk}\left[T_B \cdot \pi R_B^2 + T_C \cdot \pi\left(R_a^2 - R_i^2\right)\right] \quad [W/m] \tag{34}$$

when R_B is the fuel radius, Ra, Ri are the outer and inner radii of the clad.

The heat fluxes out of the pins are

$$\phi_{ijk} = \chi_{ijk} / (2\pi R_a) \tag{35}$$

The set a) of coefficients is used to calculate the radial power distribution Q_n (n = 0,1...NN) in the fuel. From the relation

$$\left(\frac{\text{Power in fuel volume } V_n}{\text{Fuel power}}\right)_{ijk} = \left(\frac{Q_{Bn} V_{Bn}}{Q \cdot T_B V_B}\right)_{ijk} = \left(\frac{f_n V_{Bn}}{\sum_0^{NN} f_n V_{Bn}}\right)_{ijk} \tag{36}$$

we derive

$$\left(Q_{Bn}\right)_{ijk} = \left(\frac{f_n Q T_B V_B}{\sum_0^{NN} f_n V_{Bn}}\right)_{ijk} . \tag{37}$$

V_{Bn} is the volume of the fuel cell within the cylindrical surfaces of radii $R_{n-1/2}$, $R_{n+1/2}$.

Following main FORTRAN symbols are used in the programme:

$FACR_n$	for	f_n
QZ_j		z_j
QRT_{ik}		a_{ik}

FAK	for	$Q_{i,j,k}\, T_B\, V_B \,/\, \Sigma_m f_m V_{Bm}$	in (37)
$VØLBR_{ijk}$		$V_{B\,i,j,k}$	
$VBRZ_j$		$\Sigma_{i,k} V^*_{i,j,k}$	in (31)
$VQRT_j$		$\Sigma_{i,k} \alpha_{i,k} V^*_{i,j,k}$	
$QlVØ_j$		$\bar{Q}^{(n)}_j$	in (30)
$QGRT_j$		$\bar{Q}_j$	in (30)
$QVØLL_{ijk}$		$Q_{i,j,k}$	in (33)
$QVØLLO_{ijk}$		$Q_{i,j,k}$	at t=0
$QVØLLA_{ijk}$		$Q_{i,j,k}$	at t_{n-1}
$QQQl_{ijk}$		$\phi_{i,j,k}$	in (35)
$QLIN_{ijk}$		$\chi_{i,j,k}$	in (34).

6.4 Check of mass balance

The coolant mass unbalance is given for every control cell by the continuity equation C.2 (1)

$$D^*_{i,j,k} = \varepsilon_{i,j,k} \frac{\rho^{n+1}_{i,j,k} - \rho^{n}_{i,j,k}}{\Delta t_n} + \tag{38}$$

$$+ \vartheta_c \frac{\varepsilon_{i,j,k}}{\Delta z_j}\left[(\rho w)^{n+1}_{i,j+1/2,k} - (\rho w)^{n+1}_{i,j-1/2,k}\right] + (1-\vartheta_c)\frac{\varepsilon_{i,j,k}}{\Delta z_j}\left[(\rho w)^{n}_{i,j+\frac{1}{2},k} - (\rho w)^{n}_{i,j-1/2,k}\right] +$$

$$+ \frac{\vartheta_c}{\Delta x_i}\left[(\psi F \rho u)^{n+1}_{i+1/2,j,k} - (\psi F \rho u)^{n+1}_{i-1/2,j,k}\right] + \frac{(1-\vartheta_c)}{\Delta x_i}\left[(\psi F \rho u)^{n}_{i+1/2,j,k} - (\psi F \rho u)^{n}_{i-1/2,j,k}\right] +$$

$$+ \frac{\vartheta_c}{\Delta y_k}\left[\left(\frac{\varphi \rho v}{\cos\beta}\right)^{n+1}_{i,j,k+1/2} - \left(\frac{\varphi \rho v}{\cos\beta}\right)^{n+1}_{i,j,k-1/2}\right] + \frac{1-\vartheta_c}{\Delta y_k}\left[\left(\frac{\varphi \rho v}{\cos\beta}\right)^{n}_{i,j,k+1/2} - \left(\frac{\varphi \rho v}{\cos\beta}\right)^{n}_{i,j,k-1/2}\right] = 0$$

$$\left[D^*_{i,j,k}\right] = \left[kg/m^3 s\right]$$

In the programme we check the mass conservation in terms of mass flow by means of:

$$D_{i,j,k} = D^{*}_{i,j,k} \cdot V_{i,j,k} = D^{*}_{i,j,k} \cdot S_t \, \Delta z_j \quad [kg/s]. \tag{39}$$

The value of D_{ijk} gives an information about the convergence behaviour of the numerical scheme used for the numerical solution of the Poisson equation. A good convergence is achieved when $\max|D_{ijk}|$ is less than about 10^{-5}.
In the steady state the mass unbalance is given by

$$\begin{aligned} D_{0\,i,j,k} = {} & (\rho w)_{i,j+1/2,k} \cdot S_{ft} - (\rho w)_{i,j-1/2,k} \cdot S_{fb} + \\ & + (\rho u)_{i+1/2,j,k} \cdot S_{fe} - (\rho u)_{i-1/2,j,k} \cdot S_{fi} + \\ & + (\rho v)_{i,j,k+1/2} \cdot S_{fp} - (\rho v)_{i,j,k-1/2} \cdot S_{fm} \quad [kg/s]. \end{aligned} \tag{40}$$

6.5 Check of enthalpy balance

The enthalpy balance requires that in the steady state the power supplied corresponds to the sum of the power transported by the coolant and of the power lost beyond the hexagonal can.

In the transient case the temperature increment in every medium must account for the difference between power generation and power lost or transported by the coolant.

The power transported by the fluid P_H equals the difference between the enthalpy flows at outlet and at inlet of the bundle per unit time

$$P_H = H_N - H_S. \qquad \underline{\bar{W}} \tag{41}$$

The enthalpy flows per unit time at outlet (North) and inlet (South) of the bundle are given by

$$H_N = \sum_{2}^{NC} i \sum_{2}^{NTH} k \; h_{i,Mz,k} \cdot (\rho w)_{i,Mz,k} \cdot S_{fi,k} \quad [W] \tag{42}$$

$$H_S = \sum_{2}^{NC} i \sum_{2}^{NTH} k \; h_{i,1,k} \cdot (\rho w)_{i,1,k} \cdot S_{fi,k} \quad [W] \tag{43}$$

The power lost beyond the hexagonal can is

$$P_X = \sum_{2}^{MC}{}_j \sum_{2}^{NTH}{}_K \left[\alpha_W F_W \left(T_S - T_W \right) \right]_{j,K} \qquad [W] \tag{44}$$

where

α_W = heat transfer coefficient structure to surrounding medium ($W/m^2\ ^oC$)

F_W = outer surface of hexagonal can per unit axial length (m)

T_S = hexagonal can temperature (^oC)

T_W = surrounding medium temperature (^oC).

In the steady state it holds

$$P = P_H + P_X \tag{45}$$

where P is the input power.

The power stored in the sodium during a transient is

$$P_K = \frac{1}{\Delta t_m} \sum_{2}^{NC}{}_i \sum_{2}^{MC}{}_j \sum_{2}^{NTH}{}_K \left(h^{m+1}_{i,j,K} - h^{m}_{i,j,K} \right) \rho^{m+1}_{i,j,K} \Delta z_j \, S_{f\,i,j,K} \tag{46}$$

where h is the coolant enthalpy.

The powered stored in the fuel during a transient is

$$P_B = \frac{1}{\Delta t_m} \left\{ \sum_{2}^{NC}{}_i \sum_{2}^{MC}{}_j \sum_{2}^{NTH}{}_K \sum_{0}^{NN}{}_n \left[\left(\rho c_p \right)_B V_B \left(T_B^{m+1} - T_B^{m} \right) \right]_{i,j,K,n} \right\} FAC_{i,K} \tag{47}$$

where T_B is the fuel temperature. V_B is the volume of the fuel associated to the radial fuel node n, between the cylindrical surfaces of radii $r_{n\pm1/2}$ (see section A.2). FAC_{ik} is the fraction of fuel pin associated to the control cell (i,j,k).

The power stored in the clad during a transient is

$$P_C = \frac{1}{\Delta t_m} \left\{ \sum_{2}^{NC} \sum_{2}^{MC} \sum_{2}^{NTH} \sum_{1}^{3} \left[(\rho c_p)_C V_C \left(T_C^{m+1} - T_C^{m} \right) \right]_{i,j,k,\ell} \right\} \cdot FAC_{ik} \quad (48)$$

The index ℓ refers to the three nodes considered in the clad.

The power stored in the hexagonal can during a transient is

$$P_S = \frac{1}{\Delta t_m} \sum_{2}^{MC} \sum_{2}^{NTH} \left[(\rho c_p)_S V_S \left(T_S^{m+1} - T_S^{m} \right) \right]_{jk} . \quad (49)$$

The overall enthalpy balance requires that during a transient

$$P = P_H + P_K + P_B + P_C + P_S + P_X \qquad [W] . \quad (50)$$

In a steady state $P_K \simeq P_B \simeq P_C \simeq P_S \simeq 0$ and eq. (50) reduces to (45).

The power P calculated with eq. (50) differs in general from the specified input power

$$P_D = \sum_{2}^{NC} \sum_{2}^{MC} \sum_{2}^{NTH} \left(Q \cdot V^* \right)_{ijk} \quad (51)$$

where Q_{ijk} $[W/m^3]$ is the power density calculated as explained in section 6.3.

The relative error

$$e = \frac{P - P_D}{P_D} \quad (52)$$

gives a measure of the accuracy of the calculation. Typically is $e \approx 10^{-3}$. The programme calculates also the energy released from the beginning of the transient by integrating the instantaneous power over the subsequent time steps:

$$P^C = \int_0^t P(t)\, dt \qquad [J] \quad (53)$$

$$P_D^C = \int_0^t P_D(t)\, dt \qquad [J] . \quad (54)$$

For consistency the percentual error

$$e^C = \left| P^C - P_D^C \right| / P_D^C \quad (55)$$

should vanish with increasing time in a quasi-stationary calculation run with constant power.

6.6 Time step control

Previous programme versions were run using the Alternating Direction Implicit (ADI) method for the solution of the Poisson equation with a constant time step in the range 1 - 4 msec. A reduction of the CPU time in the calculation of the pressure field of up to fifty percent has been obtained with a time step optimization which works as follows.

We call tolerance $\left[= \max \left((p_{ijk}^{r+1} - p_{ijk}^{r}) / p_{ijk}^{r+1} \right) \right]$

the maximum of the relative pressure change in the full definition domain in two subsequent iterations with the ADI method. The iterative sweeps must be repeated till the tolerance decreases below an input value TOL (about 10^{-5}). The calculation practice has shown that

i) the tolerance which can actually be reached is inversely proportional to the time step Δt;

ii) the mass unbalance D_{ijk} (see Section 6.4) is roughly proportional to the product of the tolerance with the time step;

iii) the number of iterations (ITER) necessary to reach a given tolerance is directly proportional to the time step and inversely proportional to the tolerance itself. Therefore following empirical relations can be written:

$$TOL \cdot \Delta t \simeq C_1 \tag{56}$$

$$D_{ijk} \propto TOL \cdot \Delta t \tag{57}$$

$$ITER = C_2 \frac{\Delta t}{TOL} = \frac{C_2 \Delta t^2}{C_1} \tag{58}$$

where C_1, C_2 are constants and the symbol $\propto$ means proportionality.

The problem of minimizing the calculation time (t_{CPU}) necessary to simulate a problem time t_p consists in finding the optimum time step (or, for (58), the optimum number of iterations) which allows to approach the extremum of the function $t_{CPU} / t_p = f(\Delta t)$.

Let assume to calculate a transient problem for a bundle with a number of NC, MC and NTH control cells in the radial, axial and azimuthal directions respectively, and introduce the following calculation time normalized to the problem time

$$\gamma = \frac{1}{NC \cdot MC \cdot NTH} \quad \frac{t_{CPU}}{t_P} \; . \tag{59}$$

The normalized time is given by the following equation, derived from the calculation practice,

$$\gamma = \frac{1}{\Delta t} (a + b \cdot ITER) \tag{60}$$

or, by means of (58),

$$\gamma = \frac{a}{\Delta t} + \frac{C_2 b}{C_1} \; . \; \Delta t \tag{61}$$

When using the IBM 3033 computer the constants in eqs. (60), (61) have the values: $a = 1.16 \times 10^{-3}$ (sec), $b = 9.15 \times 10^{-5}$ (sec). The constant a represents the CPU time necessary to make the explicit calculation within one time step while the constant b represents the CPU time for one iteration sweep in the numerical solution of the Poisson equation, which then must be multiplied by the number of iterations.

A plot of the normalized time γ as function of the iteration number is shown in Fig. 10. The corresponding values of the time step are also shown in the plot for a case $C_2/C_1 = 10^{-6}$ sec^{-2} which holds for a slow transient. The minimum of γ is obtained differentiating with respect to Δt in eq. (61) and imposing the extremum condition, which yields, with the above given proportionality constant,

$$\begin{aligned} \Delta t &= (aC_1/bC_2)^{1/2} = 3.5 \times 10^{-3} \text{ sec} \\ \frac{C_2}{C_1} \Delta t^2 &= ITER \simeq 13 \end{aligned} \tag{62}$$

If we allow a deviation up to about 5% from the minimum ζ, which corresponds to the optimum $ITER_{opt} = 13$, the iteration number can vary in the range

$$6 \simeq \frac{1}{2} \; ITER_{opt} \leq ITER \leq 2 \cdot ITER_{opt} \simeq 26 \qquad (63)$$

This range for ITER has been found acceptable for all calculations made with different transient conditions and bundle sizes.

The computer programme changes automatically the time step to insure that the iteration number remains in the above range. In practice, this is done as follows: the mean iteration number is calculated over twenty time steps. If it exceeds the upper boundary in (63) the time step is divided by $\sqrt{2}$, rounded to half-millisecond steps (for instance 0.00141 rounded to 0.0015), and then kept constant for the following twenty time steps. Conversely, if the iteration number becomes smaller than the lower boundary in (63), the time step is multiplied by $\sqrt{2}$.

Moreover, we use the relation (57) to ensure that the mass unbalance D_{ijk} always remains just smaller than an input value (OMEGA $\simeq 10^{-6}$), (without needing to become smaller by a large factor). This implies that a reduction of Δt can be accompanied by an increase of the given tolerance for the solution of the Poisson equation. Conversely, a larger Δt implies a smaller (sharper) tolerance.

As a rule, after optimizing the time step with the method explained above, we check if the following constraint is satisfied (see Ref. /27/):

$$\Delta t \leq \min_{i,j,k} \left\{ \frac{1}{2\left[\frac{|\bar{w}|}{\Delta z} + \frac{|\bar{u}|}{\Delta x} + \frac{|\bar{v}|}{\Delta y} + \frac{2\nu}{\Delta z^2} + \frac{2\nu}{\Delta x^2} + \frac{2\nu}{\Delta y^2} \right]} \right\} \qquad (64)$$

where

$$\bar{w} = \frac{1}{2}\left(w_{i,j+1/2,k} + w_{i,j-1/2,k} \right) \qquad (65)$$

$$\bar{u} = \frac{1}{2}\left(u_{i+1/2,j,k} + u_{i-1/2,j,k} \right) \qquad (66)$$

$$\bar{v} = \frac{1}{2}\left(v_{i,j,k+1/2} + v_{i,j,k-1/2} \right) \qquad (67)$$

$$\nu = \mu / \rho. \qquad (68)$$

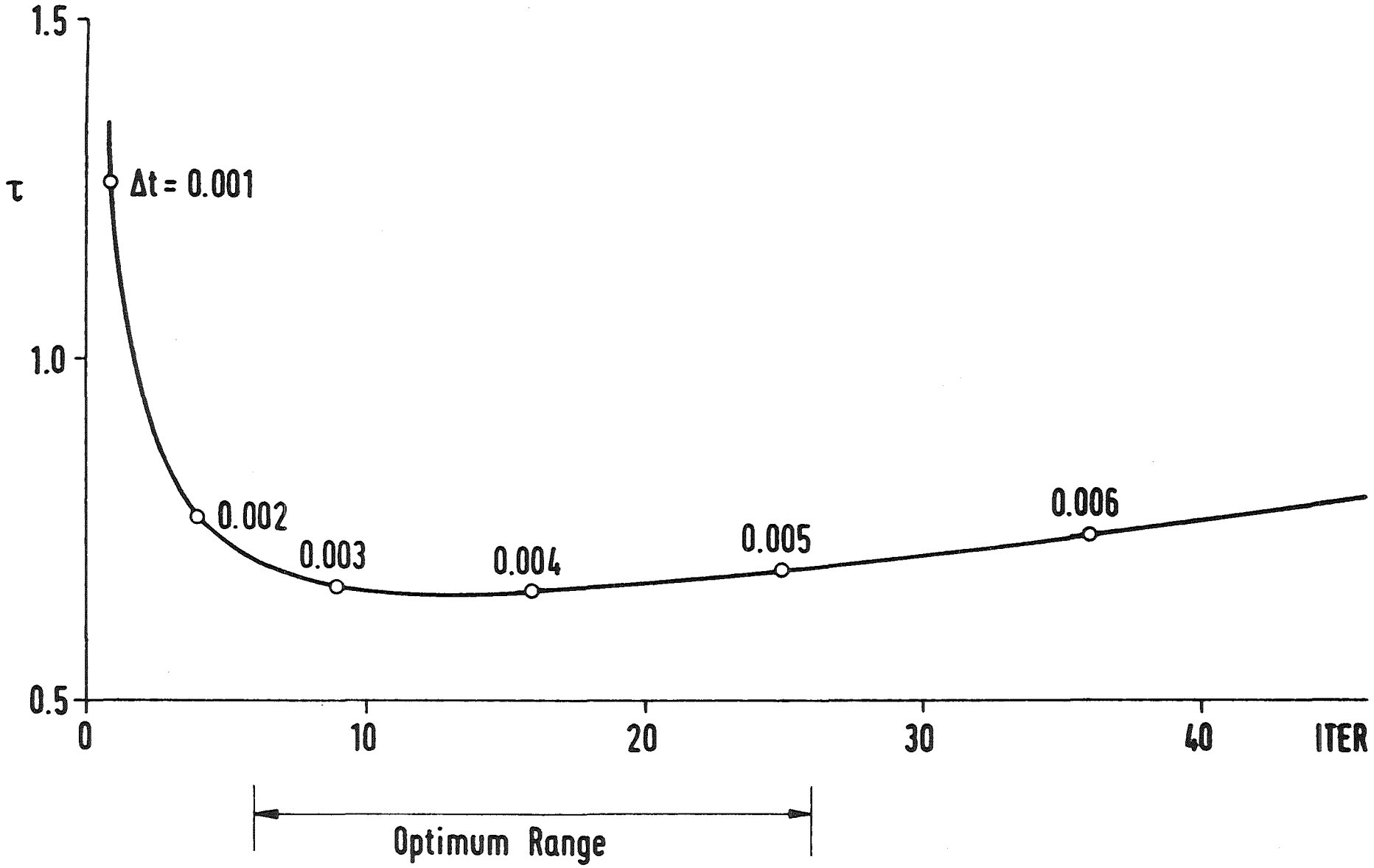

Fig. 10: Normalized calculation time versus number of iteration sweeps with the ADI method.

List of symbols

(Only symbols used throughout the report are listed)

c = $(dp/d\rho)^{1/2}$ sound velocity (m/s)

c_p = specific heat (J/kg)

D = pin diameter (m) / drag force per unit surface ($kg/m\ sec^2$)

$\vec{D}_o$ = drag force per unit volume (kg/m^2s^2)

D_h = hydraulic diameter (m)

f = friction coefficient

F = geometric factor (See eq. B.1.14)

g = gravity acceleration (m/s^2)

h = specific enthalpy: (J/kg)

K = resistance coefficient

$\vec{n}$ = unit vector

Nu = Nusselt number

p = pressure (N/m^2)

P = pitch (m)

P_r = Prandtl number

q,Q = specific power (W/m^3)

r = radial coordinate (m)

R = radius (m)

s = azimuthal coordinate (m)

S = surface (m^2)

t = time (s)

T = temperature (^oC)

u = radial component of coolant velocity (m/s)

v = azimuthal component of coolant velocity (m/s)

V = volume (m^3) /velocity vector (m/s)

w = axial component of coolant velocity (m/s)

z = axial coordinate (m)

Greek symbols

α	heat transfer coefficient ($W/m^2\ ^oC$)
$\tilde{\alpha}$	thermal diffusivity (m^2/s)
β	angle between planes through the bundle axis bounding an azimuthal control volume (See Fig. 9)
ε	volume porosity and surface permeability with respect to the axial direction
ϑ	time discretization parameter
λ	thermal conductivity ($W/m\ ^oC$)
μ	dynamic viscosity (kg/ms)
ν	kinematic viscosity (m^2/s)
ξ	surface permeability with respect to the azimuthal direction
ϱ	density (kg/m^3)
χ	friction coefficient
ψ	surface permeability with respect to the radial direction

Indices

b	bottom
B	fuel
e	exterior
f	fluid
g	grid
H	cladding
i	interior/identifier of cells in radial direction
j	identifier of cells in axial direction
k	identifier of cells in azimuthal direction
K	coolant
l	laminar
m	minus (previous-one in azimuthal direction)
n	time discretization
p	plus (subsequent in azimuthal direction)
S	structure (hexagonal can)
t	top/turbulent
w	wall

References

/1/ G. Basque, D. Grand, B. Menant:
"BACCHUS-P: un code permanent de thermohydraulique simple et double phase en grappe". CEA/CENG Note Technique Nr. 565, February 1979

/2/ D. Grand, G. Basque:
"Two-dimensional Calculation of Sodium Boiling in Sub-Assemblies". ANS/ENS Proc. International Meeting on Fast Reactor Safety Technology, Seattle, Washington, August 19-23, 1979, Vol. V, pp. 2502-2511, American Nuclear Society (1979).

/3/ B. Basque, D. Grand, L. Delapierre, M. Bottoni, B. Dorr, C. Homann, D. Struwe:
"Thermohydraulic analysis of LMFBR subassemblies with the BACCHUS programme". ANS/ENS Int. Topical Meeting on LMFBR Safety and related Design and operational aspects, Lyon, July 19-23, 1982.

/4/ J. Aberle, A.J. Brook, W. Peppler, H. Rohrbacher, K. Schleisiek:
"Sodium Boiling Experiments in a 7-Pin Bundle under Flow Run Down Conditions". KFK-2378 (1976)

/5/ D.W. Peaceman, H.H. Rachford:
"The numerical solution of parabolic and elliptic differential equations", Journal of the Society for Industrial and Applied Mathematics, Vol. 1, Nr. 1 (1955), pp. 28-41

/6/ H.H. Delhaye:
"General equations of two-phase systems; a series of five lectures given at the Von Karman Institute for Fluid Dynamics"(Rhode-Saint-Genese, Belgium), April 1978

/7/ L.H. Thomas:
"Elliptic problems in linear difference equations over a network" Watson Scientific Computing Lab., Columbia Univ., New York, 1949

/8/ J.R. Bodoia:
"The finite difference analysis of confined viscous flows" - Thesis presented at the Carnegie Institute of Technology, July 1959.

/9/ F.H. Harlow, A.A. Amsden:
"A numerical fluid dynamics calculation method for all flow speeds". Journal of Computational Physics, 8 (1971), pp. 197-213

/10/ J. Douglas:
"On the numerical integration of $\partial^2 u/\partial x^2 + \partial^2 u/\partial y^2 = \partial u/\partial t$ by implicit methods", Journal of the Society for Industrial and Applied Mathematics, Vol 3, Nr. 1 (1955), pp. 42-65

/11/ E.L. Wachpress:
"Iterative Solution of Elliptic Systems", Prentice-Hall Inc., 1966

/12/ D.M. Young:
"Iterative Solution of Large Linear Systems", Academic Press, 1971

/13/ U. Schumann:
"Über die direkte Lösung der diskretisierten Poisson-Gleichung mittels zyklischer Reduktion", KFK-Ext. 8/75-6, Januar 1976

/14/ J.W. Cooley, J.W. Tukey:
"An algorithm for the machine calculation of complex Fourier series", Mathematics of Computation, Vol. 19 (1965) p. 297

/15/ G.E. Forsythe, W.R. Wasow:
"Finite difference methods for partial differential equations". J. Wiley and Sons Inc., 1960

/16/ Y. Wallach, A. Barlevi:
"Inversion of a Blockwise Tridiagonal Matrix". Computing 7 (1971), pp. 357-363.

/17/ J.M. Varah:
"On the Solution of Block-Tridiagonal Systems arising from certain Finite-Difference Equations". Mathematics of Computation, 26, Nr. 120 (1972), pp. 859-868.

/18/ D. Young:
"Iterative methods for solving partial difference equations of elliptic type". Trans. Amer. Math. Soc. 76 (1954), pp. 92 - 111.

/19/ S.P. Frankel:
"Convergence rates of iterative treatments of partial differential equations". Math. Tables Aids Comput. 4, (1950), pp. 65-75

/20/ R.S. Varga:
"Matrix Iterative Analysis". Prentice-Hall, Inc. 1962.

/21/ E.H. Novendstern:
"Turbulent flow pressure drop model for fuel rod assemblies utilising a helical wire-wrap spacer system".
Nuclear Engineering and Design, 22 (1972), pp. 19-27

/22/ G. Trippe:
"Experimentelle Untersuchungen turbulenter Strömungen in axial durchströmten Stabbündeln ohne und mit gitterförmigen Abstandshaltern"
KfK 2834, Juli 1979

/23/ M. Bottoni, B. Dorr, C. Homann, D. Struwe:
"Progress in development and verification of the BACCHUS-3D programme".
IV IAHR Working Group, Grenoble, 9-11 December 1981

/24/ R. Möller, H. Tschöke, M. Kolodziej:
"Experimentelle Bestimmung von Temperaturfeldern in natriumdurchströmten Bündeln mit hexagonaler Stabanordnung und gitterförmigen Abstandshaltern". KfK 2356, Januar 1977.

/25/ S.T. Hsu:
"Engineering Heat Transfer". D. Van Nostrand Company, Inc., 1963.

/26/ J.E. Welch, F.H. Harlow, J.P. Shannon, B.J. Daly:
"The MAC method - A computing technique for solving viscous, incompressible, transient fluid-flow problems involving free surfaces".
Los Alamos Sci. Lab., Rep. No. LA-3425

/27/ J.Noye Ed.:
"Numerical Simulation of Fluid Motion". North Holland Publishing Company, 1978.

Acknowledgement

The authors wish to express their gratitude to the colleagues Drs. J. Costa, D. Grand, G. Basque from the Grenoble Nuclear Research Centre CENG of the French Commissariat à l'Energie Atomique (CEA) and Mrs. L. Delapierre from Compagnie Internationale de Services en Informatique (CISI), Grenoble, for delivering the steady-state and the transient two-dimensional versions of the BACCHUS programme, which formed the basis of the further developments documented in this report.

We would also like to thank Mrs. Stephany for her excellent work of typing the manuscript, Miss Stutz and Mrs. Oberacker for the preparation of the figures.